Compact Passive Wireless UHF Sensors for Packaged Food Monitoring

by

Robin Raju

A Thesis submitted to the Faculty of Graduate Studies of

The University of Manitoba

in partial fulfilment of the requirements of the degree of

DOCTOR OF PHILOSOPHY

Department of Electrical and Computer Engineering

University of Manitoba

Winnipeg, Manitoba, Canada

Copyright © 2022 by Robin Raju

Abstract

Package to package monitoring of food commodities using printed RFID-based sensors offers a low-cost, environmentally friendly and bio-compatible alternative to traditional electronic sensors. The lack of batteries and expensive electronic components enable their integration into a sustainable food production and distribution model easily. Some of the essential properties essential for the practical implementation of such sensors include small size, easy detectability, and long detection range. Though a vast amount of research has been demonstrated towards the development of chipless and passive RFIDs little work has been carried out in literature for their application in food monitoring applications. This thesis presents the study of compact passive wireless sensors operating in the giga-hertz range for application in packaged food monitoring. Firstly, a radar-cross-section (RCS) based compact wireless humidity sensor with a built-in reference signature and time-gated measurement is presented. This novel approach of integrated reference in the same scattering element gives the differential sensing ability and thereby immunity to frequency detuning effects from the dielectric loading in the immediate environment of the sensor without an increase in the size of the tag. Environmental clutter is one of the biggest problems towards the practical implementation of RCS-based tags. The thesis thus further focuses on tackling this problem. One of the solutions to this is a polarimetry-based depolarizing tag that scatters orthogonally polarized fields. The next part of the thesis thereby presents the first of its kind compact depolarization-based sensing tag for acidic/basic volatile sensing. Further improvement in the clutter performance can be achieved using frequency diversity between the interrogator transmitted and sensor retransmitted signal. In the final part of the thesis a novel compact harmonic sensor with integrated transmit, receive antennas and non-linear doubling circuit integrated on an annular slot antenna is demonstrated for the first time. The sensor is suitable for monitoring of high-value food items like fish and meat. The non-linear sensor has the advantage of not needing background calibration for practical applications commonly needed for detection of chipless sensors passive sensors. Milk and ammonia monitoring are demonstrated using the presented sensors.

Contributions

The research contributions of this Ph.D. thesis are reported in the form of four published peer-reviewed journal papers, and one peer-reviewed conference paper. In all of these, the first author is the author of the thesis and the other author is the candidate's advisor with the supervisory role, with the exception of [J1]. [J1] is a review paper and section II on low frequency coupled coil sensors was contributed by a third author.

It should be noted that the candidate's other conference articles that are listed here are not included in the thesis directly. Some sections of these papers, however, conceptually integrate into one or more of the chapters in the thesis. Specifically, [J1], [J2] , [J3] ,[J4] and [C1] from the list of the publications presented below, have been included in this thesis in the form of chapters.

Journal Articles

[J1] **R. Raju,** G. E. Bridges, and S. Bhadra, "Wireless passive sensors for food quality monitoring: Improving the safety of food products," *IEEE Antennas Propag. Mag.*, vol. 62, no. 5, pp. 76–89, Oct. 2020.

© [2020] IEEE. Reprinted, with permission, from [R. Raju, G. E. Bridges, and S. Bhadra, Wireless passive sensors for food quality monitoring: Improving the safety of food products, IEEE Antennas Propag. Mag, Oct. 2020]

[J2] **R. Raju** and G. E. Bridges, "Radar Cross Section-Based Chipless Tag With Built-In Reference for Relative Humidity Monitoring of Packaged Food Commodities," in *IEEE Sensors Journal*, vol. 21, no. 17, pp. 18773-18780, 1 Sept.1, 2021.

© [2021] IEEE. Reprinted, with permission, from [R. Raju and G. E. Bridges, Radar Cross Section-Based Chipless Tag With Built-In Reference for Relative Humidity Monitoring of Packaged Food Commodities, IEEE Sensors Journal, Sept, 2021]

[J3] **R. Raju** and G. E. Bridges, "A Compact Passive wireless harmonic sensor for packaged food quality monitoring," IEEE Trans. Microw. Theory Tech., 2022 (early access).

© [2022] IEEE. Reprinted, with permission, from [R. Raju and G. E. Bridges, A Compact Passive wireless harmonic sensor for packaged food quality monitoring, IEEE Trans. Microw. Theory Tech., 2022]

[J4] **R. Raju** and G. E. Bridges, "A compact wireless passive harmonic sensor for ammonia sensing in packaged food," IEEE Sensors Lett., 2022 (early access).

© [2022] IEEE. Reprinted, with permission, from [R. Raju and G. E. Bridges, A compact wireless passive harmonic sensor for ammonia sensing in packaged food, IEEE Sensors Lett., 2022]

Conferences and Abstracts

[C1] **R. Raju** and G. E. Bridges, "RCS based depolarizing passive tag with improved clutter rejection for potentiometric gas sensing," in *2019 IEEE SENSORS*, 2019, pp. 1–4.

© [2019] IEEE. Reprinted, with permission, from [R. Raju and G. E. Bridges, RCS based depolarizing passive tag with improved clutter rejection for potentiometric gas sensing, IEEE Sensors conf., 2019]

[C2] **R. Raju** and G. E. Bridges, "Radar Cross Section Based Passive Wireless Sensor for Volatile Sensing," *Proc. - ANTEM 2018 2018 18th Int. Symp. Antenna Technol. Appl. Electromagn.*, vol. 2018-August, Dec. 2018.

[C3] **R. Raju** and G. E. Bridges, "Radar Cross Section based dual-band dual-polarized humidity sensing tag," in *XXXIInd URSI General Assembly*, 2017.

[C4] **R.Raju** and G. E. Bridges, "In-Package Humidity Sensing RFID Tag for Monitoring Fresh Vegetables", in *CSBE/SCGAB 2017 Annual Conference*, Aug. 2017.

[C5] S. Bhadra, **R. Raju**, and G. E. Bridges, "Stacked Coupled-Coil Approach for Multi-Parameter Passive Wireless Sensing," *17th Int. Symp. Antenna Technol. Appl. Electromagn. ANTEM 2016*, pp. 2–3, Aug. 2016.

Acknowledgement

First and foremost, I would like to express my most sincere gratitude to my advisor, Prof. Greg. Bridges, for his guidance and support during every stage of my Ph.D. research. I will always be thankful to him for the knowledge, confidence and independence that he nurtured in me through his supervision. I would also like to extend my gratitude for the time taken by my examining committee members: Prof. Doughlas Thomson and Prof. Nazim Cicek from the University of Manitoba, and my External Examiner, in reviewing this work.

Thanks to Cory Smit, Zoran and James Dietrich for the endless support they had provided me with the fabrication and setting-up of the measurement apparatus used during the experiments.

Thank you to all my friends and colleagues of the Microsystems and bio-sensors measurement laboratory for their support, engaging discussions and fun-filled conversations that made the graduate school life very enjoyable. Special thanks to Amy Dario, for her administrative support, unlimited supplies of candies and meet-ups she organized, alleviating some of the stress of long hours in the lab.

The funding and support by the Natural Science and Engineering Research Council of Canada (NSERC), the University of Manitoba Graduate Scholarship (UMGF), Graduate Students Association (GSA) and Canadian Microelectronics Corporation (CMC), is greatly appreciated.

Finally, I would like to thank my wife and my parents for the continued love and support they have given me throughout the course of the research work.

Contents

Abstract ii
Contributions iii
Acknowledgement v
Contents vi
List of Figures ix
List of Tables xv
Chapter 1. Introduction – Motivation and Purpose of the Thesis 1
1.1. Chipless wireless sensors and various transduction schemes for food monitoring 3
1.2. Considerations with Microwave Passive Wireless Sensors 4
1.2.1. Size of the Sensor 4
1.2.2. Immunity to Environmental Loading and Clutter 5
1.3. Smart Packaging for Extended Shelf Life and Spoilage Detection 7
1.3.1. Gas Sensors for Packaged Food Monitoring 8
1.3.2. Electrochemical transduction 8
1.3.3. Semiconductor based electronic transduction 8
1.3.4. Dielctric and Mass sensitive transduction 9
1.3.5. Optical transduction 10
1.4. Objectives of the Thesis 10
References 12
Chapter 2. Wireless Passive Sensors for Food Quality Monitoring 18
2.1. Abstract 18
2.2. Introduction 18
2.3. High-Frequency Passive Sensors 22
2.3.1. LC resonators measuring dielectric permittivity 23
2.3.2. Passive RFID based HF sensor. 24
2.3.3. LC resonator measuring volatiles. 26
2.4. UHF Sensors for Food Quality Monitoring 29
2.4.1. Chipless UHF Sensors 30
2.4.2. Limitations of Chipless UHF Sensors 34

2.5. Discussion 36
2.6. Conclusion 37
2.7. References 38
Chapter 3. Radar Cross Section Based Chipless Tag with Built-in Reference for Relative Humidity Monitoring of Packaged Food Commodities 46
3.1. Abstract 46
3.2. Introduction 46
3.3. Sensor Design 49
3.3.1. Sensing Transducer Characterization 49
3.3.2. Tag Design and Sensor Operation 52
3.4. Experimental Results 54
3.4.1. RCS Measurement Method 54
3.4.2. Wireless Relative Humidity Monitoring 57
3.5. Conclusion 61
3.6. Acknowledgment 62
3.7. References 62
Chapter 4. RCS Based Depolarizing Passive Tag with Improved Clutter Rejection for Potentiometric Gas Sensing 67
4.1. Abstract 67
4.2. Introduction 67
4.3. Concept of Operation, Sensor design and Simulation Results 69
4.4. Experiments and Discussion of Results 71
4.5. Conclusion 75
4.6. References 75
Chapter 5. A Compact Passive Wireless Harmonic Sensor for Packaged Food Quality Monitoring Applications 79
5.1. Abstract 79
5.2. Introduction 79
5.3. Sensor Design and Operation 82
5.3.1. Antenna Design and Simulation 82
5.3.2. Harmonic Generation for Retransmission 86
5.3.3. Sensor Integration 89

5.4. Sensor interrogation and characterization 90
5.5. Sensor Application to pH Sensing 93
5.5.1. Milk Spoilage Monitoring 94
5.6. Conclusion 96
5.7. References 98
Chapter 6. A Compact Wireless Passive Harmonic Sensor for Ammonia Sensing in Packaged Food 102
6.1. Abstract 102
6.2. Introduction 102
6.3. Sensor Design and Operation 104
6.3.1. Hydrogel Coated pH Electrode 106
6.4. Ammonia Sensing Application 107
6.5. Conclusion 109
6.6. References 110
Chapter 7. Conclusion and Future Work 113
7.1. References 116

List of Figures

Fig. 1.1 A broad classification of chipless passive RF sensors based on their principle of operation. 3

Fig. 2.1 Passive wireless sensor system concepts for packaged food monitoring……20

Fig. 2.2 Schematic of steps for wrapping and adhering silk LC resonators onto foods. 1) Water vapor is exposed to the back of non-crystalline functionalized silk films, resulting in 2), a functionalized film in which the back surface of the film is partially melted and acting as glue. 3) This melted surface is conformally applied to arbitrary surfaces with gentle pressure, resulting 4), applied functional sensors on a variety of food [29]. [© 2012 WILEY-VCH Verlag GmbH & Co. KGaA, Weinheim] 23

Fig. 2.3 Measured resonant frequency the during banana ripening process. Conducted at room temperature (22° C) with a relative humidity of 30% [29]. [© 2012 WILEY-VCH Verlag GmbH & Co. KGaA, Weinheim] 24

Fig. 2.4 Fig. 2.1 Modified commercial RFID tag with printed PTS-PAni layer [34]. [© 2018 American Chemical Society] 25

Fig. 2. 5 (a) The real-time responses of sensor in terms of S_{11} and f_0 towards 5, 10, 20, and 40 ppm of NH_3. (b) The sensor's application for meat spoilage monitoring [34]. [© 2018 American Chemical Society.] 25

Fig. 2.6 (a) Prototype volatile absorption sensor with hydrogel coated MMO and Ag/AgCl electrodes. (b) An equivalent circuit diagram of the sensor [8]. [© 2014 Elsevier B.V.] 26

Fig. 2.7 (a) Resonant frequency of the sensor after reaching equilibrium state as a function of NH_3 concentration at 24ºC (20mins. after initial exposure to each concentration of NH_3. (b) Experimental setup for wireless tilapia spoilage test. A 25 g tissue sample of fish and the wireless sensor are placed in a jar. The sensor's resonant frequency is measured using the interrogator coil connected to an impedance analyzer [8]. [© 2014 Elsevier B.V.]..... 27

Fig. 2. 8. Resonant frequency of the sensor and bacterial population in fresh tilapia kept at 4ºC over a period of 4.5 days. Bacterial data are the average of two replicates [8]. [© 2014 Elsevier B.V.]..... 28

Fig. 2.9 Resonant frequency response of embedded sensor and pH measured over 4 days for milk left at room temperature. (b) Milk container with encapsulated sensor inside measured with an impedance analyser at 5 cm distance [37]. 29
Fig. 2.10 (a) Retransmission based sensing in time domain with single BST resonator for temperature sensing. (b) Measured resonant frequency of the sensor for various temperature conditions [51]. [©2012 IEEE] 30
Fig. 2.11 (a) Stepped impedance resonator for humidity sensing (b) measured insertion loss of the sensor corresponding to different humidity conditions [52] [©2012 IEEE] 31
Fig. 2.12 (a) Experimental setup used for measuring radar cross section of the annular slot ring antenna. The sensing tag is placed at a distance of 80 cm from the interrogating antenna, inset is the example of measured RCS of the tag (b) Measured percentage change in resonant frequency with time for different saturated salt solutions. Note the initial room humidity was not controlled and thus the initial resonant frequency varies in the measurements [61]. 32
Fig. 2.13 (a) Asymmetric circular split ring resonator coated with sensing material for temperature threshold detection. (b) Measured performance of the sensor with pure coconut oil as the sensing material [62]. [© 2019, IEEE] 33
Fig. 2.14 (a) Inkjet-printed flexible Van-Atta reflect-array prototype, next to a standard "credit-card" size RFID tag package. (b) Plot of measured resonance frequency of the inkjet-printed Van-Atta array as a function of ambient humidity level. [63]. [© 2016, IEEE] 34
Fig. 2.15 (a) Fabricated circuit and the complete tag setup with antennas and pH electrode (b) Measured phase change for harmonic operation at different pH [69]. [© 2019, IEEE]..... 35
Fig. 2.16 (a) Experimental set-up and fabricated depolarizing tag used for volatile sensing. (b) Change in resonant frequency of the depolarizing RCS based sensor to different concentration of ammonia gas (inset is the measured normalized RCS response showing the reference and sensing signatures). [74] .....36https://d.docs.live.net/a1409a91ffbe894f/PhD/Thesis/New folder/RR_Thesis_Combined_20211114.docx - _Toc87904279
Fig. 3.1 Schematic representation showing headspace monitoring of packaged food commodity using the proposed passive chipless radar cross section (RCS) based sensor. 47
Fig. 3.2 (a) Experimental set-up used for humidity sensing and characterization of the interdigitated capacitor. (b) The measured impedance response of the capacitor and the curve fitted

data obtained from the extracted equivalent circuit. Inscribed is the equivalent circuit model (without PVA coating R_{eqv}=3.15 k**Ω**, C_{eqv}=545 fF, and L_{eqv}= 4 **nH**). 49
Fig. 3.3 (a) Measured relative humidity in the chamber for each of the salt solutions. Change in equivalent circuit parameters (b) capacitance C_{eqv} and (c) resistance R_{eqv} of the PVA coated interdigitated capacitor for different saturated salt solutions. 50
Fig. 3.4 Per-unit-length capacitance and resistance for the interdigitated capacitor vs percent relative humidity (obtained using different saturated salt solutions). 52
Fig. 3.5 (a) Dual-polarized annular slot antenna loaded with a functionalized interdigitated capacitor (all dimensions are in mm). (b) aperture field distributions for the two orthogonal modes. 53
Fig. 3.6 Experimental setup used for measuring radar cross section of the annular slot ring sensing tag. The sensing tag is placed inside a humidity-controlled chamber at a distance 80 cm from the interrogating antenna, both the antennas are rotated 90^0 to measure the two polarizations. 55
Fig. 3.7 Measured RCS of the tag showing the effect of time gating with different window width ($\boldsymbol{\tau}$) on the frequency domain response of the tag. An interfering tag with the same resonant frequency is placed at a distance of 80 cm further away from the sensing tag. 56
Fig. 3.8 HFSS simulation results showing the vertically polarized RCS_S and horizontally polarized RCS_R response of the proposed annular slot tag with PVA coated IDC. PVA material properties corresponding to various humidity conditions were obtained from [32]. 56
Fig. 3.9 Measured resonant frequency of the vertically polarized RCS_S and horizontally polarized RCS_R (a) magnitude and (b) phase sampled at two different humidity conditions obtained using the saturated salt solution method. 57
Fig. 3.10 Measured and simulated differential resonant frequency vs the equilibrium relative humidity for the annular slot ring sensor with a PVA coated IDC. Discrete markers indicate data points, and the solid line is the non-linear interpolated fit. The measured data were obtained using the 800 min data points of the time response obtained using the saturated salt solution test (see Fig. 11). Circles indicate the HFSS simulation results obtained using the per-unit-length parameters of Fig. 4. Red squares-indicate the HFSS simulation results obtained using the permittivity values from [32]. 58
Fig. 3.11. Change in resonant frequency of the sensing tag with adsorption and desorption of water vapor for the saturated KCl test. Inset shows the fabricated sensor with functionalized IDC. 59

Fig. 3.12 Measured time response of the resonant frequency with time for different saturated salt solutions obtained using the wireless interrogation setup shown in Fig. 6. Note that the initial room humidity is not controlled and varies with background room RH when measurements were carried out. 59

Fig. 4.1 (Left) Annular slot antenna with capacitive loading at two orthogonal sites. (Bottom) The current distribution at resonance of the annular slot antenna when excited by an incident vertically polarized plane wave. 70

Fig. 4.2 HFSS simulation results showing the X-pol response of the proposed wireless sensor, C1 corresponds to the sensing capacitance and C2 corresponds to the reference capacitance. 71

Fig. 4.3 Experimental results showing the generated potential of an MMO-Ag/AgCl combination electrode pair to different concentrations of ammonia vapor inside a sealed chamber. 72

Fig. 4.4 (Left) Experimental setup used for the measurement of the cross-polarization measurement of the annular slot antenna. (Right) Fabricated tag with fixed capacitor loading .. 72

Fig. 4.5 (Left) Experimental set up used to demonstrate the clutter rejection capability of the depolarizing antenna. (Right) Measurement results showing the RCS co-pol and cross-pol response of the capacitively loaded annular slot in the presence of scattering elements inside the radian sphere of the tag. 73

Fig. 4.6 Measurement results showing the RCS co-pol and cross-pol responses of the capacitively loaded annular slot antennas. 73

Fig. 4.7 (a) Experimental set-up and fabricated depolarizing tag used for volatile sensing. (b) Change in resonant frequency of the depolarizing RCS based sensor to different concentration of ammonia gas (inset is the measured normalized RCS response showing the reference and sensing signatures obtained using late time short time fourier transform resoponse). 74

Fig. 5.1 Concept diagram representation of the passive harmonic sensor. The swept frequency interrogation signal at $\boldsymbol{f0}$ is orthogonally polarized to the re-transmitted signal at $\boldsymbol{2f}$.....81

Fig. 5.2 Exploded diagram showing the different functional parts of the harmonic sensor. 82

Fig. 5.3 Geometry of the annular slot antenna operating at two distinct frequencies and polarizations, used for HFSS simulations. The antenna is excited using two driven ports to obtain the simulation results without the doubler circuitry. 83

Fig. 5.4 HFSS simulation showing $|\boldsymbol{S11}|$ plot for the antenna mode corresponding to the (a) receiving mode at $\boldsymbol{f0}$ and (b) transmitting mode at $\boldsymbol{2f0}$, for different capacitance values modeling

the varactor diode under different bias conditions. Insets show the surface current distribution for reach of the modes. 84
Fig. 5.5 Gain patterns of the dual polarized annular slot antenna operating at two distinct frequencies (a) at 2.5 GHz and (b) 5 GHz 85
Fig. 5.6 (a) Circuit schematic showing the harmonic frequency doubler and (b) printed circuit board layout on an FR4 board of thickness 0.7874 mm. The location of the feedlines and the dimensions of meander lines were chosen such that the circuit can be easily integrated with the annular ring antenna of Fig. 2. 86
Fig. 5.7 (a) Wideband harmonic balance EM-circuit co-simulation results of the frequency doubling circuit of the layout shown in Fig. 5b obtained using Keysight ADS simulation software. The input power at the fundamental frequency was swept from 2 to 3 GHz while the power was kept constant at 0 dBm. (b) The fundamental and harmonic power at the output port at a fixed frequency of 2.5 GHz. 87
Fig. 5.8 (a) Measured conversion loss for an output frequency of 5 GHz. (b) Measured frequency response for different input power to the frequency doubling circuit. Inset in (a) shows the fabricated frequency-doubling circuit with connectors added for testing purposes. 88
Fig. 5.9 Fabricated harmonic sensor with the annular slot and the doubling circuit integrated with an external pH electrode. 89
Fig. 5.10 Block diagram of the interrogator for wireless harmonic tag sensing. 90
Fig. 5.11 (a) Resonant frequency change and (b) received signal signature of the sensor for different applied voltages across the varactor diode in the forward and reverse bias conditions. Markers indicate the measured data points, and the solid lines are the linear and 4th order polynomial fits in (a) and (b), respectively. 92
Fig. 5.12 3-point calibration of the commercial pH electrode using buffer solutions measured using Agilent 34401A digital multimeter. The electrode has a sensitivity of ~55mV per unit pH change. 92
Fig. 5.13 (a) Normalized received signal from the harmonic sensor for different pH buffers, (b) the time response of the sensor's doubled resonant frequency for different pH buffer solutions and (c) the received doubled resonant frequency of the sensor vs the pH of the buffer solution. (data points in (c) are takin from the t=15 min points in (b)) 93

Fig. 5.14. Study of stability of the sensor in two different pH buffer solutions over 25 hour period. 94

Fig. 5.15 (a) Experimental setup used for monitoring of milk spoilage and (b) the resonant frequency measured using the harmonic sensor and corresponding pH change measured using a commercial pH electrode with a voltmeter during milk souring process (no temperature compensation). 95

Fig. 6.1 Concept diagram representation of the passive harmonic sensor for volatile gas sensing in packaged food items. 103

Fig. 6.2 (a) Schematic of the frequency doubler circuit on the back side. (b) Dual frequency orthogonal polarized annular ring antenna on the front side and (c) the fabricated sensor and schematic of the amorphous hydrogel coated pH-electrode structure. 104

Fig. 6.4 (a) The power received (P_{rec}) by the interrogator for different transmitted power (P_{out}) when the sensing tag is placed at a fixed distance of 80 cm from the reader. (b) The frequency response for the signal received by the interrogator for different **Pout**. Discrete points are actual measured values and solid lines indicates the interpolated data. 105

Fig. 6.3 Block diagram of the interrogator used for harmonic wireless sensing. 105

Fig. 6.5 The measured pH response of the MMO-Ag/AgCl electrode pair. The inset shows the time response of the electrodes to different buffer solutions. 106

Fig. 6.6 Experimental setup used for ammonia sensing. Inset shows the schematic of the sensing chamber with the sensor tag inside. Details of the interrogator are in Fig. 3. 107

Fig. 6.7 (a) Interpolated normalized magnitude of the received signal at 50 min intervals (b) resonant frequency change with time for different ammonia concentrations introduced into the chamber, and (c) the resonant frequency versus the logarithm of the equilibrium ammonia concentration in ppm (solid line indicates linear interpolation and markers indicate the actual measured points). 108

List of Tables

Table 1.1 21
Table 3.1 50
Table 3.2 60
Table 5.1 97

Chapter 1.
Introduction – Motivation and Purpose of the Thesis

About 55% (35.5 million tons) of all food produced in Canada is lost in the form of food waste according to the research in [1]. 77% of these losses come from the stages of production, processing, manufacturing, distribution, and retail stages of the food supply chain. This accounts for 31.95 billion dollars in economic loss. Avoidable food waste also accounts for 9.8 million tonnes of CO_2 equivalent to 2.1 million cars on the road [2]. Some of the key factors of avoidable food waste are the confusion between expiry and best before dates, inappropriate labelling, and improper packaging. Intelligent packaging and monitoring of food quality of food items effectively and efficiently are therefore inevitable from both consumer safety, economical perspective, and environmental standpoint.

Food quality is affected by factors internal to the food commodity and external storage conditions. Internal factors include moisture content, pH, and catalysts which influence the enzymatic activity inside the food material. External factors include light, temperature, mechanical pressure, temperature, and humidity. Humidity (water activity), temperature, and pH have been identified to be the three most crucial factors affecting food quality [3]. These three factors when monitored and controlled have shown to significantly increase the shelf life of packaged food commodities. Though controlling internal pH can be challenging, monitoring pH provides information pertaining to the early detection and quantitative indication of microbial activity inside the food material. Studies on food spoilage indicate emission of various acidic and basic volatiles as a by-product of fungal and bacterial metabolism [4][5]. For instance, microorganisms with proteolytic (capable of breaking down proteins) activity can act on proteins, breaking them down into simpler compounds of amino acids. These compounds further undergo oxidative deamination and desulfurization, resulting in the emission of basic gasses like ammonia and hydrogen sulphide [6]. These basic gases can be used as quality indicators of meat products. Similarly, foods rich in carbohydrates like desserts are broken down into simpler molecules like organic acids, ethanol and CO_2 due to microbial action [7], which can be used as their quality indicators. Integration of food packaging with wireless sensors capable of providing quantitative information about such quality

indicators, thereby, delivers an unparalleled solution to item-level tagging and monitoring food commodities.

Deployment of traditional wireless sensors for package-to-package monitoring has always been challenging in terms of the associated cost. Recent advancements in material science and printing technology have however vastly changed this scenario [8]. The fabrication and deployment of bio-compatible, environment-friendly micro-sensors have become much simpler and more cost-effective. Though these sensors allow real-time monitoring of quantities about health care, food, and environment [9], control of food quality, and spoilage [10], the finite-capacity batteries, which are often hazardous, limit their application. Nevertheless, a significant amount of work has been done on the development of energy-efficient systems for a longer lifetime [11]. Passive sensors, which do not require any local source of power, hence present a new paradigm in low-cost wireless sensing [12]. Several such sensors have been successfully developed and studied previously for the detection of food spoilage and smart packaging applications [13]. These sensors like others in [14] [15], utilize near field coupling for their activation, this constrains the read range of the sensor considerably. One way to increase the range is by using active transponders in the sensor which are powered remotely, however, increases the cost of the sensor substantially, limiting large-scale deployment as required in food packaging [16]. Passive wireless sensors at microwave frequencies, with considerable range and that are devoid of integrated chips thereby strike a balanced alternative to both sensors with active transponders and low frequency coupled coil sensors in terms of cost, maintenance, and detection range.

The goal of this thesis is to design and implement a low-cost wireless passive gas sensor capable of operating in the gigahertz range, for monitoring chemical and/or physical changes in packaged food to improve its self-life or/and detect spoilage. The high (microwave) frequency design gives them a longer read range and compact size. The manufacturing cost thus can be kept under 0.1% of the food commodity when mass-produced [16], making them suitable for package to package monitoring of food products. The applications of these sensors may also further be extended to the healthcare and petrochemical industries for chemical sensing.

1.1. Chipless wireless sensors and various transduction schemes for food monitoring

Traditional wireless sensors can be classified broadly into two categories: active and passive. Active sensors are the class of sensors that are battery powered and are often integrated with other electronic devices like microcontrollers, radio and sensor circuits. These sensors have the advantage of long-range and superior data handling capacity. The power requirement and active integrated circuits however make these devices expensive and incompatible with low-cost roll-to-roll printing technology. Some popular examples of such sensors are IoT platform-based CC3200 from Texas Instruments [17] and sensor tags by CAO Gadgets LLC [18]. Passive sensors on the other hand do not require a battery, based on whether they have an active integrated chip, these can be classified into chip-based and chipless sensors. Chip-based sensors obtain the power required for the activation of the chip through energy harvesting [19] or from the interrogating signal sent out by the reader. Commercial RFID tags utilize such an approach, where the interrogation signal is used both for the radio front end reception, and transmission of identification signal through modulated backscattering scheme [16]. The presence of a chip in these sensors however makes them expensive and incompatible with the current planar printing technology, thereby limiting their applications in package to package labelling of commodities. Chipless radio

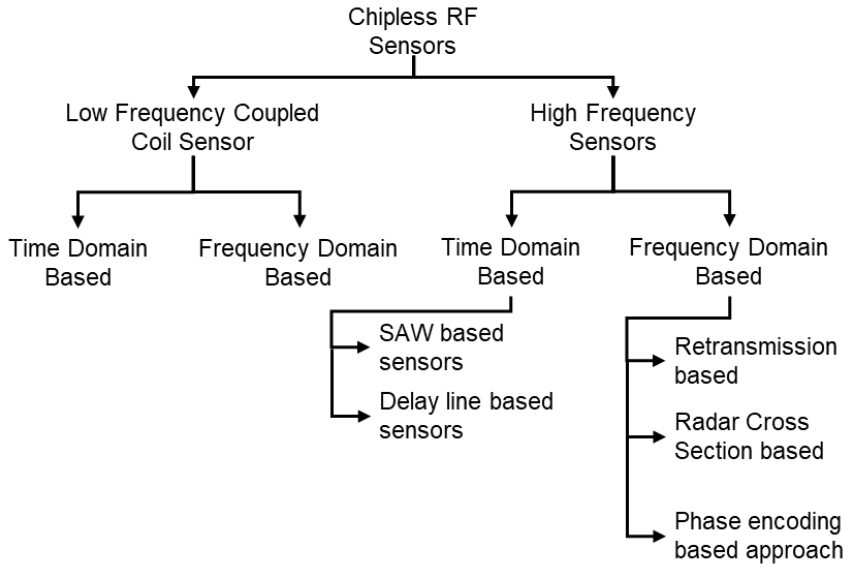

Fig. 1.1 A broad classification of chipless passive RF sensors based on their principle of operation.

frequency sensors offer the benefits of longer life, lower cost, and printability over chip-based sensors.

A broad classification of chipless radio frequency sensors based on their operation is shown in Fig. 1.1. Chapter 2 presents a literature survey of the application of passive wireless sensors for packaged food quality monitoring, in section 1.2, the key design challenges of chipless passive sensors operating in the microwave frequency range are discussed. Section 1.3 presents common transduction schemes and their applicability to food packaged quality monitoring.

1.2. Considerations with Microwave Passive Wireless Sensors

Some of the key factors that have to be taken into account in designing microwave passive sensors are- its compatibility with low-cost printing technology, its integration with RFID technology for product identification, its size, and its clutter rejection capability. Advancements in printed electronics have expanded the possibilities of using various shapes (2D and 3D) and materials for the substrate and the conducting layouts. The performance of printed active devices like diodes has also made considerable progress, enabling their application in passive sensors if needed. By utilizing sensors of the same architecture as that of the RFID tags, their integration together can be easily achieved without a considerable increase in the complexity of reader design. The size of the sensor and its clutter rejection capability are the most crucial factors that are needed to be considered from an RF engineer's design point of view. These are discussed briefly in the following sections.

1.2.1. Size of the Sensor

As the passive sensors mainly rely on the number of sensing elements for measuring multiple parameters and the number of encoded bits, the size of these sensors becomes a key factor to be considered in their design. Often the retransmission-based sensors are significantly larger in size compared to the RCS based sensors, this is because in these sensors the structural scattering is of higher magnitude than the antenna mode, thus the delay provided by the transmission lines for the retransmitted signal has to be large enough for the sensing information to be easily distinguished. As electromagnetic waves have higher speeds than mechanical and acoustic waves, they require long transmission lines for obtaining the desired delay, this increases the size of the sensor.

Some of the alternatives used by researchers are surface acoustic wave (SAW) sensors or metamaterial-inspired negative delay lines [20][21][22] or, the use of orthogonally polarized backscatter schemes [23]. Both SAW-based sensors and negative group delay lines are slow-wave structures, thereby reducing the length of the delay lines required for the retransmitted pulse. SAW-based sensors often consist of a piezoelectric transducer to convert the interrogation signal into an acoustic signal. The acoustic wave travels along the piezoelectric surface, thus acting as an acoustic a delay line. Slots along the piezoelectric act as discontinuities (reflectors) which partially reflects the acoustic wave towards the reader, the delay between the reflected waves can be controlled by the spacing between the slots. Both the delay and phase information can be used to encode the required information [24]. A SAW-based temperature sensor is presented in [25], where the delay between the reflected signals changes with the temperature due to the temperature coefficient of delay of the piezoelectric substrate material. SAW sensors however are nonplanar and often use difficult manufacturing processes. Other traditional techniques like the use of high permittivity or high permeability material, meandering of the transmission line to reduce the effective length may also be used for the reduction in the size of the transmission lines [26]. In the case of RCS-based sensors, little work has been done in the literature towards their miniaturization. Most miniaturization techniques used for antenna miniaturization like dielectric loading, lumped element loading and modified geometry for extended current paths may be employed for their size reduction [26].

1.2.2. Immunity to Environmental Loading and Clutter

Clutter is the unwanted signal scattered by the environment, picked up by the interrogator. Chipless sensors being of small size, the signatures may be overwhelmed by large objects in the environment, making the detection difficult. In retransmission-based techniques, clutter rejection can easily be achieved by using separate receiving and transmitting antennas. The antennas are oriented orthogonal to each other, such that polarization diversity between the received and transmitted signals can be achieved. As the polarization of the scattered signal from common clutter is largely in the direction of the interrogating signal, orthogonally polarized received signal can be distinguished. This however increases the size of the sensor considerably.

Since RCS-based sensors solely rely on the scattering from the sensing antenna, which almost always needs to be polarization matched to the incident interrogating signal, clutter reduction for these sensors becomes challenging. One of the ways by which the effect of environmental clutter can be reduced is to make the scattering from the sensing element as large as possible. This has been done using two methods, one is by using retrodirective array antenna like Van-Atta reflectarray antenna as the scattering element [27][28], and the second is by using active negative resistance load on the scattering antenna [29][30] [31][32]. A hybrid combination of both, using a reflection amplifier with the retrodirective reflector-Van Atta array has also been demonstrated in [33] [34]. Van-Atta reflectarray itself being of large size, it is generally suited for applications in higher millimeter-wave frequencies. Negative resistance loading on the other hand requires an active element and related biasing circuit on the sensor making it incompatible with roll-to-roll printing technology.

Another method to reduce the clutter is by using a depolarizing/cross-polarizing scattering element like a dipole oriented at 45° to the polarization of the incident interrogating wave as proposed in [35][36][37]. Though this technique has successfully been shown to eliminate clutter close to the scatterer for an RFID system, little work has been done towards integrating them for sensors application. Similarly, frequency diversity between the incident interrogation signal and the scattered/retransmitted signal may be used in quasi-chipless sensors for clutter rejection. This may be achieved by utilizing a highly nonlinear device like a diode, either as a passive harmonic frequency generator or a passive mixer to produce a transmit signal either the harmonic of the incident wave or the product of two incident waves respectively. This technique has been demonstrated in sensing of various physical parameters like crack and strain [38][39], liquid level [40], temperature [41][42][43], and humidity [44], these tags have also been reported for tracking of small insects like bees [45][46]. One of the disadvantages of using passive harmonic sensors however is that they require high transmitted power in the interrogating signal, this is attributed to the power loss associated with the passive generation of the harmonic frequency. These sensors are larger compared to the radar cross-section (RCS) counterpart, as most of them utilize separate antennas for reception and transmission.

In addition to the above-mentioned techniques, time-domain gating is often implanted to block unwanted scattering from the scatterer. In this technique, a time-domain window is implemented

in software or hardware to receive the signal only for a specific duration of time corresponding to the sensor under interrogation. This is done under the assumption that the scattered clutter is reasonably farther away from the sensor, thereby taking a long time to travel back to the receiver.

1.3. Smart Packaging for Extended Shelf Life and Spoilage Detection

Traditionally food packaging is used for the protection, convenience, and containment of food products, where the packaging materials are made to have minimal interaction with the food materials. Smart packaging techniques on the other hand are designed to interact with the food material and its packaged environment to provide a positive change or indication for the extended shelf life of food products. The shelf life of food is dictated by one or more of the several quality indicators like colour, texture, odour or micro-organism count. These quality indicators may degrade due to both internal compositional factors and external environmental factors. Some of the compositional factors are pH, micro-organism levels and other catalysts like enzymes and trace metals [3]. Environmental factors which affect food quality are temperature, humidity, light, mechanical stress and pressure. Smart food packaging focuses on keeping these factors at the optimal levels using active and/or intelligent packaging techniques. Active packaging involves the use of strategies like temperature control, oxygen removal using oxygen scavengers, carbon dioxide control using absorbers and emitters, moisture control using moisture absorbing pads or desiccants like silica gel, the addition of chemicals to change the internal parameters like pH of the food product, and the use of an antimicrobial coating to retard the microbial growth in the package [47].

Intelligent packaging on the other hand focuses mainly on the ability to monitor the conditions of the packaged food or its environment. It adds the functionality of detection, sensing and recording of the conditions in which the food is stored. This is done by using sensors and indicators. The common include biosensors, gas sensors, chemical sensors, freshness indicators, time-temperature indicators for storage temperature history and integrity indicators to detect leaks. Biosensors are used to detect biological reactions using bio receptors like a specific antibody to detect a target analyte or pathogens [48]. Most biosensors are however need active electronic devices to translate the sensed biochemical signals into quantitative information, these sensors are

thus often used with a dye for colorimetric qualitative visual indication of the food freshness. Chemical bi-products resulting from the activity of pathogens like acidic or basic chemicals namely, lactic acid, acetic acid or basic amines can be detected using pH-based chemical sensors [13].

1.3.1. Gas Sensors for Packaged Food Monitoring

Unlike biosensors and chemical sensors, gas sensors offer contactless monitoring of food products. These sensors can give quantitative information on pathogenic activity by indirectly sensing the gaseous bi-products resulting from their metabolic activity. Depending on the material and principle of transduction, gas sensors can be classified into several types: electrical, mass sensitive, magnetic, optical, thermoelectric and electrochemical. A brief overview of each of these is discussed in the following section.

1.3.2. Electrochemical transduction

Electrochemical sensors are amperometric [49] or potentiometric sensors [50]. These sensors make use of the charge transfer between a solid or liquid electrolyte and an electrode for their sensing mechanism. These sensors consist of a sensing/working electrode and a reference electrode, and often a third counter electrode. The electrodes are dipped in a conducting electrolyte, which forms the electrochemical cell. The electrolyte can be liquid, solid or polymer-based. Amperometric and potentiometric sensors respectively give an output current and voltage, proportional to the concentration of the electroactive species at the working electrode with respect to the reference electrode. Often electrochemical cells used in gas sensing also consist of a gas-permeable membrane through which the gas diffuses into the cell and prevents loss of electrolyte from the cell. The gas-permeable membrane or the working electrode can be made selective to certain gases for gas identification [51].

1.3.3. Semiconductor based electronic transduction

Electronic transduction involves the use of semiconducting devices for the sensing of gases. Most of these sensors are based on the principle of reversible gas adsorption at the surface for sensing. Adsorption of a foreign species on the surface of a semiconductor provides surface states,

the electrical properties of these surface states change based on the sorption and/or reaction at the surface. The metal oxide-based sensing devices have been more successfully employed for gas sensing applications than the organic semiconductors and elemental or compound semiconducting counterparts [52]. Commonly used metal oxides for gas sensing include ZnO, TiO_2, SnO_2 and WO_3. When the temperature of these metals is elevated (>300° C), in addition to reacting with the oxygen in the atmosphere, the surface and grain boundary resistance of the oxide is affected by the gas adsorbed on the surface. Intrinsic n-type conductors are suitable for detecting reducing gases and p-type semiconductor are suitable for the detection of oxidizing gases. The metal oxides are usually deposited on a silicon substrate containing a micro heating element to elevate the temperature of the metal oxide. A field-effect transistor (FET) based device has also been of interest for gas sensing applications. A FET is a three-terminal device, a voltage the gate terminal controls the flow of charge carriers from the source terminal to the drain terminal. By using catalytic materials like palladium as the gate material, these FET devices have been shown to produce high sensitivity to Hydrogen and hydrogen-containing gases at high temperatures [53]. Conducting polymer-coated FET devices have gained recent interest for gas sensing applications. This is due to their inherent advantage of room-temperature operation and ease of deposition. Here the gate terminal of the FET is replaced by a gas-sensitive polymer like polypyrrole, polystyrene-co-butadiene or polyvinyl carbazole [54]. Alternatively, the gate-terminal can be constructed using an ion-sensitive electrode, coated with an electrolyte to form the ion-sensitive field-effect transistors (ISFET). ISFETs have the advantage of fast response time and low-temperature operation. These sensors however can only detect gases that are ionic when dissolved in an electrolyte [55].

1.3.4. Dielectric and Mass sensitive transduction

Similar to the semiconducting sensors discussed above, dielectric and mass-sensitive sensors work based on the adsorption to the surface of a gas-sensitive layer. This adsorption changes either the permittivity and mass of the sensor surface and permittivity and/or mass sensitive device transduces this change in mass to some property of the substrate/supporting material. Two of the most common mass-sensitive devices are surface acoustic wave (SAW) devices and microcantilevers. The change in mass is often monitored by measuring the change in the resonant frequency of the device. For maximum sensitivity, the entire SAW device is coated with gas

adsorbing material like polyvinyl alcohol (for humidity sensing) [56]. For the case of a microcantilever, however, only the tip of the cantilever needs to be coated for getting maximum sensitivity [57]. The common dielectric change-based sensors use a direct coating of a resonant element with the gas sensitive material or by using an interdigitated capacitor coated with the gas sensitive material to get the resonant frequency and capacitance change respectively.

1.3.5. Optical transduction

Optical sensors work based on the change of one or more optical properties like transmission and reflection, of visible or near-visible waves, due to the interaction with the gas analyte. Optical transducers for gas sensing usually consist of a monochromatic light source, a waveguiding structure like an optical fibre sensitized with a gas adsorbing material and a detector. The gas adsorbing material may be coated as the cladding of the fibre for transmission-based analysis or the coating may be coated at the end of the fibre reflective property analysis. Both transmissive and reflective properties of the wave depend on the real and imaginary parts of the refractive index of the gas adsorbing material and the gas being analyzed [58]. Other properties that can also be used are fluorescence and chemiluminescence need an indicator medium [59]. Indicator dyes that change optical properties when they react to certain gases, in this case, the optical property of the gas under analysis does not have to be sensitive to be directly sensitive, instead, the compound formed after the reaction of the gas with the dye is what is responsible for the sensing.

1.4. Objectives of the Thesis

As presented in the previous discussions, item-level tagging of food products with wireless sensors that can monitor compositional and environmental parameters play a vital role in the future of sustainable food production and distribution. Tagging of every packaged item using traditional RFID sensors, however, requires expensive integrated chips and sometimes even potentially hazardous built-in batteries. Printable passive, chipless wireless tags show remarkable advantages over such tags in terms of cost and maintenance.

Two approaches are common in passive wireless and chipless sensors. The first is based on the retransmission of the reader signal, and the second is the RCS-based tag. The RCS-backscatter approach on the other hand has the advantage of being considerably smaller in size and requires

narrower bandwidth but suffers from being prone to environmental clutter. Little work has been carried out towards the feasibility of their practical application towards packaged food monitoring. Furthermore, though a number of transduction techniques exist to detect microbial activity directly or indirectly using their chemical bi-products, most of these require active signal conditioning circuitry for their operation. Two techniques can be identified to be amenable for their passive operation and integration into chipless RFID sensors – electrochemical transduction scheme and dielectric change-based capacitive transduction scheme. Capacitive transduction gives frequency modulation based sensing scheme, this provides

Frequency modulation-based sensors is advantageos over amplitude modulation-based sensing because the amplitude measurement suffer from the limitations like sensitivity to measurement distance and multi-path. The sensitivity of passive sensors that work based on frequency modulation is defined as $f_0/\Delta f$, here f_0 is the initial resonant frequency and Δf is the change in resonant frequency for 1 unit change in sensing parameter. Discrete frequency points and Gaussian noise in the interrogated signal affect the accurate detection of the resonant frequency of the signal. A quadratic polynomial-based fit is used to obtain accurately the resonant frequencies of the signal, this gives less stringent requirements on frequency resolution and signal-to-noise [60]. Systemic errors from the reader like the amplitude stability of the integrator oscillator, and scattering from the environment however are much bigger contributors to the errors in discerning resonant frequencies.

The aim, therefore, is to design and develop compact, low-cost wireless-passive sensors that operate in the microwave frequency range giving a longer range than the low-frequency coupled coil passive counterpart and utilize passive transduction like a dielectric or electrochemical scheme for packaged food quality monitoring applications.

Below are the objectives formulated for the thesis-

- Relative humidity is one of the most important components for an extended shelf life of various food items. The first objective of the thesis is to design and build an RCS-based tag with a built-in reference for humidity monitoring. The sensor will utilize a PVA coated interdigitated capacitor and an orthogonally polarized integrated reference operating at two slightly different frequencies providing differential sensing. This gives the sensor immunity to the loading effect

from the immediate environment like the packaging material itself that causes frequency de-tuning and at the same time keeps the sensor compact, which has not been demonstrated before. Together with a time-gated measurement, the clutter rejection capability and its feasibility for packaged food commodity monitoring is studied.

- The second objective is to design and demonstrate the operation of a new sensor design consisting of depolarizing/ cross polarizing scattering elements with acidic/basic gas sensing capability is presented. Depolarizing tags, eliminate the dominant clutter polarized in the direction of the incident interrogating signal. Volatiles like ammonia, hydrogen-sulphide, carbon-di-oxide and acetic acid are produced as gaseous secondary bi-products, resulting from the metabolic actives of micro-organisms in various kinds of food items. A low frequency coupled coil passive pH electrode-based transduction technique for gas monitoring application has been successfully implemented in [15] [61]. Research work is carried out to integrate the pH electrode into the depolarizing tag, giving it a longer range compared to LF coil-based tags.

- Though differential sensing and depolarizing tags offer advantages over traditional chipless sensors, they often require a well-calibrated environment to operate effectively. The third objective of the thesis is to design and demonstrate a novel compact harmonic tag-based pH and volatile sensor. The sensor utilizes a nonlinear element like a diode to generate a harmonic frequency, providing frequency diversity between the interrogator transmitted and received signal. This gives superior detection against environmental clutter and eliminates the need for calibration techniques like background subtraction and other signal processing techniques, that are often necessary for functional detection of chipless tags. The utilization of a single antenna for re-transmission at the doubled frequency and the integration of the sensor into a compact form factor is the novel aspect of this part of the thesis. The application of the sensor in the milk souring process and volatile sensing is also demonstrated, this also a novel aspect.

References

[1] L. Nikkel *et al.*, “The Avoidable Crisis of Food Waste: Roadmap; Second Harvest and Value Chain Management International,” Ontario, 2019.

[2] “Food Waste – City of Toronto.” [Online]. Available: https://www.toronto.ca/services-

payments/recycling-organics-garbage/long-term-waste-strategy/waste-reduction/food-waste/. [Accessed: 25-Mar-2021].

[3] R. S. Singhal, P. R. Kulkarni, and D. V. Rege, *Handbook of indices of food quality and authenticity*. Woodhead Pub, 1997.

[4] L. H. Ledenbach and R. T. Marshall, "Microbiological Spoilage of Dairy Products," in *Compendium of the Microbiological Spoilage of Foods and Beverages*, New York, NY: Springer New York, 2009, pp. 41–67.

[5] A. E. Ghaly, D. Dave, and A. E. Ghaly, "Meat Spoilage Mechanisms and Preservation Techniques: A Critical Review," *Am. J. Agric. Biol. Sci.*, vol. 6, no. 4, pp. 486–510, 2011.

[6] C. Rukchon, A. Nopwinyuwong, S. Trevanich, T. Jinkarn, and P. Suppakul, "Development of a food spoilage indicator for monitoring freshness of skinless chicken breast.," *Talanta*, vol. 130, pp. 547–54, Dec. 2014.

[7] A. Nopwinyuwong, S. Trevanich, and P. Suppakul, "Development of a novel colorimetric indicator label for monitoring freshness of intermediate-moisture dessert spoilage.," *Talanta*, vol. 81, no. 3, pp. 1126–32, May 2010.

[8] "ChainLink Research : Research :The Future of RFID." [Online]. Available: http://www.chainlinkresearch.com/research/detail.cfm?guid=B28189C8-3048-79ED-9940-3594856D6F93. [Accessed: 09-Feb-2016].

[9] M. Engin, A. Demirel, E. Z. Engin, and M. Fedakar, "Recent developments and trends in biomedical sensors," *Measurement*, vol. 37, no. 2, pp. 173–188, Mar. 2005.

[10] A. Loutfi, S. Coradeschi, G. K. Mani, P. Shankar, and J. B. B. Rayappan, "Electronic noses for food quality: A review," *J. Food Eng.*, vol. 144, pp. 103–111, Jan. 2015.

[11] E. Romero, R. O. Warrington, and M. R. Neuman, "Energy scavenging sources for biomedical sensors.," *Physiol. Meas.*, vol. 30, no. 9, pp. R35-62, Sep. 2009.

[12] J. K. S. Karmakar, Nemai Chandra, Emran Md Amin, Ed., *Chipless RFID Sensors*. John Wiley & Sons, 2015.

[13] S. Bhadra, "Electrode-based wireless passive pH sensors with applications to bioprocess and food spoilage monitoring," Elsevier, 2011.

[14] B. E. Horton, S. Schweitzer, A. J. DeRouin, and K. G. Ong, "A Varactor-Based, Inductively Coupled Wireless pH Sensor," *IEEE Sens. J.*, vol. 11, no. 4, pp. 1061–1066, Apr. 2011.

[15] S. Bhadra, G. E. Bridges, D. J. Thomson, and M. S. Freund, "Electrode Potential-Based

Coupled Coil Sensor for Remote pH Monitoring," *IEEE Sens. J.*, vol. 11, no. 11, pp. 2813–2819, Nov. 2011.

[16] E. Perret, *Radio Frequency Identification and Sensors: From RFID to Chipless RFID*. John Wiley & Sons, 2014.

[17] "CC3200 Application notes, User guides, Selection guides, Solution guides, White papers, Design files, More literature, Blogs." [Online]. Available: http://www.ti.com/product/CC3200/technicaldocuments. [Accessed: 15-Dec-2017].

[18] "Wireless Sensor Tag." [Online]. Available: http://wirelesstag.net/specs.html. [Accessed: 15-Dec-2017].

[19] R. M. Ferdous, A. W. Reza, and M. F. Siddiqui, "Renewable energy harvesting for wireless sensors using passive RFID tag technology: A review," *Renew. Sustain. Energy Rev.*, vol. 58, pp. 1114–1128, May 2016.

[20] C. Mandel, M. Schussler, M. Maasch, and R. Jakoby, "A novel passive phase modulator based on LH delay lines for chipless microwave RFID applications," in *2009 IEEE MTT-S International Microwave Workshop on Wireless Sensing, Local Positioning, and RFID*, 2009, pp. 1–4.

[21] C. Mandel, H. Maune, and M. Maasch, "Passive wireless temperature sensing with BST-based chipless transponder," in *German Microwave Conference (GeMIC)*, 2011.

[22] M. Schueler, C. Mandel, M. Puentes, and R. Jakoby, "Metamaterial Inspired Microwave Sensors," *IEEE Microw. Mag.*, vol. 13, no. 2, pp. 57–68, Mar. 2012.

[23] B. Kubina, C. Mandel, M. Schussler, M. Sazegar, and R. Jakoby, "A wireless chipless temperature sensor utilizing an orthogonal polarized backscatter scheme," in *2012 42nd European Microwave Conference*, 2012, pp. 61–64.

[24] S. Harma, W. G. Arthur, C. S. Hartmann, R. G. Maev, and V. P. Plessky, "Inline SAW RFID tag using time position and phase encoding," *IEEE Trans. Ultrason. Ferroelectr. Freq. Control*, vol. 55, no. 8, pp. 1840–1846, Aug. 2008.

[25] J.-H. Sun *et al.*, "Wireless Saw-Based Tags with Temperature Sensors that Utilize High-Resolution Delay-Time Measurements," *J. Mech.*, vol. 32, no. 04, pp. 435–440, Aug. 2016.

[26] J. L. Volakis, C.-C. Chen, and K. (Kyōhei) Fujimoto, *Small antennas : miniaturization techniques & applications*. McGraw-Hill, 2010.

[27] J. G. D. Hester and M. M. Tentzeris, "Inkjet-Printed Flexible mm-Wave Van-Atta

Reflectarrays: A Solution for Ultralong-Range Dense Multitag and Multisensing Chipless RFID Implementations for IoT Smart Skins," *IEEE Trans. Microw. Theory Tech.*, vol. 64, no. 12, pp. 4763–4773, Dec. 2016.

[28] J. A. Vitaz, A. M. Buerkle, M. Sallin, and K. Sarabandi, "Enhanced Detection of On-Metal Retro-Reflective Tags in Cluttered Environments Using a Polarimetric Technique," *IEEE Trans. Antennas Propag.*, vol. 60, no. 8, pp. 3727–3735, Aug. 2012.

[29] R. F. Harrington, "Small Resonant Scatterers and Their Use for Field Measurements," *IEEE Trans. Microw. Theory Tech.*, vol. 10, no. 3, pp. 165–174, May 1962.

[30] R. F. Harrington, "Field Measurements Using Active Scatterers (Correspondence)," *IEEE Trans. Microw. Theory Tech.*, vol. 11, no. 5, pp. 454–455, Sep. 1963.

[31] J. Kimionis, M. M. Tentzeris, A. Georgiadis, and A. Collado, "Inkjet-printed reflection amplifier for increased-range Backscatter radio," *Eur. Microw. Week 2014 Connect. Futur. EuMW 2014 - Conf. Proceedings; EuMC 2014 44th Eur. Microw. Conf.*, vol. 1, pp. 5–8, 2014.

[32] F. Amato, C. W. Peterson, M. B. Akbar, and G. D. Durgin, "Long range and low powered RFID tags with tunnel diode," *2015 IEEE Int. Conf. RFID Technol. Appl. RFID-TA 2015*, pp. 182–187, 2016.

[33] F. Farzami, S. Member, S. Khaledian, and S. Member, "Reconfigurable Dual-Band Bidirectional Reflection Amplifier With Applications in Van Atta Array," vol. 65, no. 11, pp. 1–10, 2017.

[34] P. Chan and V. Fusco, "Bi-Static 5.8 GHz RFID Range Enhancement using Retrodirective Techniques," no. October, pp. 976–979, 2011.

[35] A. Vena, E. Perret, and S. Tedjni, "A depolarizing chipless RFID tag for robust detection and its FCC compliant UWB reading system," *IEEE Trans. Microw. Theory Tech.*, vol. 61, no. 8, pp. 2982–2994, 2013.

[36] O. Rance, R. Siragusa, P. Lemaitre-Auger, and E. Perret, "RCS magnitude coding for chipless RFID based on depolarizing tag," *2015 IEEE MTT-S Int. Microw. Symp. IMS 2015*, pp. 2–5, 2015.

[37] F. Costa, S. Genovesi, and A. Monorchio, "Chipless RFIDs for Metallic Objects by Using Cross Polarization Encoding," *IEEE Trans. Antennas Propag.*, vol. 62, no. 8, pp. 4402–4407, Aug. 2014.

[38] C. Cho, X. Yi, D. Li, Y. Wang, and M. M. Tentzeris, "Passive Wireless Frequency Doubling Antenna Sensor for Strain and Crack Sensing," *IEEE Sens. J.*, vol. 16, no. 14, pp. 5725–5733, 2016.

[39] V. Palazzi *et al.*, "Demonstration of a chipless harmonic tag working as crack sensor for electronic sealing applications," *Wirel. Power Transf.*, pp. 1–8, Oct. 2015.

[40] H. Huang, P.-Y. Chen, C.-H. Hung, R. Gharpurey, and D. Akinwande, "A zero power harmonic transponder sensor for ubiquitous wireless μL liquid-volume monitoring.," *Sci. Rep.*, vol. 6, p. 18795, Jan. 2016.

[41] B. Kubina, C. Mandel, M. Sch, R. Jakoby, M. Schussler, and R. Jakoby, "Compact Quasi-Chipless Harmonic Radar Sensor with a Dielectric Resonator Antenna," *2015 IEEE MTT-S Int. Microw. Symp. IMS 2015*, pp. 2–4, Jul. 2015.

[42] B. Kubina, J. Romeu, C. Mandel, M. Schüßler, and R. Jakoby, "Quasi-chipless wireless temperature sensor based on harmonic radar," *Electron. Lett.*, vol. 50, no. 2, Jan. 2014.

[43] V. Viikari, H. Seppä, T. Mattila, and A. Alastalo, "Wireless Ferroelectric Resonating Sensor," *IEEE Trans. Ultrason. Ferroelectr. Freq. Control*, vol. 57, no. 4, pp. 785–791, Apr. 2010.

[44] A. Lazaro, R. Villarino, and D. Girbau, "A Passive Harmonic Tag for Humidity Sensing," *Int. J. Antennas Propag.*, vol. 2014, pp. 1–11, 2014.

[45] N. Tahir and G. Brooker, "Toward the Development of Millimeter Wave Harmonic Sensors for Tracking Small Insects," vol. 15, no. 10, pp. 5669–5676, 2015.

[46] B. G. Colpitts and G. Boiteau, "Harmonic Radar Transceiver Design : Miniature Tags for Insect Tracking," vol. 52, no. 11, pp. 2825–2832, 2004.

[47] K. B. Biji, C. N. Ravishankar, C. O. Mohan, and T. K. Srinivasa Gopal, "Smart packaging systems for food applications: a review," 2015.

[48] Y. W. Park, S. M. Kim, J. Y. Lee, and W. Jang, "Application of biosensors in smart packaging," *Mol. Cell. Toxicol.*, vol. 11, no. 3, pp. 277–285, Sep. 2015.

[49] J. R. Stetter and J. Li, "Amperometric gas sensors--a review.," *Chem. Rev.*, vol. 108, no. 2, pp. 352–66, Feb. 2008.

[50] U. Guth, F. Gerlach, M. Decker, W. Oelßner, and W. Vonau, "Solid-state reference electrodes for potentiometric sensors," *J. Solid State Electrochem.*, vol. 13, no. 1, pp. 27–39, 2009.

[51] R. O. Ansell and A. McNaughtan, "Electrochemical sensors," in *Sensor Systems for Environmental Monitoring*, Dordrecht: Springer Netherlands, 1997, pp. 100–126.

[52] A. M. Azad, S. A. Akbar, S. G. Mhaisalkar, L. D. Birkefeld, and K. S. Goto, "Solid-State Gas Sensors: A Review," *J. Electrochem. Soc.*, vol. 139, no. 12, p. 3690, 1992.

[53] J. A. Covington, J. W. Gardner, D. Briand, N. F. Rooij, and N. F. De Rooij, "A polymer gate FET sensor array for detecting organic vapours," *Sensors Actuators B Chem.*, vol. 77, no. 1–2, pp. 155–162, Jun. 2001.

[54] J. A. Covington, J. W. Gardner, P. N. Bartlett, and C.-S. Toh, "Conductive polymer gate FET devices for vapour sensing," *IEE Proc. - Circuits, Devices Syst.*, vol. 151, no. 4, p. 326, 2004.

[55] C. Jimenez-Jorquera, J. Orozco, and A. Baldi, "ISFET Based Microsensors for Environmental Monitoring," *Sensors*, vol. 10, pp. 61–83, 2010.

[56] C. Caliendo *et al.*, "Advances in SAW-based gas sensors," *Smart Mater. Struct.*, vol. 6, no. 6, pp. 689–699, Dec. 1997.

[57] Wu Pan and Ning Li, "Micro-cantilever array and its application in gas sensor," in *2008 International Conference on Microwave and Millimeter Wave Technology*, 2008, pp. 1547–1550.

[58] J. Hodgkinson and R. P. Tatam, "Optical gas sensing: a review," *Meas. Sci. Technol. Meas. Sci. Technol*, vol. 24, no. 24, pp. 12004–59, 2013.

[59] J. R. Bates and M. Campbell, "Gas sensors and analysers," in *Sensor Systems for Environmental Monitoring*, Dordrecht: Springer Netherlands, 1997, pp. 127–178.

[60] M. P. Robinson and J. Clegg, "Improved determination of Q-factor and resonant frequency by a quadratic curve-fitting method," *IEEE Trans. Electromagn. Compat.*, vol. 47, no. 2, pp. 399–402, May 2005.

[61] S. Bhadra, "Coupled Resonant Coil Sensors for Remote Passive Monitoring Applications," University of Manitoba, 2010.

Chapter 2.

Wireless Passive Sensors for Food Quality Monitoring

This chapter presents a literature survey of wireless passive sensors in packaged food monitoring applications. It also incorporates the results of chapters 3 and 4 for comparison to coupled coil sensors and the state-of-the-art passive ultra-high-frequency (UHF) sensors. This chapter is based on the published article "**R. Raju,** G. E. Bridges, and S. Bhadra, "Wireless passive sensors for food quality monitoring: Improving the safety of food products," *IEEE Antennas Propag. Mag.*, vol. 62, no. 5, pp. 76–89, Oct. 2020.". It should be noted that section 2.3 of the chapter was contributed by the third author.

2.1. Abstract

Food waste amounts to roughly one-third of its total production every year. There is an unprecedented demand to improve long-term storage of food products while preserving quality and safety in every stage of its processing, from post harvesting to pre-consumption. Different technologies, such as total viable count (TVC), metal oxide semiconductor sensors, fluorescence spectroscopy, dye and polymer-based colorimetric sensors, as well as RFIDs, are currently applied for monitoring food products. This article provides an overview of current developments in near-field and UHF wireless passive sensors for monitoring of food quality indices and food spoilage indicators. Solutions based on coupled-coil resonator and UHF chipless RFID sensors with application to bacterial-count detection, volatile gas concentration, humidity and pH monitoring are highlighted.

2.2. Introduction

Food quality is an important issue for both the consumer and the food processing industry. Spoiled food is not only a human health concern, but it also causes major economic loss due to food wastage [1], [2]. In the present day, distance between consumer and production zone is increasing leading to a complex supply and management requirement. Therefore, new methods for preserving and monitoring food quality is needed. Traditionally, food packaging is only used for

protection, convenience and containment of food products, and the packaging materials are made to have minimal interaction with the food materials. Smart packaging techniques, on the other hand, are designed to interact with the food material and its packaged environment in order to provide an extended shelf life of the food products. The shelf life of food is dictated by one or more quality indicators such as colour, texture, odor or micro-organism count [1]. Environmental factors that affect food quality are temperature, humidity, light, mechanical stress and pressure. Smart food packaging focuses on keeping these factors at optimal levels using active and/or intelligent packaging techniques. Active packaging or modified atmosphere packaging employs strategies like temperature control, oxygen removal using oxygen scavengers, carbon dioxide control using absorbers and emitters, moisture control using moisture absorbing pads or desiccants, the addition of chemicals to change the internal parameters of the food product like its pH, and the use of antimicrobial coatings to retard microbial growth in the package [2]. Intelligent packaging focuses mainly on the ability to monitor the conditions of packaged food or its environment. It adds the functionality of detection, sensing and recording of the conditions and quality indicators in which the food is stored. Common indicators include freshness indicators, time-temperature indicators and integrity indicators to detect leaks. Of all the parameters of interest, humidity (water activity), temperature and pH have been identified to be the three most crucial factors affecting food quality [1]. These three factors, when monitored and controlled for each specific food commodity, have shown to significantly increase shelf life.

In addition to environmental parameters, biosensors, gas sensors and chemical sensors can be employed for early pathogenic activity detection in packaged food. Biosensors detect biological reactions using bioreceptors incorporating specific antibodies to detect target analytes or pathogens [3]. The activity of pathogens also produces chemical bi-products as acidic or basic chemicals namely, lactic acid, acetic acid or basic amines which can also be detected [4], [5], [6], [7]. Many of the biproducts are volatile in nature and thus gas sensors, which offer contactless monitoring, have been used as an alternative solution as an index of food quality. For instance, in spoilage of meat products three main mechanisms occur - microbial spoilage, lipid oxidation and autolytic enzymatic spoilage [5]. Microbial spoilage involves the action of micro-organisms like various molds and bacteria species. The breakdown of the proteins (protein degradation) and fats (lipid oxidation) results in the production of new compounds which changes the meat flavor, odour and texture. The action of common microorganisms in meat, such as *Enterobacteriaceae*,

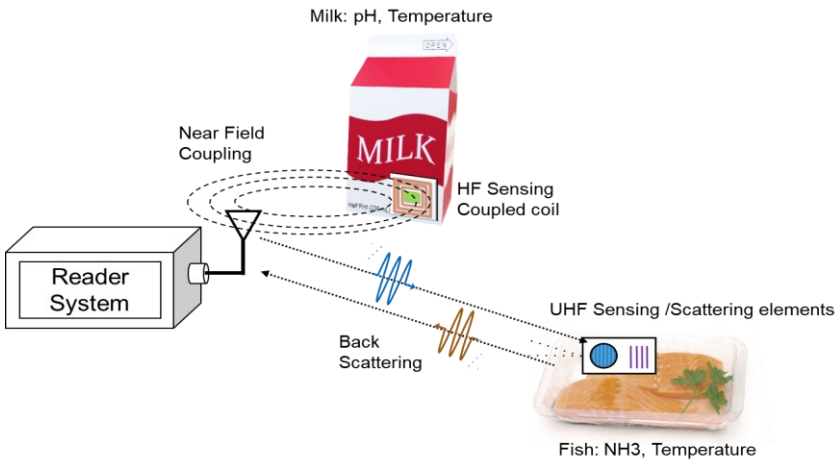

Fig. 2.1 Passive wireless sensor system concepts for packaged food monitoring

Pseudomonas fluorescens and *Lactobacillus sake* have been shown to produce various volatile compounds like sulfur-containing molecules, alcohols, acetone, fatty acids, amines and carbon-dioxide [5]. Similarly, foods rich in carbohydrates such as desserts are broken down into simpler molecules like organic acids, ethanol and CO_2 due to microbial action [6]. Total volatile base nitrogen (TVB-N) and trimethylamine (TMA) are used worldwide as indicators of fish quality and decomposition [7]. The detection of spoilage due to microbial action using its volatiles in different kinds food can be very distinct from one another. It is important to note that gas sensors give quantitative information on pathogenic activity by indirectly sensing the gaseous bi-products resulting from their metabolic activity [8].

Several different transduction schemes can be employed for food quality monitoring, namely, electrochemical [9], [10], electronic [11], mass sensitive and optical. Optical transducers are based on indicator dyes that change one or more optical properties such as color, fluorescence and chemiluminescence when they react to specific analytes [12]. pH-sensitive dye and polyaniline (PAni) colorimetric sensors have been demonstrated for monitoring spoilage of Cod, Cardinal, Round nose grenadier and milk, fish [13], [14]. These sensors change color in response to the TVB-N level in the package headspace. Electrochemical sensors typically employ amperometric [9] or potentiometric approaches [10]. These sensors make use of charge transfer between a solid or liquid electrolyte and an electrode and give an output current or voltage proportional to the concentration of the electroactive species at the working electrode with respect to a reference electrode. As the electrodes are in contact with the food material biocompatibility must be addressed. Most electronic transduction sensors are based on a field-effect transistor (FET)

Table 1.1

Comparison of wireless sensing modalities.

Passive Sensing Technology	Visual Access	Typical Range	Reader Technology	Tag Cost	Calibration Required
Optical colorimetric	Yes	Line of sight	Camera	Low	Yes
Active RFID	No	> 10 m	RF Transceiver	High	No
HF - passive RFID	No	0.1-0.5 m	NFC Devices	Medium	No
HF - LC resonator	No	2-5 cm	Impedance Analyzer	Low	Yes
UHF- passive RFID	No	10 m	Commercial hardware	Medium	No
UHF- chipless RFID	No	0.2-0.5 m	Custom RF Electronics	Low	Yes

structure where the gate is a chosen material or functionalized surface for adsorption of a specific gas or analyte [15], [16]. Monitoring change in permittivity and conductivity of food material or gas-sensitive polymers is another common transduction scheme that is widely used [17].

The advancements in printed electronics and material science have led to the easy integration of different transduction mechanisms into wireless sensors [18]. RFID sensors are categorized as active RFID, passive RFID or chipless RFID. Active RFID sensors are finding increased use in food-chain monitoring as data loggers, most commonly tracking temperature (time-temperature indicators) [19]. They can operate over long distances but require a battery and are expensive. Passive wireless sensors, on the other hand, do not require a battery, thereby, making them low cost and environment friendly. Such sensors present new opportunities in low-cost food quality monitoring. Based on whether they have an integrated circuit (IC), these can be classified as chip-based or chipless sensors. Chip-based passive sensors acquire power required for activation through energy harvesting or from the reader [20]. Commercial RFID tags utilize this approach [21]. Chipless radio frequency sensors do not employ ICs and offer the benefits of longer life and lower cost. Passive RFID sensors are also compatible with planar technology allowing them to be produced by roll-to-roll processing, decreasing the unit cost. Fig. 2.1 shows the generalized concept of different passive sensing systems for packaged food monitoring.

Table 1.1 shows a comparison of different sensing modalities used for food quality monitoring. Depending on the modality, architecture, complexity and system requirements differ. High-frequency passive RFID is compatible with many commercially available readers including NFC enabled devices such as smartphones. For sensing applications, additional electronics are incorporated within the RFID increasing their cost. The sensing electronics typically do not need

calibration. High-frequency LC resonator-based sensors require measuring the impedance characteristics of the tag. Expensive and operationally complex impedance analyzing electronics is typically required to receive/analyze the data. Recently, however, low-cost passive LC resonator readers have emerged [22], [23]. LC-resonator sensors provide quantitative measurement (of pH, permittivity, bacteria count change, etc.) of the food, but can be affected by environment parameters and require calibration. Typically, during food spoilage or quality monitoring, high-frequency passive RFID sensors measure volatiles or analytes in food package whereas the LC resonator-based sensors measure dielectric permittivity. Chip-based passive UHF RFID systems are a mature technology and have been widely commercialized for asset tracking applications. In addition to the power, processing and modulation circuitry, additional active sensing components can be integrated for sensing applications. This makes them comparatively more expensive. Chipless RFID on the other hand mainly relies on passive transduction mechanisms, like dielectric or capacitance change, for their operation making them less expensive. The readers for chipless RFID, however, require complex and specialized architectures based on their mode of operation. Examples of reader architectures include time delay/pulse position based readers [24], UWB impulse radar-based readers [25], frequency domain readers for multi-resonant tags [26] and synthetic-aperture radar imaging based readers [27]. A detailed review and comparison of different chipless RFID systems can be found in [28].

In this chapter an overview of current developments in HF and UHF wireless passive sensors for monitoring food quality indices and food spoilage is provided. HF passive sensors, as categorized depending on their principle of operation and presence of chip, are described in the following sections. For UHF passive sensors, the development and applications of chipless UHF sensors to food monitoring are highlighted. For both HF and UHF passive sensors, effect of humidity, temperature and distance between sensor and reader is discussed along with prospects and challenges for future commercialization of wireless passive food sensors.

2.3. High-Frequency Passive Sensors

A complete HF passive sensor system consists of a reader such as a smartphone and a responder such as a sensor tag. The reader wirelessly energizes the sensor tag and reads data from the sensor

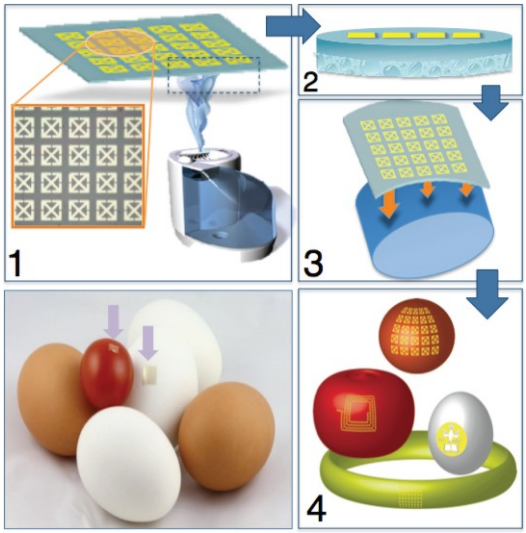

Fig. 2.2 Schematic of steps for wrapping and adhering silk LC resonators onto foods. 1) Water vapor is exposed to the back of non-crystalline functionalized silk films, resulting in 2), a functionalized film in which the back surface of the film is partially melted and acting as glue. 3) This melted surface is conformally applied to arbitrary surfaces with gentle pressure, resulting 4), applied functional sensors on a variety of food [29]. [© 2012 WILEY-VCH Verlag GmbH & Co. KGaA, Weinheim]

tag through inductive coupling. HF passive food sensors can be categorized into three classes depending on their principle of operation.

2.3.1. LC resonators measuring dielectric permittivity.

These sensors consist of a simple inductor-capacitor (LC) resonator. The resonator's capacitor is proximity coupled to the food item so that it is dependent on the dielectric permittivity of the food. As food ripens and spoils, its chemical composition changes resulting in change in its dielectric properties [17]. This changes the coupled capacitance, and in turn the resonant frequency of the sensor. These sensors are either attached to food package or placed on the surface of the food itself. The approach has been demonstrated using conformal adhesive LC resonators attached on the surface of a banana skin or cheese surface [29], as a 3-D printed LC resonator integrated in a milk package cap [30], and as a planar LC resonator attached to a milk package surface [31].

For example, researchers have developed LC resonators on a biocompatible flexible silk substrate which can be directly adhered on the food surface [29]. In [26] the fabrication processes of the planar LC resonators by patterning gold on silk substrate is described which are based on

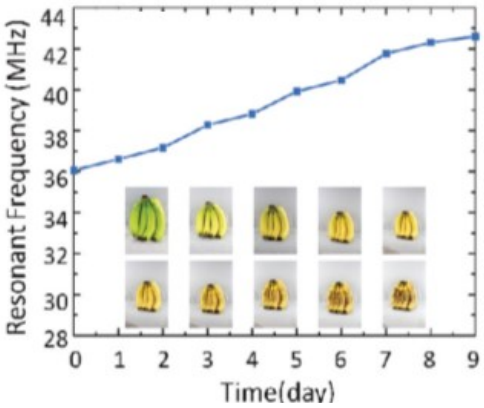

Fig. 2.3 Measured resonant frequency the during banana ripening process. Conducted at room temperature (22° C) with a relative humidity of 30% [29]. [© 2012 WILEY-VCH Verlag GmbH & Co. KGaA, Weinheim]

transferring gold patterns onto silk substrates using inkjet printing, shadow mask deposition, silk transfer micropatterning, or contact transfer which directly transfers nano-patterns from a donor substrate onto the silk substrate [29]. Methods to conformally wrap the sensor on a non-planar surface and then adhere to the food surface have also been developed. Fig. 2.2 shows the schematic of the wrapping and adhering process. The conformal LC resonator sensor closely interacts with the food underneath it. The depth of interaction between the food and sensor (penetration depth) depends on the operating frequency of the sensor, electric conductivity and dielectric polarization loss of the food. For high loss-tangent materials the penetration depth is inversely proportional to the square root of the operating frequency of the sensor. Hence, for sensors operating at HF-frequencies the fields will penetrate well below the surface of the food. Fig. 2.3 shows how the resonant frequency of a 36 MHz LC-resonator sensor changes during the banana ripening process [29]. Impedance changes were measured using a coil connected to a network analyzer as the reader. Bananas were initially green and underwent transition to yellow and then brown appearance over a 9-day period. A significant (20%) change in resonant frequency was observed, showing the potential of dielectric based food quality sensing. These types of sensors have also been used to detect food dielectric changes due to bacterial growth in cheese and in milk spoilage.

2.3.2. Passive RFID based HF sensor.

The use of HF passive RFID sensors for monitoring food spoilage or quality typically employs monitoring the volatiles produced in the food package or monitoring analytes, such as pH or KCl,

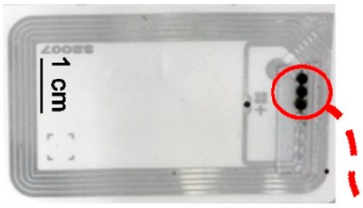

Fig. 2.4 Modified commercial RFID tag with printed PTS-PAni layer [34]. [© 2018 American Chemical Society]

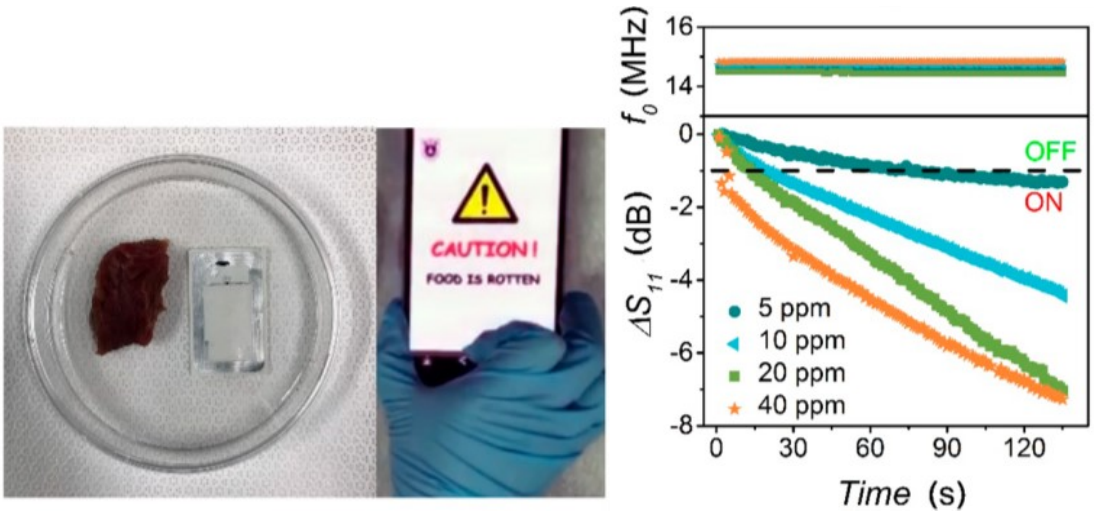

(a) **(b)**

Fig. 2.5 (a) The real-time responses of sensor in terms of S_{11} and f_0 towards 5, 10, 20, and 40 ppm of NH_3. (b) The sensor's application for meat spoilage monitoring [34]. [© 2018 American Chemical Society.]

in the food solution [32] [33] [34] [35]. Researchers have approached this by either modifying commercial RFID tags with gas or analyte sensing polymer coatings [34], [32], or using custom made RFID tags with an interface to a polymer-based gas sensing resistive circuit or to analyte sensing electrodes [33], [35]. In [34] the group developed an ammonia sensitive PTS−PAni layer that is inkjet printed on the coils of a commercial RFID tag. Fig. 2.4 shows the modified commercial RFID tag with a printed PTS-PAni layer (black dots in the figure). The sensor employs the large change in electrical properties of the PTS-PAni coating when exposed to TVB-N. Under ambient, low TVB-N, conditions the coating conductivity is high, this acting to produce a large shunt conductance between the tag coils, dramatically reducing its Q-factor. When exposed to

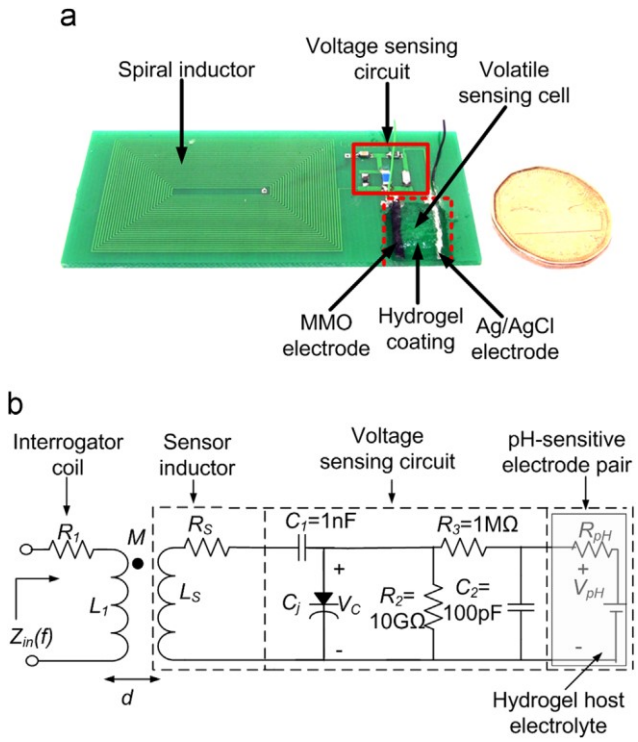

Fig. 2.6 (a) Prototype volatile absorption sensor with hydrogel coated MMO and Ag/AgCl electrodes. (b) An equivalent circuit diagram of the sensor [8]. [© 2014 Elsevier B.V.]

amine gas the PAni changes to an insulating state, and the Q-factor is increased. The researchers used this to develop an Off-to-On tag where the impedance mismatch of the coil-tag IC is used to monitor TVB-N threshold level using a smartphone NFC reader. Under low TVB-N condition, when the food is safe, the coil is mismatched and the tag can not respond to the reader. As food spoils TVB-N concentration in its package gradually increases, reducing the mismatch, and at a certain threshold the tag turns on and can respond to the reader. The researchers have demonstrated the applicability of this sensor for meat spoilage monitoring [34]. Fig. 2.5 shows the sensor's response (S11 at the reader measured using a network analyzer) for different concentration of NH_3.

2.3.3. LC resonator measuring volatiles.

Based on an LC-resonator approach, sensors for monitoring volatiles or pH in food products has been developed by the authors. A hydrogel coated pH-electrode-based near-field passive wireless sensor for determining acidic and basic volatile concentration is described in [36]. The sensor has been applied to detection of fish spoilage by measuring TVB-N levels [8]. The prototype sensor

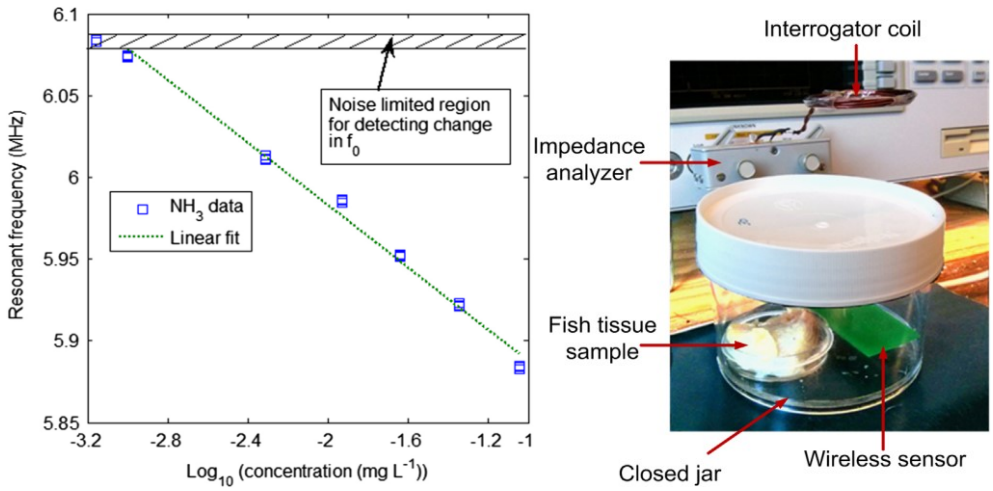

(a) **(b)**

Fig. 2.7 (a) Resonant frequency of the sensor after reaching equilibrium state as a function of NH_3 concentration at 24°C (20mins. after initial exposure to each concentration of NH_3. (b) Experimental setup for wireless tilapia spoilage test. A 25 g tissue sample of fish and the wireless sensor are placed in a jar. The sensor's resonant frequency is measured using the interrogator coil connected to an impedance analyzer [8]. [© 2014 Elsevier B.V.]

consists of two parts, a hydrogel coated pH-electrode pair and a varactor-based passive LC-resonator. For the hydrogel coated pH electrode, a mixed metal oxide (MMO) pH sensitive electrode and silver/silver chloride (Ag/AgCl) reference electrode are coated with a thin layer of hydrogel. The hydrogel acts to contain the electrolyte [8]. The sensor, shown in Fig. 2.6a, is designed to have a resonant frequency near 6 MHz and was fabricated with a rectangular coil inductor, surface-mount capacitors, resistors and a varactor. An equivalent circuit diagram of the sensor is shown in Fig. 2.6b. The coil inductor is connected in parallel with a varactor-based voltage sensing circuit and a hydrogel coated pH-sensitive electrode pair. L_S is the inductance of the spiral inductor. Basic or acidic volatiles produced in a closed environment due to food spoilage are absorbed by the hydrogel. As a result, the hydrogel pH changes which in turn changes the voltage, V_{pH}, across the pH-sensitive electrode pair. The varactor capacitance, $C(V_{pH})$, changes in response to the low frequency change of the biasing voltage. The spiral inductor and capacitor form a resonant circuit with a resonant frequency, f_0,

$$f_0 = \frac{1}{\sqrt{L_S C(V_{pH})}} \quad .$$

In this manner the sensor's resonant frequency is directly related to the basic volatile absorbed by the hydrogel. This corresponds to the volatile concentration in the package and the microbial count generating the volatile. For fish spoilage monitoring the sensor needs to respond to NH_3. Fig. 2.7a shows the sensors resonant frequency response for different concentration of NH_3. The response time of the sensor is 20 mins. This response time is adequate for fish spoilage monitoring as the increase TVB-N in a fish package occurs over a period of several hours to days. The resonant frequency has a linear relationship with the logarithm of NH_3 concentration. The NH_3 concentration can be measured with an accuracy of 13% and the detection limit of NH_3 is 0.001 mgL^{-1}.

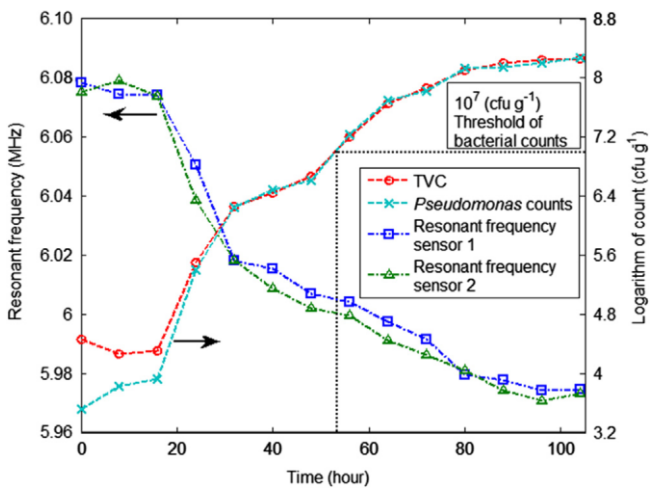

Fig. 2.8. Resonant frequency of the sensor and bacterial population in fresh tilapia kept at 4ºC over a period of 4.5 days. Bacterial data are the average of two replicates [8]. [© 2014 Elsevier B.V.]

The sensor was used to measure spoilage of Tilapia fish in an enclosed environment as shown in Fig. 2.7b [8]. Fig. 2.8 shows the change in the sensor's resonant frequency as volatile basic nitrogen (TVB-N) was produced in the fish package as it spoiled. The fish spoilage trials were performed at 4ºC, similar to storage conditions. For each of the two trials, the sensors response was correlated directly with the bacterial population in the fish (by TVC and *Psedudomonas* count as evaluated using standard microbial counting methods). Comparison of the sensor response and bacterial count results, as shown in Fig. 2.8, demonstrate that the sensor can accurately track spoilage effectively and can distinctly identify the TVC and Pseudomonas value of 10^7 cfu g^{-1},

which is defined as the safe spoilage level for fish. This demonstrates that these types of sensors can provide quantitative measurements of bacteria count.

A similar version of the sensor, shown in Fig. 2.9, was used for monitoring pH in liquid products. In this application the hydrogel electrolyte is removed and the sensor is encapsulated to make it biocompatible and insensitive to the liquid dielectric loading [34]. The sensor was used for monitoring milk spoilage as shown in Fig. 2.9.

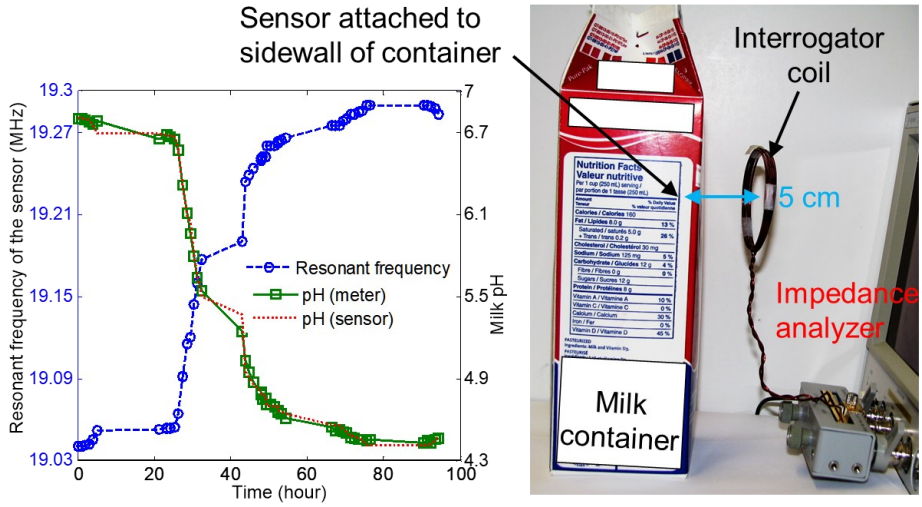

(a) **(b)**

Fig. 2.9 Resonant frequency response of embedded sensor and pH measured over 4 days for milk left at room temperature. (b) Milk container with encapsulated sensor inside measured with an impedance analyser at 5 cm distance [37].

2.4. UHF Sensors for Food Quality Monitoring

Passive RFIDs are powered by the reader, where the incident signal is rectified and used to power the active electronics (an integrated circuit bonded to a tag antenna) that stores the sensor ID and possibly sensing functions. The electronics modulates the tag antenna impedance so that the backscattered signal is encoded with the ID/sensor information [38]. Passive RFID with temperature sensing capability, [39], [40], are suited for food monitoring. Additional circuitry for sensing increases the cost and reduces the read range of these sensors. A detailed review of chipped RFID based sensors with application in the food industry can be found in [41]. Hybrid approaches have been proposed in [42], [43] for monitoring of pork and wine. These sensors use the detuning

effect between the RFID antenna and chip due to dielectric change of the food commodity for monitoring its quality. Similar techniques are used in [44], [45] for gas-based sensors where a gas-sensitive polymer is selectively coated on the RFID antenna, which intern detunes the antenna impedance. Commercial RFID tags for moisture sensing applications employ technique [46].

Chipless UHF sensors do not employ active electronics to modulate/encode the backscattered signal, instead, they use variations of their frequency response amplitude/phase, induced by passive resonances or discontinuities in transmission lines, for their operation. Even though UHF chipless sensor technology has the potential to be very inexpensive, it is still in its infancy, requires custom readers and its application to food monitoring is just being explored. Chipless UHF sensors operate in the far-field or radiative near-field region enabling increased interrogation distance as compared with their HF counterparts, which use coupled coils. Additionally, UHF (SHF) frequencies enable the use of multi-resonator elements and distributed element printed planar technologies. A review and comparison between chipped and chipless UHF RFID sensors is provided in [47]. In the following sections, we concentrate on chipless UHF sensors as possible candidates for food monitoring.

2.4.1. Chipless UHF Sensors

Chipless UHF sensors operate using retransmission or radar cross-section backscattering approaches. In the retransmission approach, as shown in Fig. 2.10, wideband antennas receive and retransmit (usually with orthogonal polarizations) the reader signal. Resonant elements, such as

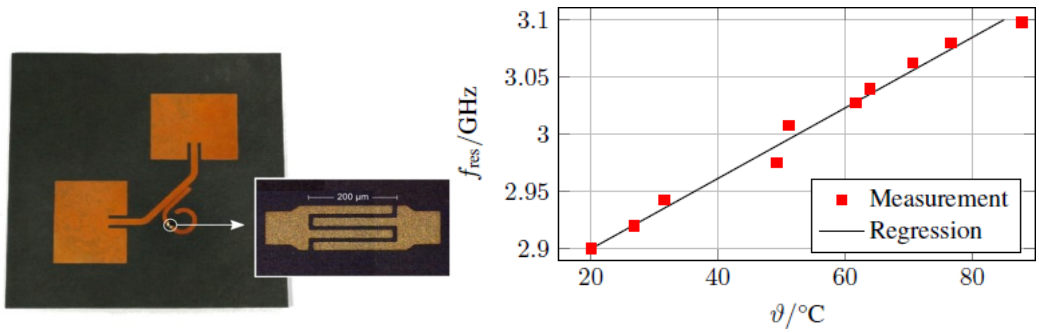

(a) **(b)**

Fig. 2.10 (a) Retransmission based sensing in time domain with single BST resonator for temperature sensing. (b) Measured resonant frequency of the sensor for various temperature conditions [51]. [©2012 IEEE]

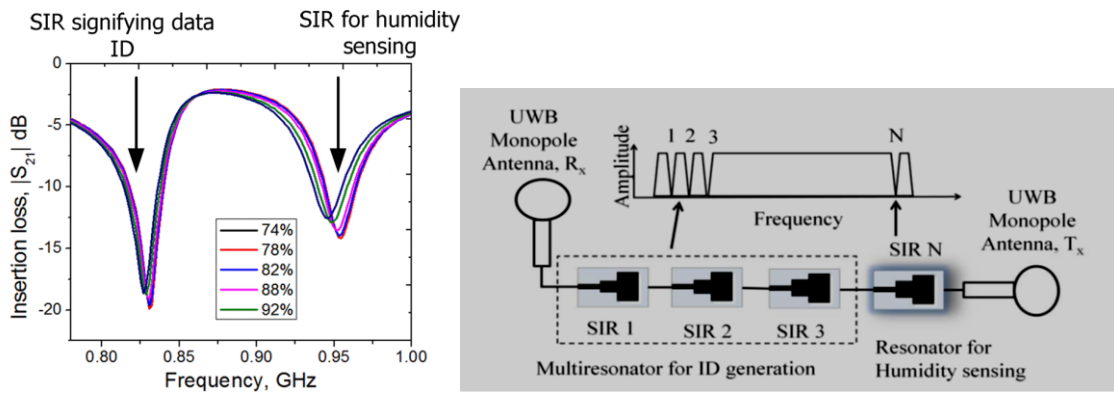

(a) **(b)**

Fig. 2.11 (a) Stepped impedance resonator for humidity sensing (b) measured insertion loss of the sensor corresponding to different humidity conditions [52] [©2012 IEEE]

stub resonators [48], split-ring resonators and spiral resonators [49] are inserted in the transmission path producing a frequency-dependent response. The resonators can be functionalized using coatings to sense humidity [49], or temperature [50] changes for example. The tag shown in Fig. 2.10, suited to food storage monitoring, uses a stub resonator with a Barium-Strontium-Titanate (BST) coated capacitor for sensing temperature changes [51]. Extension of this concept for simultaneous sensing and identification employs a multiple series of stepped impedance resonators, as shown in Fig. 2.11 [52]. Here, one of the resonators is reserved for humidity sensing using a Kapton polyamide coating while the other resonators retain a fixed frequency representative of the sensor ID. Time-domain sensors employing ultra-wideband (UWB) antennas connected to transmission lines of different lengths have also been explored [53]. Here a transmission line is loaded with a thermistor to produce a temperature-dependent delay. A UWB monopole antenna connected to a delay line with a thermistor load to sense temperature [54] or to a delay-line coated with silicon nanowires to sense humidity have been demonstrated [55].

Radar Cross Section (RCS) based sensing techniques rely on the variation of the magnitude and/or the resonance frequency of a backscattering source. The scattering element is usually a resonant antenna. Variations are brought about by a change in conductivity, permittivity or permeability of a sensing material which is deposited on or tightly coupled to the scattering element. Many types of scattering sources such as shorted dipoles [56], bent slot resonators [57],

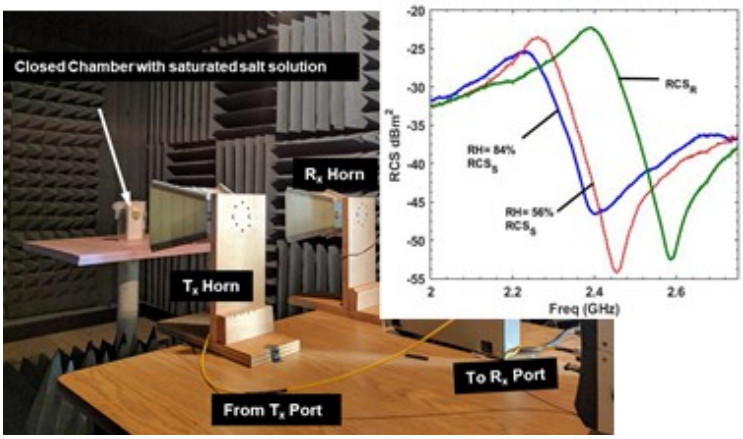

(a)

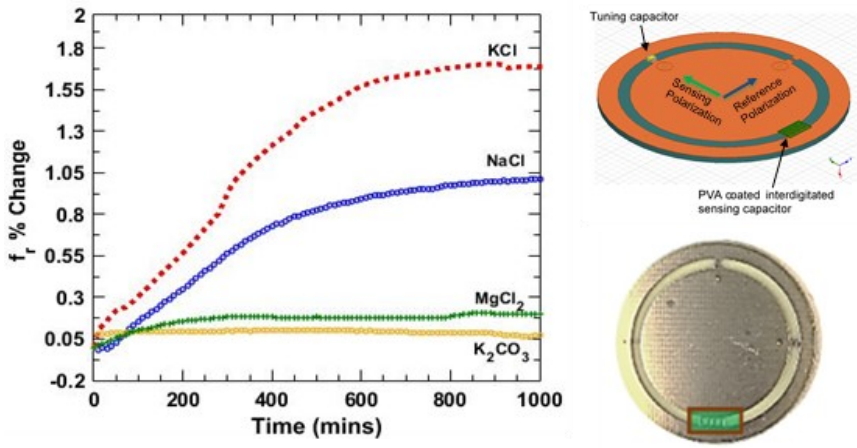

(b)

Fig. 2.12 (a) Experimental setup used for measuring radar cross section of the annular slot ring antenna. The sensing tag is placed at a distance of 80 cm from the interrogating antenna, inset is the example of measured RCS of the tag (b) Measured percentage change in resonant frequency with time for different saturated salt solutions. Note the initial room humidity was not controlled and thus the initial resonant frequency varies in the measurements [61].

circular and rectangular rings [58] have been proposed. For gas sensing applications, graphene-coated split ring resonator elements have been used [59], and humidity sensing has been demonstrated using C-shaped resonators coated with poly-vinyl alcohol (PVA) and poly-methyl methacrylate [60]. The authors have demonstrated a dual-band annular slot antenna-based element for sensing humidity in packaged grain headspace [61]. The sensor, shown in Fig. 2.12, uses the same scattering element for generating two signatures – a reference and a sensing signature. The

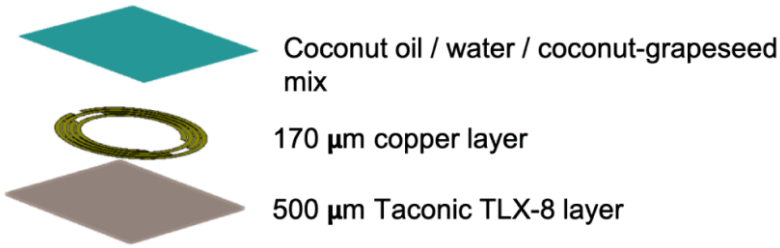

(a)

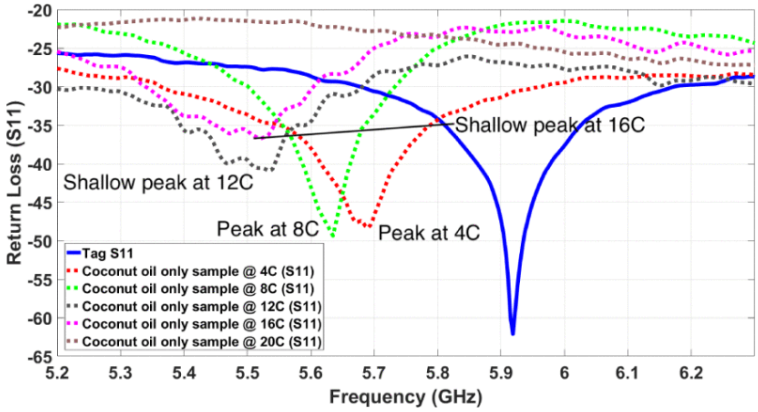

(b)

Fig. 2.13 (a) Asymmetric circular split ring resonator coated with sensing material for temperature threshold detection. (b) Measured performance of the sensor with pure coconut oil as the sensing material [62]. [© 2019, IEEE]

PVA sensing material used has high sensitivity and low loss in the low humidity regime which is desirable for monitoring packaged grains. The permittivity of PVA changes with humidity which in turn changes the resonant frequency of the annular slot. Fig. 2.12a shows the frequency response of the sensing and reference (fixed) backscattered signals for different relative humidity conditions. Fig. 2.12b shows the corresponding change in resonant frequency measured for four different relative humidity conditions, as set by different saturated salt solutions. A similar approach, shown in Fig. 2.13, was used in [62] for temperature threshold indication. Here the scattering element consists of three closely packed asymmetric circular split-ring nested resonators, one of the resonators is coated with a bio-compatible coconut oil-based material for temperature threshold detection. The sensor utilizes the phase transition of the superstrate coating that occurs with a change in temperature as a temperature threshold detector. Two resonators are insensitive and act as identifiers.

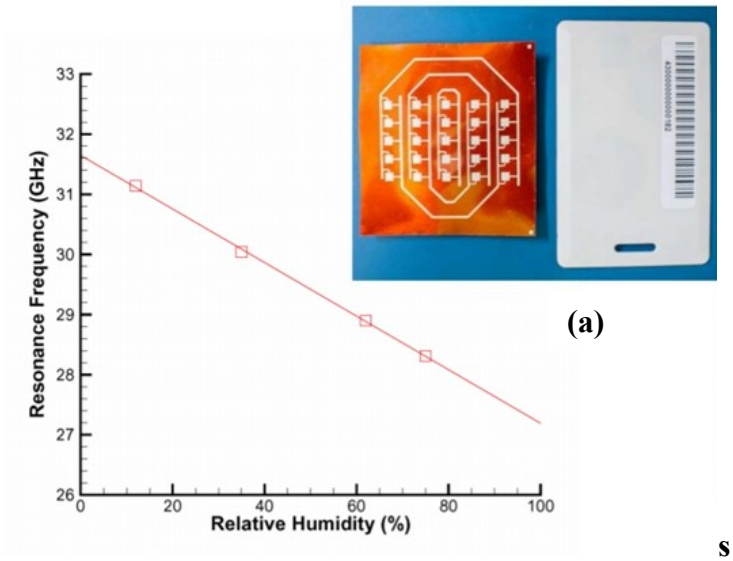

s

(b)

Fig. 2.14 (a) Inkjet-printed flexible Van-Atta reflect-array prototype, next to a standard "credit-card" size RFID tag package. (b) Plot of measured resonance frequency of the inkjet-printed Van-Atta array as a function of ambient humidity level. [63]. [© 2016, IEEE]

2.4.2. Limitations of Chipless UHF Sensors

The biggest disadvantage of chipless wireless sensors is their vulnerability to environmental clutter. This limits them from being used in many practical applications. Several techniques have been used to circumvent this, such as the Van Ata array-based retrodirective reflectarray antenna [63]. Retrodirective reflectarrays provide a much higher radar cross-section signature when compared with conventional antennas in the direction of illumination. A Van-Atta array operating at 30 GHz for humidity sensing application using a 5×5 array is shown in Fig. 2.14. The entire array is inkjet printed on a flexible Kapton HN substrate, a humidity sensitive material. A sensitivity of $(\Delta f/\Delta RH)/f_0 = 0.141$ was demonstrated for a range of 5 m and a 20 dBm transmit power and later extended to 20 m [64]. As array-based sensors are large compared to the wavelength, their application is often limited to mm-wave frequencies where the cost of electronics for building readers is often high.

Frequency diversity between the incident interrogation signal and the scattered/retransmitted signal can also be used in passive sensors for clutter rejection. This is achieved by utilizing a highly

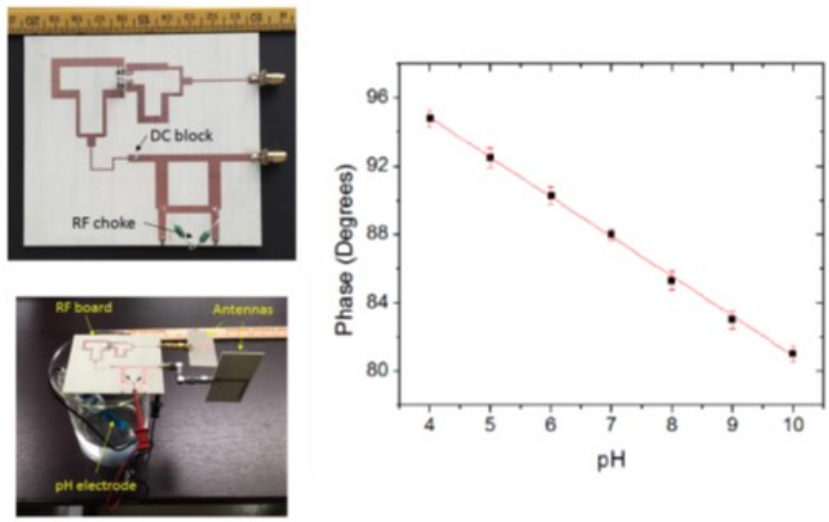

(a) **(b)**

Fig. 2.15 (a) Fabricated circuit and the complete tag setup with antennas and pH electrode (b) Measured phase change for harmonic operation at different pH [69]. [© 2019, IEEE]

nonlinear device such as a diode, either as a passive harmonic frequency generator or a passive mixer, to produce a backscattered signal at either the harmonic of the incident wave or the product of two incident waves. This technique has been demonstrated in the sensing of physical parameters such as temperature [65], [66], [67], humidity [68] and pH [69]. Fig. 2.14 shows such a harmonic sensor for pH sensing consisting of a pH combination electrode for transduction [69]. The potential generated by the pH Electrode pair is used to bias a pair of varactor diodes, which acts as a reactive element of a phase shifter. The interrogation signal is first doubled, then passed through the phase shifter to acquire a phase change proportional to the sensing varactor diode bias and retransmitted back to the interrogator. Harmonic sensors suffer from high conversion loss and require high power interrogation signals for operation.

Another method to reduce the clutter is through use of a depolarizing/cross-polarizing scattering element, such a dipole oriented at 45^0 to the polarization of the incident interrogating wave as proposed in [70], [71], [72]. Though not as effective as harmonic sensors, these radar cross-section-based sensors, when designed with high quality factor and post processed effectively with a short-time Fourier transform, have been shown to improve clutter rejection [73]. An example of a depolarizing tag based sensor developed by the authors targets sensing ammonia gas as shown in Fig. 2.15 [74]. The sensor consists of two annular slot scattering elements, where one is used as

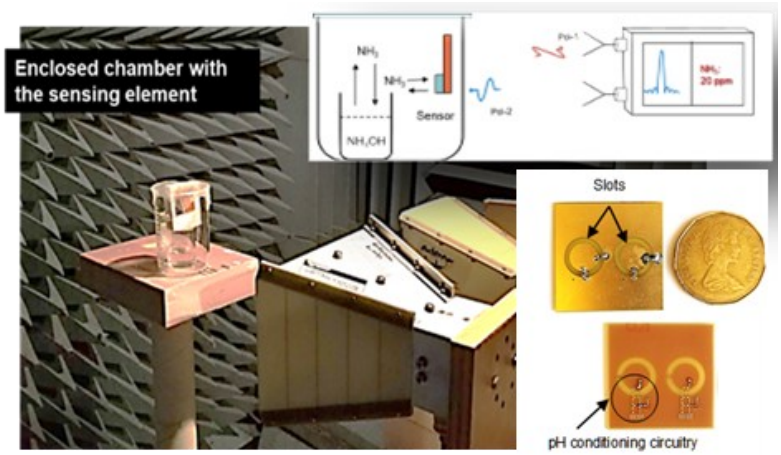

(a)

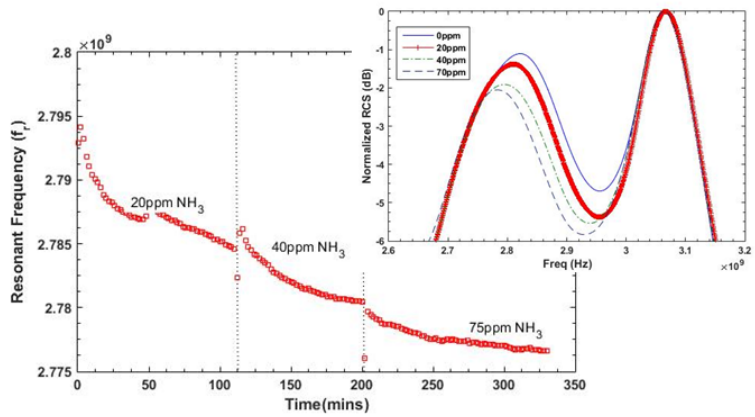

(b)

Fig. 2.16 (a) Experimental set-up and fabricated depolarizing tag used for volatile sensing. (b) Change in resonant frequency of the depolarizing RCS based sensor to different concentration of ammonia gas (inset is the measured normalized RCS response showing the reference and sensing signatures). [74]

a stable frequency reference and the other is connected to two hydrogel coated combination electrodes to sense acidic/basic volatiles [36]. The annular slots are capacitively perturbed to excite a desired cross-polarization component. Fig. 2.16 shows the measured frequency change with different ammonia gas concentration. Results demonstrate detection of lower than 20 ppm ammonia gas, making it suitable for monitoring spoilage of fish/meat products [8].

2.5. Discussion

In addition to the limitations already discussed, and depending on the transduction mechanism employed, RFID sensors can be affected by many factors, such as humidity and temperature. The

response of polymer-based gas sorption sensors can change with humidity and possibly fail at very low humidity levels [36]. Electrode based analyte or gas measurement sensors are also affected by temperature. Differential sensing or compensation using multi-parameter sensing can be used to minimize these effects [75]. Distance between and orientation of the reader-tag coils in LC resonator-based sensors can also affect the measured frequency response due to inter-coil loading [76]. Chipless UHF tags typically do not suffer from the same effects as sensor-interrogator loading is minimal.

Although many different modalities of wireless passive sensors have been explored for food spoilage or quality monitoring in research settings, currently few have been commercialized. Only active RFID HF and UHF sensors have seen widespread use for food quality monitoring, these mostly in time-temperature indication applications [19]. Looking forward though, as the demand for food security increases, passive sensors have great potential as they are cost-effective and do not require a battery. Among the different modalities passive chipped RFID systems will be relatively easy to deploy, driven by the possibility of using the NFC technology already installed in most smart phones as readers. HF and UHF chipless sensors may play a role in mass consumer product applications, where extremely low-cost tags are economical. Even though simple, quantitative measurement of quality indicators over time can be performed, such as bacteria count, the challenge to deploying them in the market is the need for custom readers. For chipless RFID sensors, readers based on low-cost impedance vector network analysis IC hardware, is now becoming available.

Biocompatibility was not considered for many of the sensors described in this paper and another challenge for deployment of future food sensors is the need to encapsulate them or make them out of biocompatible materials that can be placed inside food packaging or in contact with the food. With the advancement of material science, organic materials are being explored for electronic components and will be of importance for food sensor implementation.

2.6. Conclusion

Wireless passive sensors offer the benefits of no battery requirement, longer life and lower cost. In this article, we presented several HF and UHF passive sensors suited to food quality monitoring applications. The sensors are capable of monitoring temperature, humidity, pH or volatile which

are key indicators of packaging integrity, storage conditions or spoilage. We have shown that selective sensing of volatiles can be made with adequate sensitivity so that correlation with bacteria count is possible. With the progress in printed electronics techniques and new materials, deployment of bio-compatible and environment-friendly passive RFID and chipless sensors has become much simpler and presents a new paradigm in food quality monitoring.

2.7. References

[1] R. S. Singhal, P. R. Kulkarni, and D. V. Rege, *Handbook of indices of food quality and authenticity*. Woodhead Pub, 1997.

[2] K. B. Biji, C. N. Ravishankar, C. O. Mohan, and T. K. Srinivasa Gopal, "Smart packaging systems for food applications: a review," 2015.

[3] Y. W. Park, S. M. Kim, J. Y. Lee, and W. Jang, "Application of biosensors in smart packaging," *Mol. Cell. Toxicol.*, vol. 11, no. 3, pp. 277–285, Sep. 2015.

[4] L. H. Ledenbach and R. T. Marshall, "Microbiological Spoilage of Dairy Products," in *Compendium of the Microbiological Spoilage of Foods and Beverages*, New York, NY: Springer New York, 2009, pp. 41–67.

[5] A. E. Ghaly, D. Dave, and A. E. Ghaly, "Meat Spoilage Mechanisms and Preservation Techniques: A Critical Review," *Am. J. Agric. Biol. Sci.*, vol. 6, no. 4, pp. 486–510, 2011.

[6] A. Nopwinyuwong, S. Trevanich, and P. Suppakul, "Development of a novel colorimetric indicator label for monitoring freshness of intermediate-moisture dessert spoilage.," *Talanta*, vol. 81, no. 3, pp. 1126–32, May 2010.

[7] European Commission, "95/149/EC: Commission Decision of 8 March 1995 fixing the total volatile basic nitrogen (TVB-N) limit values for certain categories of fishery products and specifying the analysis methods to be used," Mar. 8, 1995.

[8] S. Bhadra, C. Narvaez, D. J. Thomson, and G. E. Bridges, "Non-destructive detection of fish spoilage using a wireless basic volatile sensor," *Talanta*, vol. 134, pp. 718–723, Mar. 2015.

[9] J. R. Stetter and J. Li, "Amperometric gas sensors--a review.," *Chem. Rev.*, vol. 108, no. 2,

pp. 352–66, Feb. 2008.

[10] U. Guth, F. Gerlach, M. Decker, W. Oelßner, and W. Vonau, “Solid-state reference electrodes for potentiometric sensors,” *J. Solid State Electrochem.*, vol. 13, no. 1, pp. 27–39, 2009.

[11] A. M. Azad, S. A. Akbar, S. G. Mhaisalkar, L. D. Birkefeld, and K. S. Goto, “Solid-State Gas Sensors: A Review,” *J. Electrochem. Soc.*, vol. 139, no. 12, p. 3690, 1992.

[12] J. R. Bates and M. Campbell, “Gas sensors and analysers,” in *Sensor Systems for Environmental Monitoring*, Dordrecht: Springer Netherlands, 1997, pp. 127–178.

[13] G. Ólafsdóttir *et al.*, “Methods to evaluate fish freshness in research and industry,” *Trends in Food Science and Technology*, vol. 8, no. 8. Elsevier Ltd, pp. 258–265, 1997.

[14] B. Kuswandi, Jayus, A. Restyana, A. Abdullah, L. Y. Heng, and M. Ahmad, “A novel colorimetric food package label for fish spoilage based on polyaniline film,” *Food Control*, vol. 25, no. 1, pp. 184–189, 2012.

[15] H. Yousefi, H. M. Su, S. M. Imani, K. Alkhaldi, C. D. Filipe, and T. F. Didar, “Intelligent Food Packaging: A Review of Smart Sensing Technologies for Monitoring Food Quality,” *ACS Sensors*, vol. 4, no. 4, pp. 808–821, 2019.

[16] S. Matindoust, M. Baghaei-Nejad, M. H. S. Abadi, Z. Zou, and L. R. Zheng, “Food quality and safety monitoring using gas sensor array in intelligent packaging,” *Sens. Rev.*, vol. 36, no. 2, pp. 169–183, 2016.

[17] D. Khaled, N. Novas, J. Gazquez, R. Garcia, and F. Manzano-Agugliaro, “Fruit and Vegetable Quality Assessment via Dielectric Sensing,” Sensors, vol. 15, no. 7, pp. 15363–15397, Jun. 2015.

[18] ChainLink Research "Research :The Future of RFID.”, Mar. 15, 2014.

[19] F. Bibi, C. Guillaume, N. Gontard, and B. Sorli, “A review: RFID technology having sensing aptitudes for food industry and their contribution to tracking and monitoring of food products,” *Trends in Food Science and Technology*, vol. 62. Elsevier Ltd, pp. 91–103, 01-Apr-2017.

[20] R. M. Ferdous, A. W. Reza, and M. F. Siddiqui, "Renewable energy harvesting for wireless sensors using passive RFID tag technology: A review," *Renew. Sustain. Energy Rev.*, vol. 58, pp. 1114–1128, May 2016.

[21] E. Perret, *Radio Frequency Identification and Sensors: From RFID to Chipless RFID*. John Wiley & Sons, 2014.

[22] Tagsense "LC-100 TagReader," LC-100 datasheet, 2005.

[23] Tagsense, "LC-10 Chipless TagReader," LC-10 datasheet, 2006.

[24] A. Ramos, A. Lazaro, D. Girbau, and R. Villarino, "Time-domain measurement of time-coded UWB chipless RFID tags," *Prog. Electromagn. Res.*, vol. 116, pp. 313–331, 2011.

[25] M. Garbati, R. Siragusa, E. Perret, and C. Halope, "Impact of an IR-UWB Reading Approach on Chipless RFID Tag," *IEEE Microw. Wirel. Components Lett.*, vol. 27, no. 7, pp. 678–680, Jul. 2017.

[26] M. M. Forouzandeh and N. Karmakar, "Towards the Improvement of Frequency-domain Chipless RFID Readers," in *2018 IEEE Wireless Power Transfer Conference, WPTC 2018*, 2019.

[27] N. C. Karmakar, M. Zomorrodi, and C. Divarathne, "SAR-Based Signal Processing," in *Advanced Chipless RFID*, Hoboken, NJ, USA: John Wiley & Sons, Inc., 2016, pp. 111–129.

[28] N. C. Karmakar, R. Koswatta, and P. Kalansuriya, *Chipless RFID Reader Architecture.* Artech House, 2013.

[29] H. Tao *et al.*, "Silk-Based Conformal, Adhesive, Edible Food Sensors," *Adv. Mater.*, vol. 24, no. 8, pp. 1067–1072, Feb. 2012.

[30] S. Y. Wu, C. Yang, W. Hsu, and L. Lin, "3D-printed microelectronics for integrated circuitry and passive wireless sensors," *Microsystems Nanoeng.*, vol. 1, 2015.

[31] S. Karuppuswami, L. L. Matta, E. C. Alocilja, and P. Chahal, "A Wireless RFID Compatible Sensor Tag Using Gold Nanoparticle Markers for Pathogen Detection in the Liquid Food Supply Chain," *IEEE Sensors Lett.*, vol. 2, no. 2, pp. 1–4, Apr. 2018.

[32] G. Xu *et al.*, "Passive and wireless near field communication tag sensors for biochemical

sensing with smartphone," *Sensors Actuators, B Chem.*, vol. 246, pp. 748–755, 2017.

[33] E. Smits *et al.*, "Development of printed RFID sensor tags for smart food packaging," *14th Int. Meet. Chem. Sensors*, pp. 403–406, 2012.

[34] Z. Ma *et al.*, "Highly Sensitive, Printable Nanostructured Conductive Polymer Wireless Sensor for Food Spoilage Detection," *Nano Lett.*, vol. 18, no. 7, pp. 4570–4575, 2018.

[35] P. Kassal, I. M. Steinberg, and M. D. Steinberg, "Wireless smart tag with potentiometric input for ultra low-power chemical sensing," *Sensors Actuators, B Chem.*, vol. 184, pp. 254–259, 2013.

[36] S. Bhadra, D. J. Thomson, and G. E. Bridges, "Monitoring acidic and basic volatile concentration using a pH-electrode based wireless passive sensor," *Sensors Actuators, B Chem.*, vol. 209, pp. 803–810, Mar. 2015.

[37] S. Bhadra *et al.*, "Fluid embeddable coupled coil sensor for wireless pH monitoring in a bioreactor," *IEEE Trans. Instrum. Meas.*, vol. 63, no. 5, pp. 1337–1346, 2014.

[38] C. Occhiuzzi, S. Caizzone, and G. Marrocco, "Passive UHF RFID antennas for sensing applications: Principles, methods, and classifcations," *IEEE Antennas Propag. Mag.*, vol. 55, no. 6, pp. 14–34, 2013.

[39] J. Yin *et al.*, "A system-on-chip EPC Gen-2 passive UHF RFID tag with embedded temperature sensor," in *IEEE Journal of Solid-State Circuits*, 2010, vol. 45, no. 11, pp. 2404–2420.

[40] Farsens, "EPC C1G2 Batteryless ambient temperature and relative humidity sensor," EPC C1G2 datasheet 2018.

[41] Z. Zou, Q. Chen, I. Uysal, and L. Zheng, "Radio frequency identification enabled wireless sensing for intelligent food logistics," *Philos. Trans. R. Soc. A Math. Phys. Eng. Sci.*, vol. 372, no. 2017, Jun. 2014.

[42] S. Dat Nguyen, N. N. Le, P. T. Lam, E. Fribourg-Blanc, C. M. Dang, and S. Tedjini, "A wireless sensor for food quality detection by UHF RFID passive tags," in *International Conference on Advanced Technologies for Communications*, 2016, vol. 2016-January, pp.

258–263.

[43] R. Gonçalves *et al.*, "RFID-Based Wireless Passive Sensors Utilizing Cork Materials," *IEEE Sens. J.*, vol. 15, no. 12, pp. 7242–7251, Dec. 2015.

[44] S. Manzari, A. Catini, G. Pomarico, C. Di Natale, and G. Marrocco, "Development of an UHF RFID chemical sensor array for battery-less ambient sensing," *IEEE Sens. J.*, vol. 14, no. 10, pp. 3616–3623, 2014.

[45] B. Saggin, Y. Belaizi, A. Vena, B. Sorli, V. Guillard, and I. Dedieu, "A flexible biopolymer based UHF RFID-sensor for food quality monitoring," in *2019 IEEE International Conference on RFID Technology and Applications, RFID-TA 2019*, 2019, pp. 484–487.

[46] Onsemi, Appl. Note AN-FAM1601, Oct. 2016.

[47] T. Athauda and N. Karmakar, "Chipped versus chipless RF identification: A comprehensive review," *IEEE Microw. Mag.*, vol. 20, no. 9, pp. 47–57, Sep. 2019.

[48] Y. F. Weng, S. W. Cheung, T. I. Yuk, and L. Liu, "Design of Chipless UWB RFID System Using A CPW Multi-Resonator," *IEEE Antennas Propag. Mag.*, vol. 55, no. 1, pp. 13–31, Feb. 2013.

[49] D. Dominic, S. Krafft, N. Safdari, and S. Bhadra, "Multiresonator-Based Printable Chipless RFID for Relative Humidity Sensing," *Proceedings*, vol. 1, no. 4, p. 367, Aug. 2017.

[50] E. M. Amin and N. Karmakar, "Development of a chipless RFID temperature sensor using cascaded spiral resonators," in *2011 IEEE Sensors Proceedings*, 2011, pp. 554–557.

[51] B. Kubina, C. Mandel, and M. Schüßler, "A wireless chipless temperature sensor utilizing an orthogonal polarized backscatter scheme," in *Microwave Conference (EuMC), 2012 42nd European*, 2012, pp. 61–64.

[52] E. M. Amin and N. C. Karmakar, "Development of a low cost printable humidity sensor for chipless RFID technology," in *2012 IEEE International Conference on RFID-Technologies and Applications (RFID-TA)*, 2012, pp. 165–170.

[53] A. Ramos, D. Girbau, A. Lazaro, and R. Villarino, "Time-coded chipless RFID temperature sensor with self-calibration based on a Vivaldi antenna," in *2013 IEEE MTT-S International*

Microwave Symposium Digest (MTT), 2013, pp. 1–4.

[54] D. Girbau, A. Ramos, A. Lazaro, S. Rima, and R. Villarino, "Passive Wireless Temperature Sensor Based on Time-Coded UWB Chipless RFID Tags," *IEEE Trans. Microw. Theory Tech.*, vol. 60, no. 11, pp. 3623–3632, Nov. 2012.

[55] R. S. Nair, E. Perret, S. Tedjini, and T. Baron, "A Group-Delay-Based Chipless RFID Humidity Tag Sensor Using Silicon Nanowires," *IEEE Antennas Wirel. Propag. Lett.*, vol. 12, pp. 729–732, 2013.

[56] I. Jalaly and I. D. Robertson, "RF barcodes using multiple frequency bands," *IEEE MTT-S Int. Microw. Symp. Dig.*, vol. 2005, no. C, pp. 139–142, 2005.

[57] E. M. Amin, N. C. Karmakar, and B. W. Jensen, "Fully Printable Chipless RFID Multi-parameter Sensor," *Sensors Actuators A Phys.*, Jul. 2016.

[58] A. Vena, E. Perret, and S. Tedjini, "High-Capacity Chipless RFID Tag Insensitive to the Polarization," *IEEE Trans. Antennas Propag.*, vol. 60, no. 10, pp. 4509–4515, Oct. 2012.

[59] A. Vena, L. Sydänheimo, M. M. Tentzeris, and L. Ukkonen, "A Fully Inkjet - Printed Wireless and Chipless Sensor for CO 2 and Temperature detection," vol. 15, no. c, pp. 89–99, 2014.

[60] E. M. Amin, N. Karmakar, and B. Winther-Jensen, "Polyvinyl-Alcohol (PVA)-Based RF Humidity Sensor in Microwave Frequency," *Prog. Electromagn. Res. B*, vol. 54, pp. 149–166, 2013.

[61] R. Raju and G. E. Bridges, "Radar Cross Section Based Dual-Band Dual-Polarized Humidity Sensing Tag," in *XXXIInd URSI General Assembly*, 2017.

[62] R. Bhattacharyya, S. Sarma, T. Athauda, and N. Karmakar, "Electromagnetic characterization of a food safe, organic smart material for customizable temperature threshold sensing in cold chain applications," in *2019 IEEE International Conference on RFID, RFID 2019*, 2019.

[63] J. G. D. Hester and M. M. Tentzeris, "Inkjet-Printed Flexible mm-Wave Van-Atta Reflectarrays: A Solution for Ultralong-Range Dense Multitag and Multisensing Chipless

RFID Implementations for IoT Smart Skins," *IEEE Trans. Microw. Theory Tech.*, vol. 64, no. 12, pp. 4763–4773, Dec. 2016.

[64] J. G. D. Hester and M. M. Tentzeris, "Inkjet-printed flexible mm-wave van-atta reflectarrays: A solution for ultralong-range dense multitag and multisensing chipless RFID implementations for IoT smart skins," *IEEE Trans. Microw. Theory Tech.*, vol. 64, no. 12, pp. 4763–4773, Dec. 2016.

[65] B. Kubina, C. Mandel, M. Sch, and R. Jakoby, "Compact Quasi-Chipless Harmonic Radar Sensor with a Dielectric Resonator Antenna," pp. 2–4, 2015.

[66] B. Kubina, J. Romeu, C. Mandel, M. Schüßler, and R. Jakoby, "Quasi-chipless wireless temperature sensor based on harmonic radar," vol. 50, no. 2, pp. 2–3, 2014.

[67] V. Viikari, H. Seppä, T. Mattila, and A. Alastalo, "Wireless Ferroelectric Resonating Sensor," vol. 57, no. 4, pp. 785–791, 2010.

[68] A. Lazaro, R. Villarino, and D. Girbau, "A Passive Harmonic Tag for Humidity Sensing," *Int. J. Antennas Propag.*, vol. 2014, pp. 1–11, 2014.

[69] S. Mondal, D. Kumar, and P. Chahal, "A Wireless Passive pH Sensor with Clutter Rejection Scheme," *IEEE Sens. J.*, vol. 19, no. 9, pp. 3399–3407, 2019.

[70] A. Vena, E. Perret, and S. Tedjni, "A depolarizing chipless RFID tag for robust detection and its FCC compliant UWB reading system," *IEEE Trans. Microw. Theory Tech.*, vol. 61, no. 8, pp. 2982–2994, 2013.

[71] O. Rance, R. Siragusa, P. Lemaitre-Auger, and E. Perret, "RCS magnitude coding for chipless RFID based on depolarizing tag," *2015 IEEE MTT-S Int. Microw. Symp. IMS 2015*, pp. 2–5, 2015.

[72] F. Costa, S. Genovesi, and A. Monorchio, "Chipless RFIDs for Metallic Objects by Using Cross Polarization Encoding," *IEEE Trans. Antennas Propag.*, vol. 62, no. 8, pp. 4402–4407, Aug. 2014.

[73] A. Ramos *et al.*, "Temporal Separation Detection for Chipless Depolarizing Frequency-Coded RFID," *IEEE Trans. Microw. Theory Tech.*, vol. 64, no. 7, pp. 2326–2337, Jul. 2016.

[74] R. Raju and G. E. Bridges, "RCS Based Depolarizing Passive Tag with Improved Clutter Rejection for Potentiometric Gas Sensing," in *2019 IEEE SENSORS*, 2019, pp. 1–4.

[75] S. Bhadra, D. S. Y. Tan, D. J. Thomson, M. S. Freund, and G. E. Bridges, "A wireless passive sensor for temperature compensated remote pH monitoring," IEEE Sens. J., vol. 13, no. 6, pp. 2428–2436, 2013.

[76] K. G. Ong and C. A. Grimes, "A resonant printed-circuit sensor for remote query monitoring of environmental parameters," *Smart Mater. Struct.*, vol. 9, no. 4, pp. 421–428, Aug. 2000.

Chapter 3.

Radar Cross Section Based Chipless Tag with Built-in Reference for Relative Humidity Monitoring of Packaged Food Commodities

Chapter 2 presented the background literature of wireless passive sensors for packaged food monitoring applications. Relative humidity is one critical parameter that when monitored controlled improves the shelf life of various packaged food products. This chapter presents a radar cross section-based sensor for relative humidity sensing. This chapter is based on the published paper "**R. Raju** and G. E. Bridges, "Radar Cross Section Based Chipless Tag with Built-in Reference for Relative Humidity Monitoring of Packaged Food Commodities," *IEEE Sens. J.*, pp. 1–1, Jun. 2021.", and presents a novel sensr with integrated reference and sensing signature with a compact form factor.

3.1. Abstract

Dry food commodities like grains and pulses can be stored safely for several years under controlled storage conditions. The equilibrium moisture content of the packaged grain is one of the most important parameters required to be monitored and controlled for extended safe storage. This chapter presents a single element dual-polarized sensing tag based on an annular slot antenna operating at two closely spaced resonant frequencies for radar cross-section-based monitoring of relative humidity in hermetically packaged food commodities. One of the resonant frequencies is functionalized for sensing while the other acts as a built-in reference, mitigating the effects of environmental loading. A polyvinyl alcohol coated interdigitated capacitor, integrated onto the antenna is used as a capacitive transducer for the sensing element. Laboratory scale measurements were carried out using the saturated salt solution method. Results show that the proposed sensor can be used for monitoring a wide range of humidity conditions.

3.2. Introduction

Sensing, monitoring, and regulation of compositional and environmental factors play a vital role in quality estimation and control of stored food commodities. Microorganism levels, catalytic

enzymes, and trace metals internal to the food item make up the compositional factors. Physical parameters like temperature, humidity, light, mechanical stress, and pressure in which the item is stored make-up the environmental parameters [1]. Water activity (a_w), the ratio of vapor pressure in a food material to that of pure water at the same temperature, has been identified as the one of the most important factors affecting food deterioration. It is well established that critical values of a_w can be established to extend the shelf lives of various food commodities [2]. Relative humidity of the immediate environment in which the food is stored directly affects a_w and thus is one of the key factors that affect the shelf life. This is of immense importance in the case of dry food commodities (water content class 1) that are packaged and stored in large quantities for long

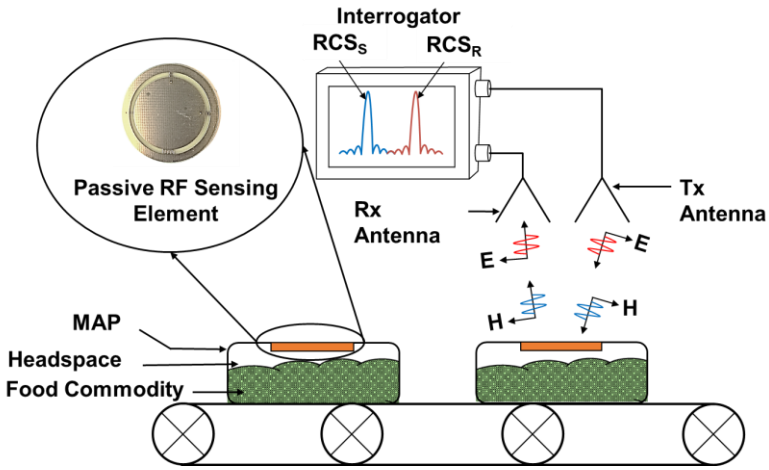

Fig. 3.1 Schematic representation showing headspace monitoring of packaged food commodity using the proposed passive chipless radar cross section (RCS) based sensor.

periods. Dry storage items like grains and pulses, for instance, can be stored for up to 10 years without quality degradation if optimal storage conditions are met. The temperature and moisture requirements of these food items are typically in the ranges of 5-10° C and 10-12%, respectively, for maximizing their safe storage periods [3]. Dried fruits like dates and figs require a humidity range of 55-75%. Even though regulatory standards mandate safe storage procedures during long term storage and transport [4], little attention is dedicated to monitoring and quality control at the packaged level.

Grains, including lentils and pulses, are often stocked in low volume hermetic bags during storage, transport, and distribution, especially in the developing parts of the world [5]. Modified atmosphere packaging (MAP) techniques, like nitrogen flushing, vacuum packaging, and gas selective packaging films are generally employed to maintain the moisture content, carbon dioxide,

and oxygen levels inside hermetically packaged grains [6]. Alternatively, the low-cost technique of naturally increasing the concentration of CO_2 in the packaged bag through respiration of the commodity has also been proven to be effective in both mold and pest control [7][8]. Hermetic bags, however, which are often made of 2-3 layers of (~250 μm thick) polyethylene plastic [9], are prone to the exchange of gases like O_2, CO_2 and water vapor over extended storage times due to their finite permeability coefficient and, perforations that may occur during storage and handling can cause significant quality degradation with time [10]. Integrity inspections and headspace analysis are hence frequently required for their quality estimation. Package-to-package inspections, however, necessitate expensive, low throughput equipment which commonly requires puncturing and resealing of the inspected item [11] [12].

Passive chipless wireless sensors can be broadly classified into two categories based on the approaches they use for their operation. The first approach is based on the retransmission of the interrogating signal. The sensing element in this technique consists of a receiving ultra-wideband antenna connected to passive sensing components, such as multi-resonant transmission lines, spiral or split-ring resonators [16][17][18][19] or a SAW element sensor [20] [21], and then finally to a transmit antenna. The second approach is based on the backscattered radar cross-section (RCS) signature of the tag. In this technique, either the resonance frequency or RCS magnitude of the back-scattered signal carries the information of the parameter being sensed [22] [23] [24] [25] [26]. The RCS-backscatter approach has the advantage of being considerably smaller in size, enabling higher data capacity for their integration with radar cross-section based radio-frequency identification systems. Though RCS based tags are prone to environmental clutter, the received signal is usually of larger magnitude compared to the retransmission-based approach. This is because, at resonance, antennas with a high reflection load tend to have a large RCS due to the in-phase superposition of the structural mode and antenna mode [27].

In this chapter, an RCS-based humidity sensing tag with an integrated reference signature is presented with its potential application in the monitoring of packaged food commodities, like grains and pulses, that require controlled moisture content for their safe storage. The tag is designed to operate in dual-frequencies with orthogonal polarizations such that the backscattered field consists of two distinct signatures independent of each other within a narrow bandwidth of operation using a single scattering element. One of these signatures is made sensitive to humidity

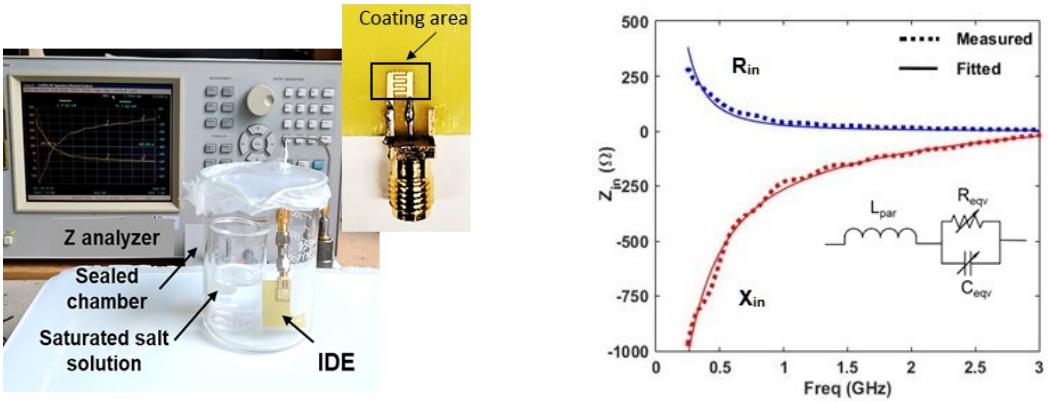

(a) **(b)**

Fig. 3.2 (a) Experimental set-up used for humidity sensing and characterization of the interdigitated capacitor. (b) The measured impedance response of the capacitor and the curve fitted data obtained from the extracted equivalent circuit. Inscribed is the equivalent circuit model (without PVA coating R_{eqv}=3.15 kΩ, C_{eqv}=545 fF, and L_{eqv}= 4 nH).

by loading it with an interdigitated capacitor coated with the humidity sensitive material, polyvinyl alcohol (PVA), which changes the resonant frequency of the sensing RCS signature (RCS_S) with a change in the humidity. The second signature serves as a built-in reference RCS (RCS_R) which provides immunity to environmental loading, like that of the package, through differential sensing capability. The second signature can also be functionalized to monitor other parameters like temperature, vital in food quality control applications. A schematic representation of the application of the sensing system to packaged grain monitoring is shown in Fig. 3.1.

3.3. Sensor Design

3.3.1. Sensing Transducer Characterization

The design of the sensing slot antenna requires proper characterization of the PVA coated capacitive transducer. The interdigitated capacitor (IDC), shown in Fig. 3.2(a), was fabricated on an FR4 board of 0.7874 mm thickness and with a finger gap and width of 0.275 mm and 0.2 mm respectively. The impedance response of the uncoated interdigitated capacitor was obtained using a calibrated Agilent E4991A RF-impedance analyzer. The equivalent circuit of the IDC was obtained using curve-fitting in MATLAB [28]. The measured impedance response, the obtained equivalent circuit, and its fitted input impedance response are shown in Fig. 3.2(b).Deposition of PVA coating over the interdigitated capacitor was accomplished by using a temporary FR4-well

Table 3.1

Sample salts and their equilibrium RH at 23°C, 1 atm [30]

Saturated Salt Solution	Equilibrium - RH%
Magnesium Chloride ($MgCl_2$)	32.78
Potassium carbonate (K_2CO_3)	43.16
Sodium Bromide (NaBr)	57.6
Sodium Chloride (NaCl)	75.29
Potassium Chloride (KCl)	84.34

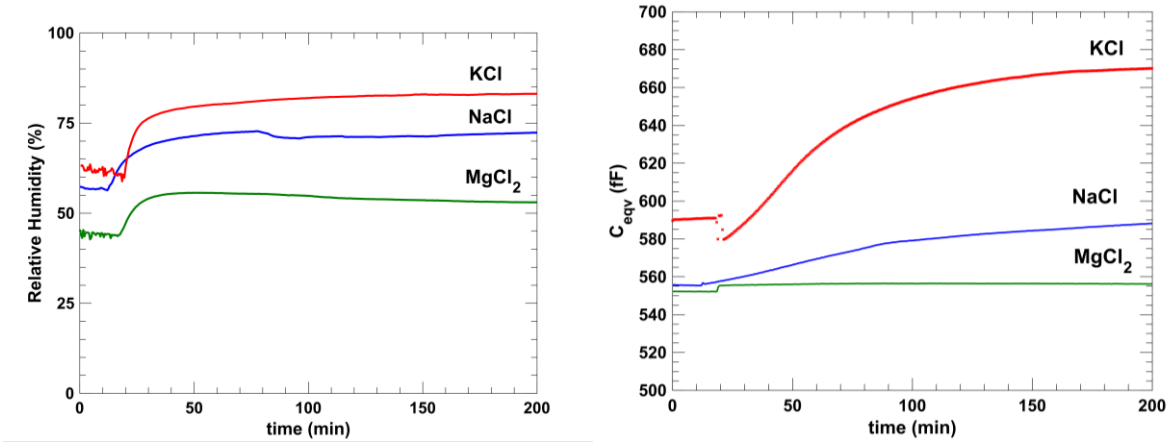

(a) **(b)**

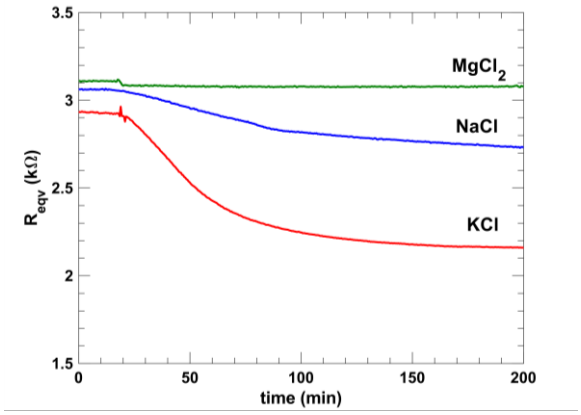

(c)

Fig. 3.3 (a) Measured relative humidity in the chamber for each of the salt solutions. Change in equivalent circuit parameters (b) capacitance C_{eqv} and (c) resistance R_{eqv} of the PVA coated interdigitated capacitor for different saturated salt solutions.

of 0.7874 mm depth around the IDCs, which is filled with a 20% PVA solution in water, followed

by drying at room temperature for 30 mins. This was repeated to get the desired thickness of PVA (20 μm), which dictates both the sensitivity and the response time of the sensor. The sensor IDC was then exposed to different humidity conditions by placing it in a 200 ml sealed beaker carrying a 20 ml solution of different saturated salts as shown in Fig. 3.2(a). The concentration of water vapor inside the chamber increases with time until an equilibrium is reached. Depending on the type of salt a different equilibrium relative humidity level is attained inside the chamber. A similar process occurs in the storage environment of food items, where an equilibrium RH is attained depending on the initial storage RH, temperature and the moisture content of the item [29]. Table 3.1 gives examples of saturated salt solutions and their equilibrium relative humidity obtained from [30]. The RH in the chamber was also monitored using a commercial sensor SHT70 [31] which has an RH accuracy of 2% and 3 sec response time.

Exposure to different RH causes a change in the measured impedance response due to the variation in capacitance and resistance of the IDC (the parasitic inductance stays constant). The equivalent capacitance and resistance changes extracted from the humidity dependent input impedance is shown in Fig. 3.3. As the humidity inside the chamber increases the capacitance of the IDC increases and the resistance decreases. These results are in agreement with the ones previously reported in [22] and [32]. PVA being a hydrophilic, hygroscopic polymer, water molecules diffuse into the polymer matrix through adsorption and absorption. This gives PVA based sensors higher sensitivity and faster response time when compared to hydrophobic polymers like polyimide [33]. The change in the equivalent circuit parameters of the IDC with a rise in the water concentration inside the PVA is ascribed to the increase in the real and imaginary parts of permittivity. When integrated with a resonant antenna, this will result in lowering of the resonant frequency and quality factor. Though a decrease in the quality factor causes a decrease in sensitivity at higher relative humidity, it may be used as an additional parameter, along with the resonant frequency shift, to improve the accuracy and reliability of the measured humidity.

The per-unit-length parameters for a given thickness of PVA give a more general indication of the change in capacitance and resistance with RH and form the basis for the design of the IDC integrated into the antenna. The total capacitance of the interdigitated capacitor can be obtained using

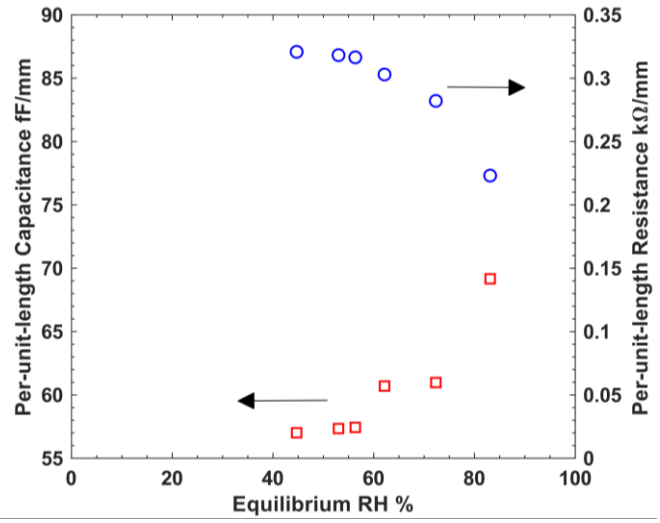

Fig. 3.4 Per-unit-length capacitance and resistance for the interdigitated capacitor vs percent relative humidity (obtained using different saturated salt solutions).

$$C = C_u(N-1)L \qquad (1)$$

where C_u is the per-unit-length capacitance of a unit cell, N is the number of electrodes and L is the length of each electrode, C_u is the sum of individual capacitive contributions, namely, gap capacitance, capacitance due to the fringing fields above the electrodes (PVA coated region), and capacitance due to the fringing fields below the electrodes (FR4 substrate region). The sensitivity of the sensor depends on the PVA coating thickness and the electrode geometry. A thicker coating of PVA provides higher sensitivity at the expense of longer response time and higher loss [34] [35]. In the current work, a thickness of 20 µm provides sufficient change to demonstrate proof of concept. Fig. 3.4 shows the change in measured per-unit-length capacitance and resistance for different RH. It should be noted that, at higher ranges of humidity values, the response to the change in humidity is also affected by the swelling of the polymer matrix causing a non-linear variation in the response [36].

3.3.2. Tag Design and Sensor Operation

A dual-band, dual-polarized annular slot ring antenna, as shown in Fig. 3.5, is employed as the backscattering element. The resonant modes of the slot ring antenna occur at the frequencies at which the circumference of the slot is an integral multiple of the guided wavelength. To a first-order approximation, the resonant frequency of the antenna when operated in the fundamental

mode can be estimated to be $\lambda_g = 2\pi r_{av}$, where r_{av} is the average of the inner and outer radius of the slot ring and λ_g is the guided wavelength of the slot line of width equal to that of the width, W_s, of a slot antenna [37].

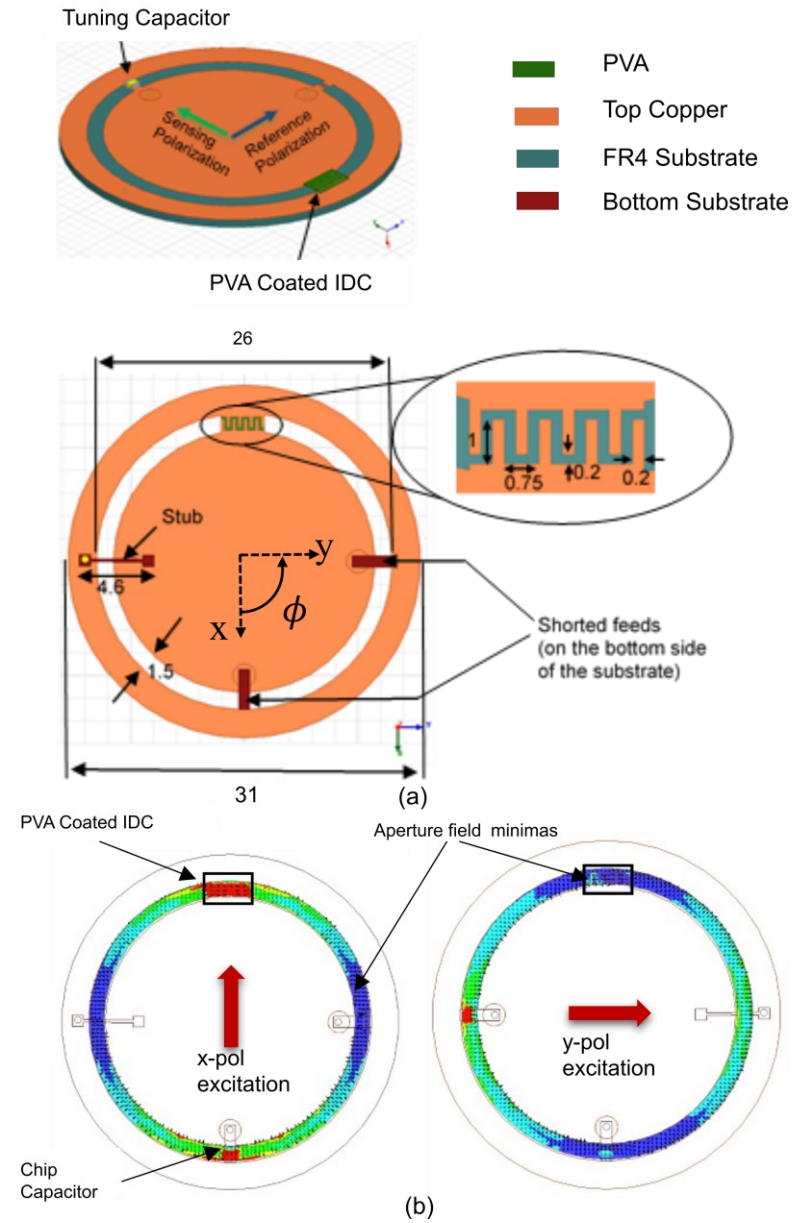

Fig. 3.5 (a) Dual-polarized annular slot antenna loaded with a functionalized interdigitated capacitor (all dimensions are in mm). (b) aperture field distributions for the two orthogonal modes.

When excited by an incident field, the aperture field induced in the slot antenna can be modeled using a magnetic current distribution described by

$$\vec{M}(\rho,\phi) = -E_{\phi}^{a}\hat{\rho} + E_{\rho}^{a}\hat{\phi}. \qquad (2)$$

For a narrow slot width ($W_s \ll \lambda_g$) and fundamental mode of operation, we have $E_{\phi}^{a} = 0$ and the $E_{\rho}^{a} = cos\,(\phi)$, giving an omnidirectional pattern with maximum radiation in the broadside direction [38]. The wide beamwidth of the radiation pattern makes the tag less sensitive to orientation effects. This mode is characterized by aperture electric field nulls in the direction orthogonal to the incident excitation field, as shown in Fig. 3.5b. In the current design, the resonant frequency of the x-polarized mode is perturbed by adding capacitive loading at the null regions of the y-polarized mode, as shown in Figure 3.5b thereby not affecting the y-polarized resonant frequency. Since the equivalent circuit of a slot antenna corresponds to a parallel resonant circuit, capacitive loading of the x-polarized mode decreases its resonant frequency from the unperturbed case [39]. This gives the antenna two distinct frequencies of operation when excited simultaneously by two orthogonally polarized incident waves.

The capacitive loading of the x-polarized mode is achieved by using an interdigitated capacitor (IDC) coated with PVA. A coating procedure identical to the one described in section 3.3.1 was used. The IDC was designed based on the per-unit-length capacitance values obtain from Fig. 3.4, to obtain an uncoated capacitance of 0.5 pF. A second tuning capacitor of 0.2 pF was optionally added in parallel at the opposite side of the slot to create sufficient frequency separation from the unperturbed y-polarized resonant frequency, but at the cost of reduced sensitivity. This fixed capacitor may also be designed using an integrated IDC. The capacitance sensitive x-polarized mode thus gives the RCS_S signature, and the unperturbed y-polarized mode gives the RCS_R signature, with $f_r^{RCS_S} < f_r^{RCS_R}$. An additional open circuit stub was added to the y-polarized component to minimize the cross coupling between the modes.

3.4. Experimental Results

3.4.1. RCS Measurement Method

Frequency domain monostatic RCS measurements were performed using a vector network analyzer in an anechoic chamber as shown in Fig. 3.6. Two identical horn antennas with a gain of 10 dBi (at 2.5 GHz) and an operating frequency range of 2 to 12 GHz were used for the

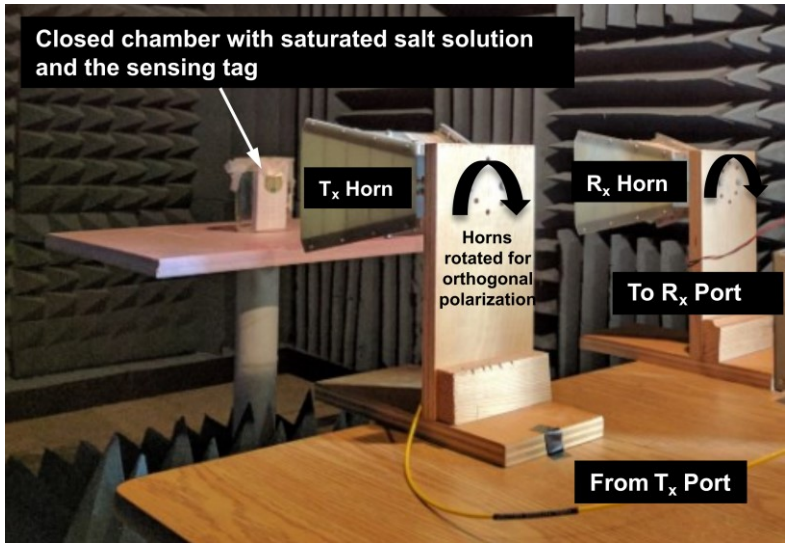

Fig. 3.6 Experimental setup used for measuring radar cross section of the annular slot ring sensing tag. The sensing tag is placed inside a humidity-controlled chamber at a distance 80 cm from the interrogating antenna, both the antennas are rotated 90^0 to measure the two polarizations (far-field distance is 48cm).

measurement of the scattering response of the tag. An (optional) amplifier with a gain of 17 dB was added to the receiver path to improve the received signal strength. The tag was placed at a distance of 80 cm from both the transmitting and receiving antennas. Before measuring the scattering from tag (S_{21}^{tag}), an isolation measurement (S_{21}^{iso}) was performed to remove static reflections from the measurement chamber and reader coupling. This was followed by a reference measurement (S_{21}^{ref}) using a 60 mm diameter circular disc with a known RCS, to remove the effects of antennas [40]. For normal incidence, the unknown RCS of the tag can then be determined using

$$\sigma_{tag} = \left(\frac{S_{21}^{tag} - S_{21}^{iso}}{S_{21}^{ref} - S_{21}^{iso}}\right)\sigma^{ref}, \tag{3}$$

where σ^{ref} is the analytical expression for the radar cross-section of the reference disc given by

$$\sigma^{ref} = 4\pi\frac{A^2}{\lambda^2} \tag{4}$$

where A is the area of the reference disc.

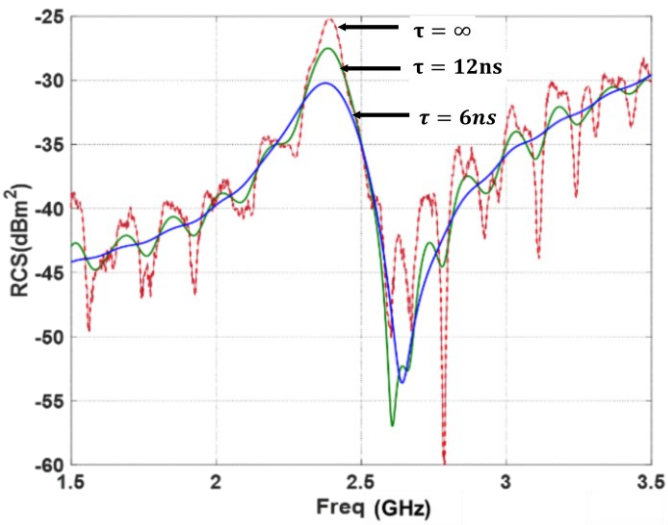

Fig. 3.7 Measured RCS of the tag showing the effect of time gating with different window width (τ) on the frequency domain response of the tag. An interfering tag with the same resonant frequency is placed at a distance of 80 cm further away from the sensing tag.

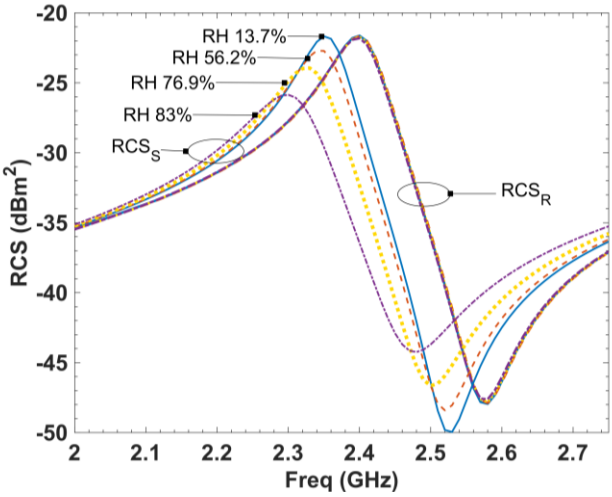

Fig. 3.8 HFSS simulation results showing the vertically polarized RCSs and horizontally polarized RCSR response of the proposed annular slot tag with PVA coated IDC. PVA material properties corresponding to various humidity conditions were obtained from [32]

Although the isolation measurement minimizes the effect of static scattering sources in the chamber, the real environment is always accompanied by dynamic scattering sources. A time-gated measurement is used to eliminate the effects of unwanted scattering sources. A Gaussian time window is used to achieve this (Gaussian shape was chosen to preserve the shape). For all the

measurements presented here a Gaussian time window with a width 3.8 ns, considering a time constant $Q/\pi f_r$, was used. A narrower window reduces the effect of clutter but this, however, deteriorates the quality factor and reduces the amplitude of the measured signal. The Q of the resonator is obtained as described in [41]. An example of the measured RCS in the presence of a clutter source is shown in Fig. 3.7. Here a second slot antenna operating in the same frequency band and placed at a distance of 80 cm behind the sensing tag is used as a secondary clutter source.

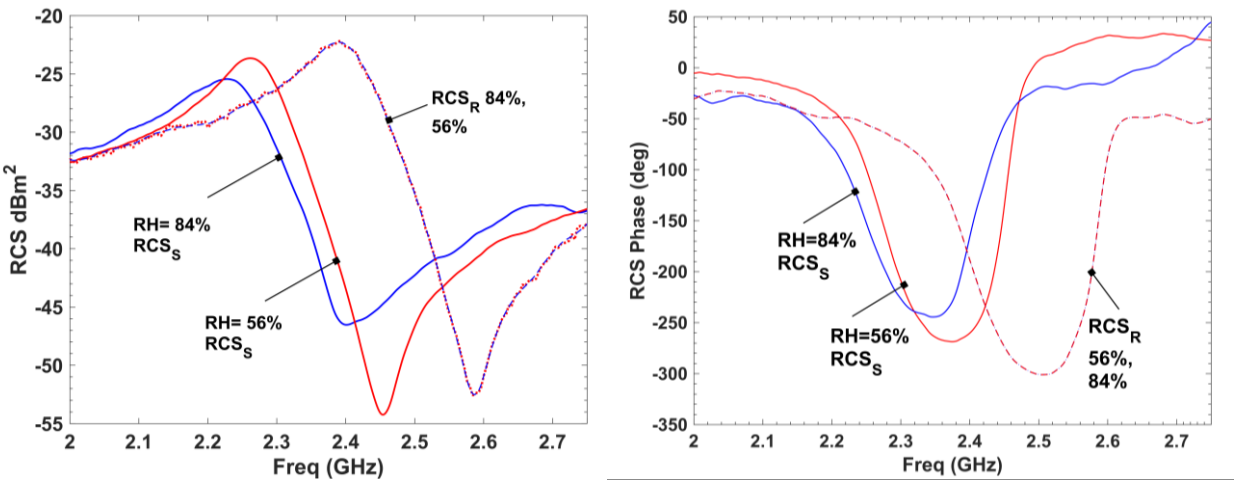

(a) (b)

Fig. 3.9 Measured resonant frequency of the vertically polarized RCS$_S$ and horizontally polarized RCS$_R$ (a) magnitude and (b) phase sampled at two different humidity conditions obtained using the saturated salt solution method.

3.4.2. Wireless Relative Humidity Monitoring

The vertically and horizontally polarized RCS responses of the sensing tag for normal plane wave incidence and different humidity conditions, simulated using Ansys HFSS, is shown in Fig. 3.8. A PVA coating of 20 µm thickness covers the IDC. The PVA complex permittivity for different humidity conditions were obtained from [32]. Fig. 3.8 shows that the sensing RCS$_S$ response decreases with increasing humidity while the reference RCS$_R$ response remains unchanged. To demonstrate the humidity sensing capability of the sensing tag and its feasibility in monitoring the equilibrium water concentration of packaged food commodities, a saturated salt solution test is used. The tag is enclosed in a 200 ml chamber together with a 20 ml saturated salt solution, such that the chamber mimics a packaged environment. The chamber is placed 80 cm

from the interrogation setup as shown in Fig. 3.6. Two sets of measurements were performed for the two orthogonal polarizations corresponding to RCS_S and RCS_R, respectively by rotating both of the transmit and receive antenna, for each saturated salt solution. Alternatively, the sensor tag may be rotated 45^0 to read both signatures simultaneously without changing the interrogator orientation antennas. Fig. 3.9 shows sample RCS responses of the sensing tag at two different humidity conditions. Both the resonant frequency and amplitude of the RCS_S signature shift with a change in relative humidity, while the RCS_R signature remains unaffected. These measurements are a very close fit to that of Fig. 3.8 in both amplitude and frequency. The quality factor and the phase response (Fig. 3.9b) of the RCS_S also decreases with an increase in the humidity. In this chapter we report the differential change in the peak amplitude of the RCS response. However, a differential phase sensing scheme can also be employed as an additional parameter to improve the reliability of the humidity measurements.

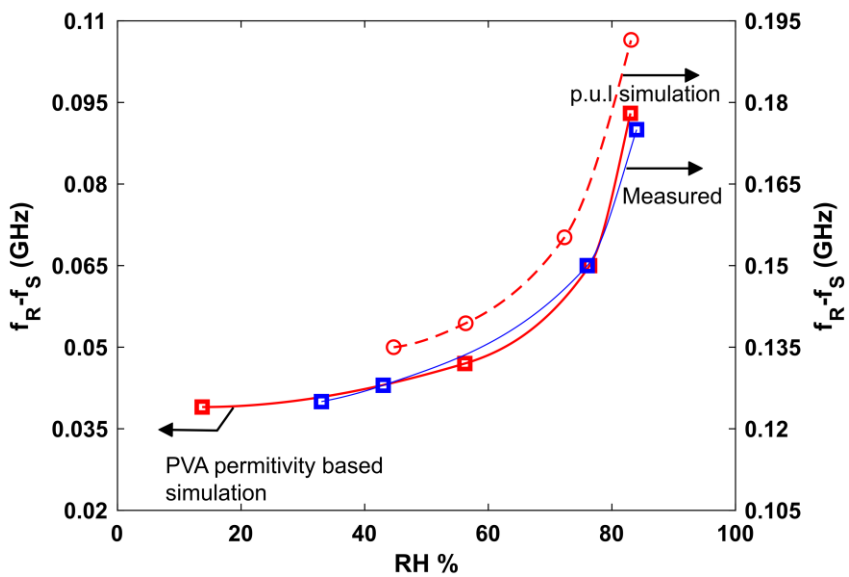

Fig. 3.10 Measured and simulated differential resonant frequency vs the equilibrium relative humidity for the annular slot ring sensor with a PVA coated IDC. Discrete markers indicate data points, and the solid line is the non-linear interpolated fit. The measured data were obtained using the 800 min data points of the time response obtained using the saturated salt solution test (see Fig. 11). Circles indicate the HFSS simulation results obtained using the per-unit-length parameters of Fig. 4. Red squares-indicate the HFSS simulation results obtained using the permittivity values from [32].

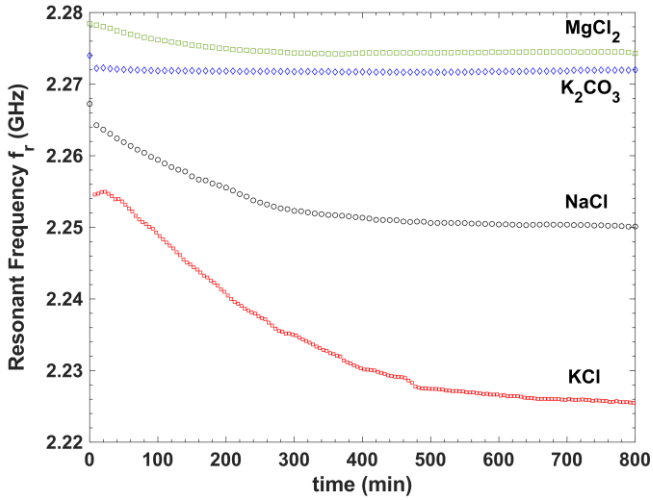

Fig. 3.11 Measured time response of the resonant frequency with time for different saturated salt solutions obtained using the wireless interrogation setup shown in Fig. 6. Note that the initial room humidity is not controlled and varies with background room RH when measurements were carried out.

Fig. 3.10 shows the comparison of the simulated and the experimentally measured differential frequency change ($f_R - f_S$) for different humidity values. The results agree with each other in terms of resonant frequency change for both the IDC model of Fig. 3.4 and the permittivity model from

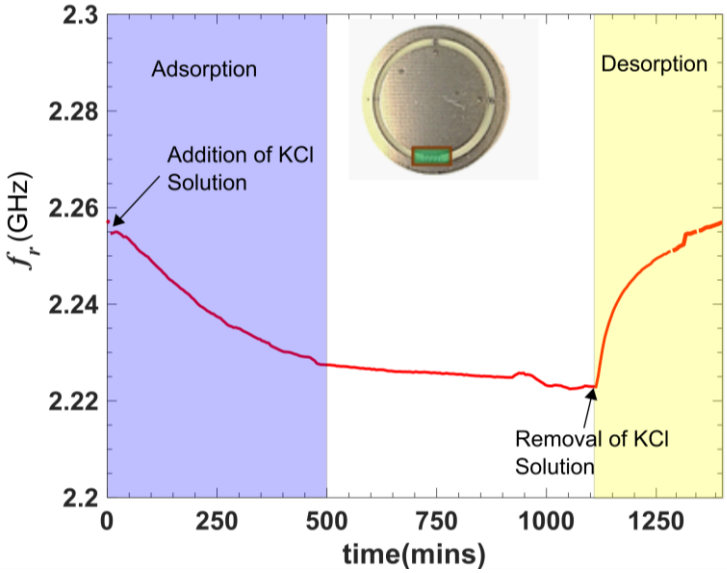

Fig. 3.12. Change in resonant frequency of the sensing tag with adsorption and desorption of water vapor for the saturated KCl test. Inset shows the fabricated sensor with functionalized IDC.

[32]. Note that though there is an offset in the frequency axes, the scales are the same. The frequency offset between the two cases may be attributed to parasitic capacitances and differences due to manufacturing tolerances, which are not included in the model.

Table 3.2

Comparison of the proposed tag with other chipless wireless humidity sensors in literature

	Resonant element	Detection method	Sensing material and coating area	Sensor size	Reference signal for differential sensing	Sensitivity * (RH range)	Printability demonstrated
[22]	Electric field coupled inductor-capacitor resonator	Transmission minima frequency change	PVA – entire resonator	0.132 λ	No	0.001 /RH% (35% - 85%)	No
[42]	Multi element loops	RCS maxima frequency change	Silicon nano-wire selective coating	0.374 λ	Additional element	0.00045 /RH% (74% - 98%)	No
[43]	Frequency selective surface	Reflection minima frequency change	Paper superstrate cover	0.45 λ	No	0.001 /RH% (50% - 90%)	Yes
[44]	Van-Atta array antenna	Processed echo response	Kapton – entire Substrate	5.92 λ	No	– (35% - 75%)	Yes
This work	Annular slot ring antenna	RCS maxima resonant frequency change	PVA coated IDC	0.285 λ	Integrated	0.001 /RH% (33% - 85%)	No

*$sensitivity = (\Delta f_{RH}/f_{RH})/\Delta RH\%$

Fig. 3.11 shows the measured time response of resonant frequency, beginning from room humidity, for different saturated salts. The resonant frequencies, in this case, were obtained by curve fitting the maxima of the RCS magnitude curves. To demonstrate the reversibility of the sensor Fig. 3.12 shows the adsorption and desorption for the KCl saturated salt case (RH of 83%). The sensor response reaches equilibrium at 500 mins and stays stable. At 1100 mins the KCl solution was removed, and the RH was allowed to return to the environment level. The resonant frequency returns to the initial level indicating minimum hysteresis of PVA as previously indicated in [22], making it suitable for a wide range of applications. Table 3.2 shows a comparison of the

sensor tag presented in this work with other chipless, passive humidity sensor in literature. The tag integrates backscattering signals for both the sensing and reference signals into the same antenna element. This enables the tag to be small in size while still providing for differential sensing capability.

3.5. Conclusion

This chapter presents a dual-band, dual-polarized annular slot ring chipless sensing tag for its application in moisture content monitoring in the headspace regions of hermetically packaged food products. The proposed chipless sensor employs an integrated reference signal within the same antenna structure. This eliminates the need for an additional antenna element for reference, keeping the size of the sensor compact. At low humidity conditions, and for the PVA thickness of 20 μm (measured it with profilometer), the sensor provides a high Q and high magnitude response but at lower sensitivity. At high humidity conditions, the sensor gives a higher sensitivity but at the expense of quality factor and RCS magnitude. An optimum response of the tag for applications involving different RH conditions for different food commodities may be achieved by appropriate selection of the PVA thickness. The integration of the reference signal into the sensor allows differential sensing and helps mitigate the detuning effects of the packaging environment. The sensor can be effectively used in low clutter environments, such as a factory or warehouse facility, this being suited to situations when the package integrity is required to be tested after packaging and before shipping. In such a scenario, the packaged commodity is usually on a moving conveyer belt, where in addition to easy background subtraction and time-gated measurements, the doppler shift caused by moving targets may be used to remove unwanted stationary clutter [45]. Additionally, signal processing techniques presented in [46] [47] can be used to reduce the effect of clutter and better estimate the resonance frequency. Techniques like, 45^0 rotation of the tag, short-time Fourier transform and matrix pencil method described in [48] [49] may also further be used to remove effects of the environmental clutter and obtain aspect independent detection.

3.6. Acknowledgment

The authors thank the University of Manitoba Imaging Laboratory and Antenna Laboratory for providing the anechoic chamber required for the experiments and the University of Manitoba's Advanced RF Systems laboratory for providing instrumentation and technical expertise.

3.7. References

[1] R. S. Singhal, P. R. Kulkarni, and D. V. Rege, *Handbook of indices of food quality and authenticity*. Woodhead Pub, 1997.

[2] G. V. Barbosa-Cánovas, *Water activity in foods : fundamentals and applications*. Blackwell Pub, 2007.

[3] B. Barker, "Post-Harvest Storage of Pulses Tips For Safe Storage Seed Moisture Content at Harvest," *Saskatchewan Pulse Growers*\.

[4] W. Strauch, Y. Wild, and R. Scharnow, *Container Handbook*, 1st ed. Germany: Marine and Loss Prevention Department of GDV, German Insurance Association, 2008.

[5] T. De Bruin, S. Navarro, P. Villers, and A. Wagh, "Worldwide use of Hermetic Storage for the Preservation of Agricultural Products," in *9th International Controlled Atmosphere & Fumigation Conference*, 2012, pp. 15–19.

[6] D. S. Jayas and S. Jeyamkondan, "PH—Postharvest Technology: Modified Atmosphere Storage of Grains Meats Fruits and Vegetables," *Biosyst. Eng.*, vol. 82, no. 3, pp. 235–251, Jul. 2002.

[7] S. N. Chulze, "Strategies to reduce mycotoxin levels in maize during storage: a review," *Food Addit. Contam. Part A*, vol. 27, no. 5, pp. 651–657, May 2010.

[8] R. Gregori, P. Meriggi, A. Pietri, S. Formenti, G. Baccarini, and P. Battilani, "Dynamics of fungi and related mycotoxins during cereal storage in silo bags," *Food Control*, vol. 30, no. 1, pp. 280–287, Mar. 2013.

[9] R. Bartosik, "An Inside Look at the Silo-Bag System," in *Int. Conf. on Controlled Atmosphere and Fumigation in Stored Products*, 2012, pp. 117–128.

[10] R. Abalone, A. Gastón, R. Bartosik, L. Cardoso, and J. Rodríguez, "Gas concentration in the

interstitial atmosphere of a wheat silo-bag. Part II: Model sensitivity and effect of grain storage conditions," *J. Stored Prod. Res.*, vol. 47, no. 4, pp. 276–283, Oct. 2011.

[11] R. Bartosik, L. Cardoso, and J. Rodríguez, "Early Detection of Spoiled Grain Stored in Hermetic Plastic Bags (Silo-bags) Using CO2 Monitoring," in *8th International Conference on Controlled Atmosphere and Fumigation in Stored Products*, 2008, pp. 550–554.

[12] V. Chelladurai, F. Jian, D. S. Jayas, N. D. G. White, A. Manickavasagan, and P. G. Fields, "Quality changes in 12% moisture content canola stored in silo bags under Canadian Prairie conditions," *J. Stored Prod. Res.*, vol. 68, pp. 33–43, Jul. 2016.

[13] P. Fathi, N. C. Karmakar, M. Bhattacharya, and S. Bhattacharya, "Potential Chipless RFID Sensors for Food Packaging Applications: A Review," *IEEE Sensors Journal*, vol. 20, no. 17. Institute of Electrical and Electronics Engineers Inc., pp. 9618–9636, 01-Sep-2020.

[14] R. Raju, G. E. Bridges, and S. Bhadra, "Wireless passive sensors for food quality monitoring: Improving the safety of food products," *IEEE Antennas Propag. Mag.*, vol. 62, no. 5, pp. 76–89, Oct. 2020.

[15] R. A. Potyrailo, N. Nagraj, Z. Tang, F. J. Mondello, C. Surman, and W. Morris, "Battery-free radio frequency identification (RFID) sensors for food quality and safety.," *J. Agric. Food Chem.*, vol. 60, no. 35, pp. 8535–43, Sep. 2012.

[16] Y. F. Weng, S. W. Cheung, T. I. Yuk, and L. Liu, "Design of Chipless UWB RFID System Using A CPW Multi-Resonator," *IEEE Antennas Propag. Mag.*, vol. 55, no. 1, pp. 13–31, Feb. 2013.

[17] D. Dominic, S. Krafft, N. Safdari, and S. Bhadra, "Multiresonator-Based Printable Chipless RFID for Relative Humidity Sensing," *Proceedings*, vol. 1, no. 4, p. 367, Aug. 2017.

[18] E. M. Amin and N. Karmakar, "Development of a chipless RFID temperature sensor using cascaded spiral resonators," in *2011 IEEE Sensors Proceedings*, 2011, pp. 554–557.

[19] E. M. Amin and N. C. Karmakar, "Development of a low cost printable humidity sensor for chipless RFID technology," in *2012 IEEE International Conference on RFID-Technologies and Applications (RFID-TA)*, 2012, pp. 165–170.

[20] J.-H. Sun *et al.*, "Wireless Saw-Based Tags with Temperature Sensors that Utilize High-Resolution Delay-Time Measurements," *J. Mech.*, vol. 32, no. 04, pp. 435–440, Aug. 2016.

[21] S. Harma, W. G. Arthur, C. S. Hartmann, R. G. Maev, and V. P. Plessky, "Inline SAW RFID tag using time position and phase encoding," *IEEE Trans. Ultrason. Ferroelectr. Freq.*

Control, vol. 55, no. 8, pp. 1840–1846, Aug. 2008.

[22] E. M. Amin, N. Karmakar, and B. Winther-Jensen, "Polyvinyl-Alcohol (PVA)-Based RF Humidity Sensor in Microwave Frequency," *Prog. Electromagn. Res. B*, vol. 54, pp. 149–166, 2013.

[23] A. Vena, L. Sydänheimo, M. M. Tentzeris, and L. Ukkonen, "A Fully Inkjet - Printed Wireless and Chipless Sensor for CO2 and Temperature detection," *IEEE Sens. J.*, vol. 15, no. c, pp. 89–99, Jan. 2014.

[24] C. Mandel, H. Maune, and M. Maasch, "Passive wireless temperature sensing with BST-based chipless transponder," in *German Microwave Conference (GeMIC)*, 2011.

[25] E. M. Amin, N. C. Karmakar, and B. W. Jensen, "Fully Printable Chipless RFID Multi-parameter Sensor," *Sensors Actuators A Phys.*, Jul. 2016.

[26] B. Kubina, C. Mandel, M. Schussler, M. Sazegar, and R. Jakoby, "A wireless chipless temperature sensor utilizing an orthogonal polarized backscatter scheme," in *2012 42nd European Microwave Conference*, 2012, pp. 61–64.

[27] R. K. Schneider, "A re-look at antenna in-band RCSR via load mismatching," in *IEEE Antennas and Propagation Society International Symposium. 1996 Digest*, vol. 2, pp. 1398–1401.

[28] J.-L. Dellis, "Zfit - Matlab Function," 2010. [Online]. Available: https://www.mathworks.com/matlabcentral/fileexchange/19460-zfit. [Accessed: 21-Dec-2017].

[29] PAMI, "Equilibrium Moisture Content Charts for Grain Storage Management," Humboldt, 2012.

[30] L. Greenspan, "Humidity fixed points of binary saturated aqueous solutions," *J. Res. Natl. Bur. Stand. Sect. A Phys. Chem.*, vol. 81A, no. 1, p. 89, 1977.

[31] Sensirion "Datasheet SHT7.", Version 5, Dec. 2011.

[32] D. Lu, M. Maasch, A. Penirschke, Y. Zheng, C. Damm, and R. Jakoby, "Broadband Permittivity Characterization of Polyvinyl-Alcohol Film for Humidity Sensing Applications," *IEEE Trans. Microw. Theory Tech.*, vol. 64, no. 10, pp. 3255–3263, 2016.

[33] D. R. Paul, "Water vapor sorption and diffusion in glassy polymers," *Macromol. Symp.*, vol. 138, no. 1, pp. 13–20, Mar. 1999.

[34] Jin Soo Kim and Dai Gil Lee, "Analysis of dielectric sensors for the cure monitoring of resin

matrix composite materials," *Sensors Actuators B Chem.*, vol. 30, no. 2, pp. 159–164, Jan. 1996.

[35] H.-E. Endres and S. Drost, "Optimization of the geometry of gas-sensitive interdigital capacitors," *Sensors Actuators B Chem.*, vol. 4, no. 1–2, pp. 95–98, May 1991.

[36] M. Penza and V. I. Anisimkin, "Surface acoustic wave humidity sensor using polyvinyl-alcohol film," *Sensors Actuators A Phys.*, vol. 76, no. 1–3, pp. 162–166, Aug. 1999.

[37] K. D. Stephan, N. Camilleri, and T. Itoh, "A Quasi-Optical Polarization-Duplexed Balanced Mixer for Millimeter-Wave Applications," *IEEE Trans. Microw. Theory Tech.*, vol. 31, no. 2, pp. 164–170, Feb. 1983.

[38] R. Garg, Ed., *Microstrip Antenna Design Handbook*. Artech, 2001.

[39] C.-S. Hong, "Small annular slot antenna with capacitor loading," *Electron. Lett.*, vol. 36, no. 2, p. 110, 2000.

[40] M. I. Grace, "Measurement of Radar Cross Section Using the 'VNA Master' Handheld VNA," *Anritsu Appl. Note*, pp. 1–9.

[41] C. W. Trueman, S. R. Mishra, C. L. Larose, and R. K. Mongia, "Computation and Measurement of the Resonant Frequencies and Q Factors of High-Permittivity Dielectric Resonators," *Symp. Antenna Technol. Appl. Electromagn.*, pp. 395–402, 1994.

[42] A. Vena, E. Perret, D. Kaddour, and T. Baron, "Toward a Reliable Chipless RFID Humidity Sensor Tag Based on Silicon Nanowires," *IEEE Trans. Microw. Theory Tech.*, vol. 64, no. 9, pp. 2977–2985, Sep. 2016.

[43] M. Borgese, F. A. Dicandia, F. Costa, S. Genovesi, and G. Manara, "An Inkjet Printed Chipless RFID Sensor for Wireless Humidity Monitoring," *IEEE Sens. J.*, vol. 17, no. 15, pp. 4699–4707, Aug. 2017.

[44] D. Henry, J. G. D. Hester, H. Aubert, P. Pons, and M. M. Tentzeris, "Long-Range Wireless Interrogation of Passive Humidity Sensors Using Van-Atta Cross-Polarization Effect and Different Beam Scanning Techniques," in *IEEE Transactions on Microwave Theory and Techniques*, 2017, vol. 65, no. 12, pp. 5345–5354.

[45] M. A. Richards, *Fundamentals of radar signal processing*, 2nd ed. New York, NY: McGraw-Hill, 2014.

[46] A. Fawky, M. Khaliel, A. El-Awamry, M. El-Hadidy, and T. Kaiser, "Novel Pseudo-Noise coded chipless RFID system for clutter removal and tag detection," in *2015 IEEE*

International Conference on RFID (RFID), 2015, pp. 100–104.

[47] F. Costa *et al.*, "Robust Reading Approach for Moving Chipless RFID Tags by Using ISAR Processing," *IEEE Trans. Microw. Theory Tech.*, vol. 66, no. 5, pp. 2442–2451, May 2018.

[48] A. Ramos, E. Perret, O. Rance, S. Tedjini, A. Lazaro, and D. Girbau, "Temporal Separation Detection for Chipless Depolarizing Frequency-Coded RFID," *IEEE Trans. Microw. Theory Tech.*, vol. 64, no. 7, pp. 2326–2337, Jul. 2016.

[49] Z. Ali, E. Perret, N. Barbot, and R. Siragusa, "Extraction of Aspect-Independent Parameters Using Spectrogram Method for Chipless Frequency-Coded RFID," *IEEE Sens. J.*, Mar. 2020.

Chapter 4.

RCS Based Depolarizing Passive Tag with Improved Clutter Rejection for Potentiometric Gas Sensing

In chapter 3 RCS based tag was presented for its application in relative humidity monitoring was presented. In the current chapter the dual-band, dual-polarized antenna is modified to operate in depolarizing mode and is applied to monitor ammonia by integrating with it a varactor coupled hydrogel-coated pH electrode. The presented sensor is smaller in size and has superior immunity to environmental clutter. This chapter is based on the published paper "**R. Raju** and G. E. Bridges, "RCS Based Depolarizing Passive Tag with Improved Clutter Rejection for Potentiometric Gas Sensing," in *2019 IEEE SENSORS*, 2019, pp. 1–4."

4.1. Abstract

This chapter presents a radar cross-section (RCS) based tag capable of detecting acidic/basic volatiles in the sensing environment. The sensor consists of two miniaturized annular slot antennas. One acts as the sensing element and the other as the reference. Both antennas are perturbed to provide a high cross-polarized scattering response. The cross-polarization-based interrogation technique provides robust detection against environmental scattering. A pH combination electrode coupled to a varactor diode provides the necessary transduction required for gas sensing. The concentration of the gas being monitored directly translates to the resonant frequency modulation of the sensing antenna.

4.2. Introduction

Passive wireless tags operating in the microwave region have been of great interest in the past decade for their application in RFID and sensing [1]-[9]. Conventional RFID tags and sensors require integrated chips and often batteries for their operation. This limits their application due to the manufacturing and maintenance cost involved. Passive, chipless tags provide the advantage of being significantly cheaper, thereby expanding their scope of application to low cost item level tagging and sensing of low value commodities such as fresh produce.

One of the biggest challenges in using chipless passive RFID sensors is making them robust to environmental clutter and loading effects. Clutter is the unwanted signal scattered by the environment, picked up by the interrogator. With chipless sensors being of small size, the signatures can be overwhelmed by large objects in the environment, making detection difficult. One of the ways by which the effect of environmental clutter can be reduced is to make the scattering from the sensing element as large as possible. This has been done using two methods, one by using a retrodirective array antenna like Van-Atta reflect array as the scattering element [10],[11], and the second by using an active negative resistance load on the scattering antenna [12]-[15]. A hybrid combination of both, using a reflection amplifier with the retrodirective reflector-Van Atta array has also been demonstrated [16], [17]. As Van-Atta reflect arrays are of large size, it is generally suited for applications in higher millimeter wave frequencies. Negative resistance loading on the other hand requires an active element and related biasing circuit on the sensor making it incompatible with low cost roll-to-roll printing technology. Frequency diversity between the incident interrogation signal and the scattered/retransmitted signal can also be used in quasi-chipless sensors utilizing a nonlinear component like a diode. This technique has been demonstrated in sensing of various physical parameters like crack and strain [18], [19], liquid level [20], temperature [21]-[23] and humidity [24]. These tags have also been reported for tracking of small insects like bees [25], [26]. One of the disadvantages of using passive harmonic sensors, however, is that they require high transmitted power for interrogation due to the power loss associated with the passive generation of the harmonic frequency. These sensors are of larger size compared to the RCS counterpart, as most of them utilize separate antennas for reception and transmission.

Another method to reduce the clutter is by using a depolarizing/cross-polarizing scattering element such as a dipole oriented at 45° to the polarization of the incident interrogating wave as proposed in [27]-[29]. Though this technique has successfully shown to eliminate clutter close to the scatterer for RCS based RFID systems, little work has been done towards integrating them for sensors application. In this chapter the objective is to design and present an RCS based pH sensing tag with a cross- polarization detection scheme. The sensor consists of two miniaturized annular slot antennas, one of which acts as a reference and the other as the sensing unit. Together with cross-polar detection, added reference and time gated measurements, the presented tag provides superior imunity against environmental scattering.

4.3. Concept of Operation, Sensor design and Simulation Results

Radar polarimetry is often used to enhance the detection of an object. Polarimetry involves the characterization of a target using its complete scattering matrix parameters. This is done by measuring the co-polarized and cross-polarized responses of the target. The co-polarized response corresponds to the case where polarizations of the transmit and receive signals the are identical, while the cross-polarized response corresponds to transmission and reception in orthogonal polarizations. The sources of scattering in the indoor environment are large reflective objects, like furniture, ground and walls. Since these objects are large compared to the wavelength at microwave frequencies, it can be reasonably assumed that the scattered field from these objects are dominantly co-polarized, meaning they have little cross-polarized scattering response. Thus, a scattering source with high cross-polarization response can be used to achieve maximum signal-to-clutter ratio. Mathematically the radar cross-section of a target can be represented by using its associated scattering matrix,

$$S = \begin{pmatrix} S_{vv} & S_{vh} \\ S_{hv} & S_{hh} \end{pmatrix}. \tag{1}$$

Here identical subscripts represent co-polarized component and dissimilar subscripts represent the cross-polarized component. The scattering matrix of manmade objects, which exhibit a dominantly co-polarized response simplifies to

$$S_{clt} \approx \begin{pmatrix} S_{vv} & 0 \\ 0 & S_{hh} \end{pmatrix}. \tag{2}$$

For a scattering element like a planar antenna, the scattered fields consist of two parts- the structural field and the antenna model or re-radiated fields. The structural field is a combination of both antenna structural scattering and the ground plane scattering. The total received field is the vectoral sum of the three fields. For enhancing the detection capability of such an antenna, the scattering field must be

$$S_{sen} = \begin{pmatrix} \sim 0 & \sim 1 \\ \sim 1 & \sim 0 \end{pmatrix}. \tag{3}$$

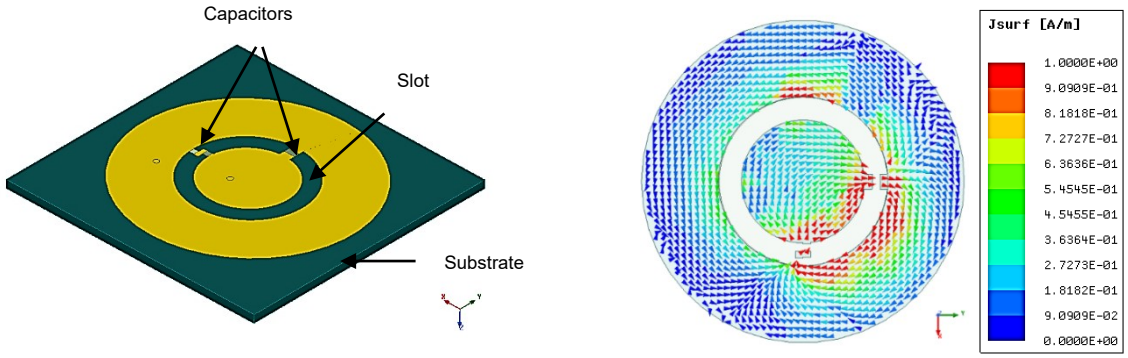

Fig. 4.1 (Left) Annular slot antenna with capacitive loading at two orthogonal sites. (Bottom) The current distribution at resonance of the annular slot antenna when excited by an incident vertically polarized plane wave.

From the total received response, $S_{tot} = S_{clt} + S_{sen}$, the scattering response of the sensing element can be easily extracted from the anti-diagonal elements of S_{tot}. To meet the antenna design objectives above and provide design flexibility, an annular ring slot is used. To achieve a high cross-polarized component for an incident vertical or horizontally polarized interrogating signal, two lumped capacitors are added in orthogonal to each other, as shown in Fig. 4.1. The capacitance however has to be large enough to provide a reasonably low impedance at the design frequency, so that the currents are perturbed adequately in the orthogonal direction to the incident signal. For a vertically polarized incident wave, significant amount of surface currents are directed towards the horizontal direction and vice versa. This is shown in Fig. 4.1

An additional radiating slot tuned to a secondary resonant frequency using a slightly different capacitive loading is added to serve as the reference signature to enable differential sensing capability. The volatile sensing capability is achieved by using the same approach as described in [30], [31]. On the sensing slot, a varactor provides the required capacitance for cross-polarization excitation and the volatile sensing capability. A bias voltage applied through a pH combination electrode consisting of a silver-silver chloride (Ag/AgCl) reference electrode and a mixed metal oxide (MMO) working electrode, modulates the varactor capacitance, which in turn changes the resonant frequency of the antenna. Fig. 4.2 (inset) shows the proposed tag structure and the simulated results of the sensor. The simulations were performed in HFSS, and the varactor was modeled as a variable lumped capacitor. As seen from the results, the reference signature remains constant and the sensing signature shows change in the resonant frequency with a change in the

capacitance. The sensing and reference antennas are on the top side of the PCB while the sensing circuit including the pH electrodes are designed to be implemented on the bottom side.

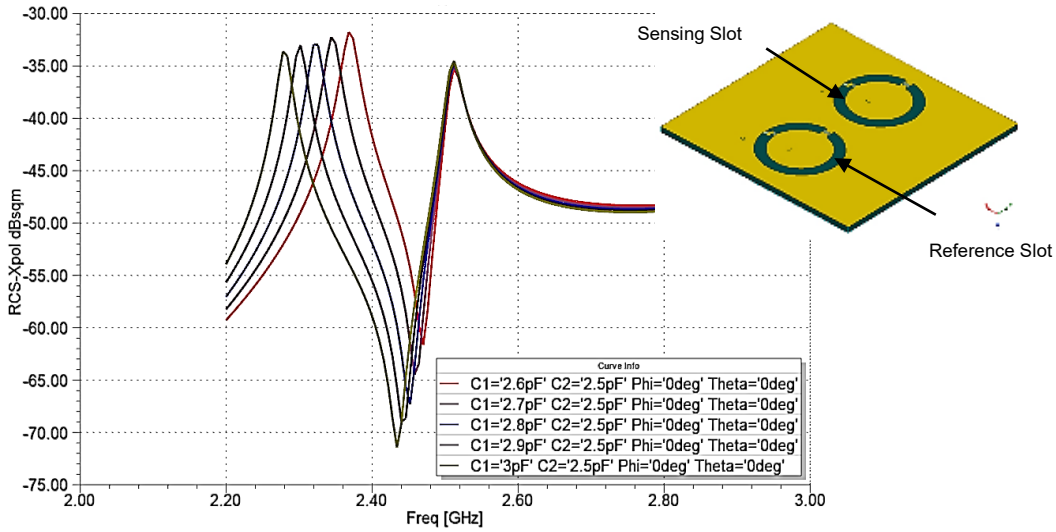

Fig. 4.2 HFSS simulation results showing the X-pol response of the proposed wireless sensor, C1 corresponds to the sensing capacitance and C2 corresponds to the reference capacitance.

4.4. Experiments and Discussion of Results

The pH combination electrode pair was first tested for different concentrations of ammonia levels, inside a sealed gas chamber as shown in Fig. 4.3. Ag/AgCl reference electrodes were fabricated using the procedure in [32]. Low cost commercial MMO electrodes were obtained from a Chinese manufacturer. The voltage generated by the electrodes was measured using Agilent 34401A multimeter. The pH electrodes produce a linear voltage response to the log concentration of the gas under test. Fig. 4.4 shows the set up used to measure the scattering response of the designed tag in an anechoic chamber. It consists of two horn antennas of 9 dBi gain connected to a VNA. The two antennas are oriented orthogonal to each other to receive the cross-polarized response of the tag. The antennas were loaded with fixed capacitors to obtain the static response for the sensor. The measured response is shown in Fig. 4.5. Tests were also done to demonstrate the clutter rejection capability of the tag. This is shown in Fig. 4.6, where scattering elements were placed inside the radian sphere region of the tag. The presence of the scattering objects has a loading effect on the antenna. However, the shape is preserved and the difference between the reference and sensing resonances remain unchanged. This difference thereby can be used further for differential sensing of the desired pH change in the environment.

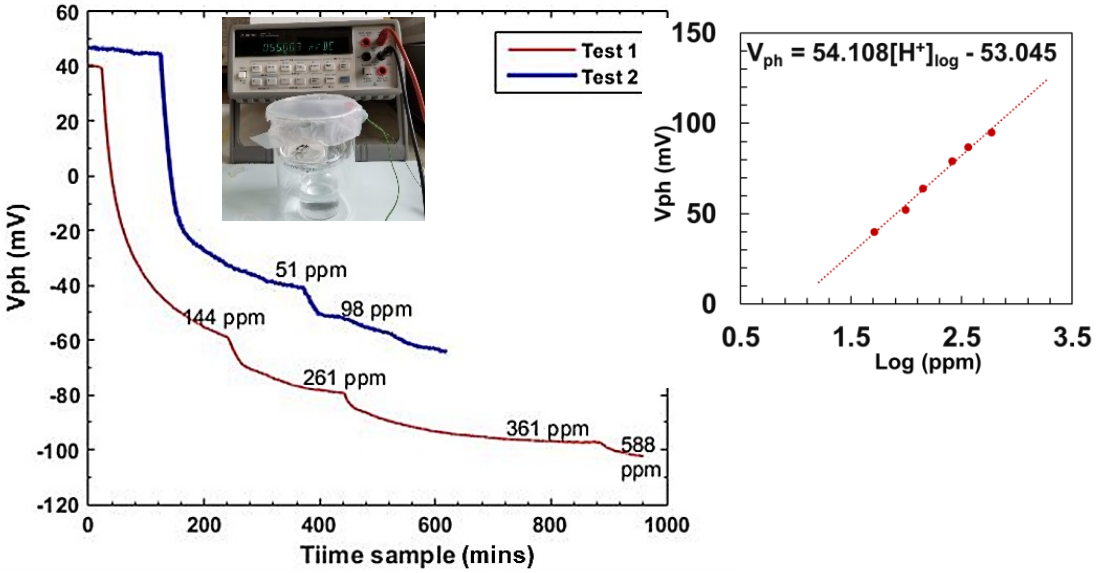

Fig. 4.3 Experimental results showing the generated potential of an MMO-Ag/AgCl combination electrode pair to different concentrations of ammonia vapor inside a sealed chamber.

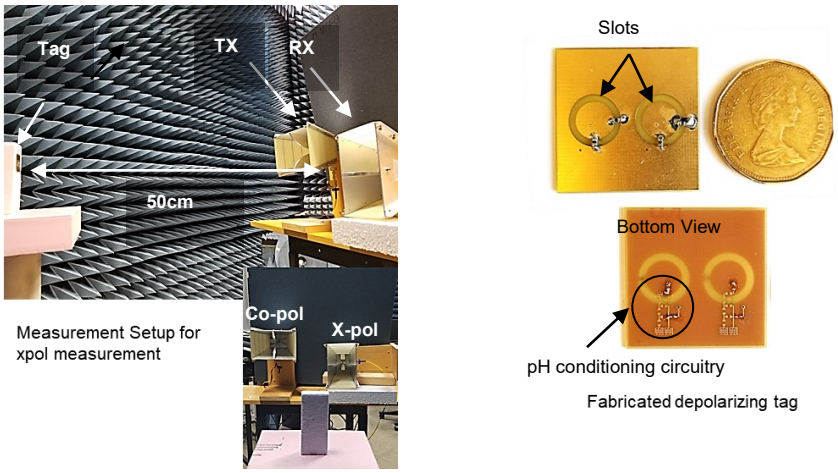

Fig. 4.4 (Left) Experimental setup used for the measurement of the cross-polarization measurement of the annular slot antenna. (Right) Fabricated tag with fixed capacitor loading

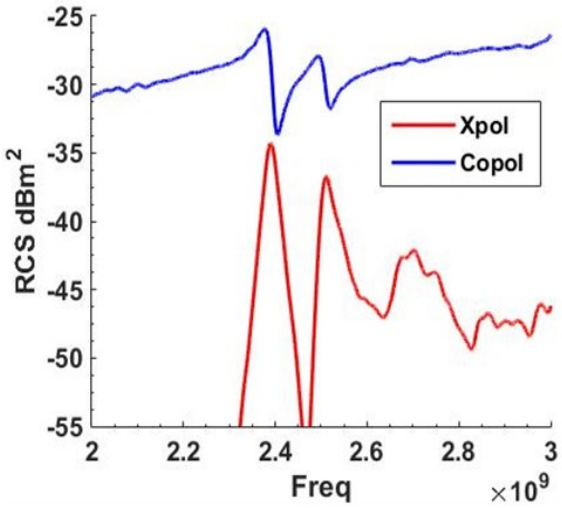

Fig. 4.5 Measurement results showing the RCS co-pol and cross-pol responses of the capacitively loaded annular slot antennas.

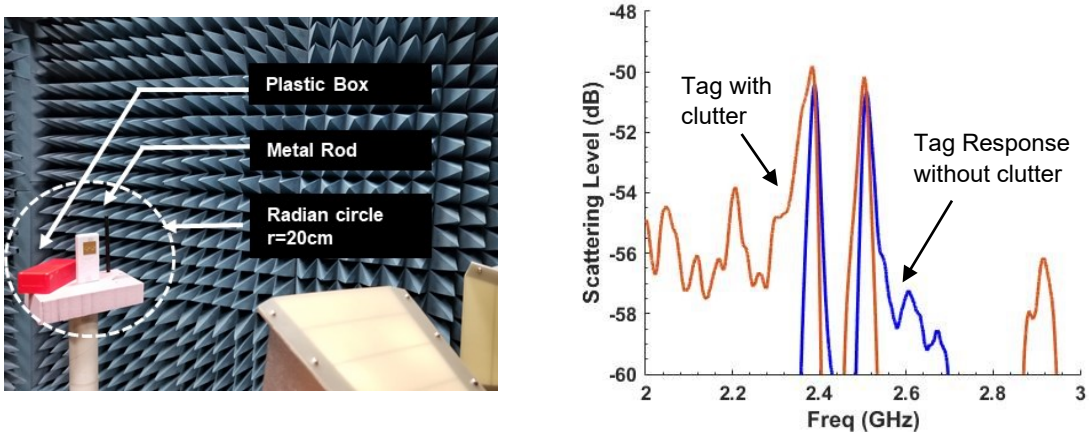

Fig. 4.6 (Left) Experimental set up used to demonstrate the clutter rejection capability of the depolarizing antenna. (Right) Measurement results showing the RCS co-pol and cross-pol response of the capacitively loaded annular slot in the presence of scattering elements inside the radian sphere of the tag.

Fig. 4.7a shows the experimental setup used to demonstrate the sensing capability of the depolarizing tag integrated with SMV1405 varactor biased using the hydrogel coated pH electrode pair presented in the previous section. The sensor was placed at a distance of 60 cm from the interrogating horn antennas inside a sealed chamber consisting of a beaker of variable ammonium

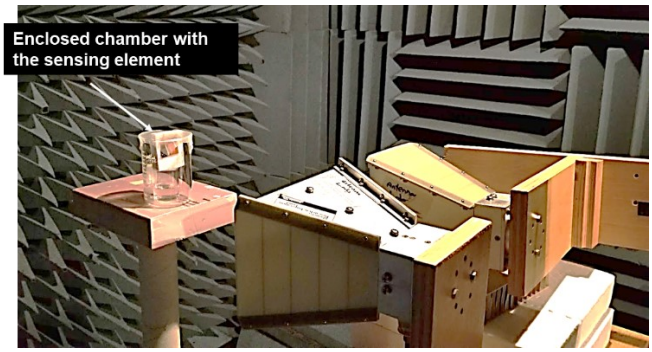

(a)

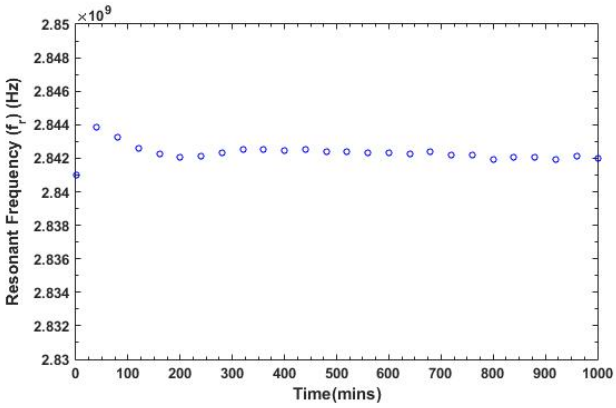

(b)

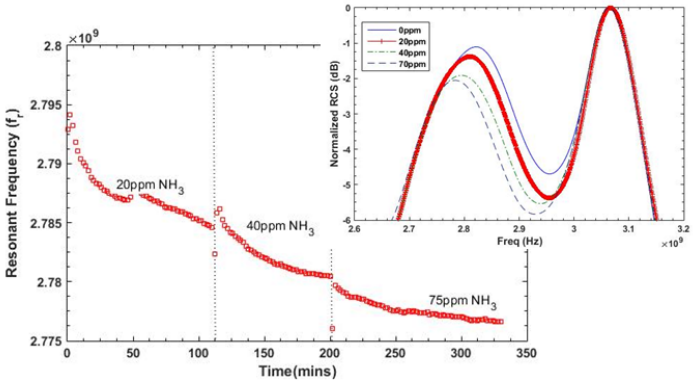

(c)

Fig. 4.7 (a) Experimental set-up and fabricated depolarizing tag used for volatile sensing. (b) Change in resonant frequency of the depolarizing RCS based sensor to different concentration of ammonia gas (inset is the measured normalized RCS response showing the reference and sensing signatures obtained using late time short time fourier transform response).

hydroxide solution. Initial experiment with 0 ppm ammonia was performed to assess the stability

of the sensor, this is shown in Fig. 4.7b. The sensor reaches a 90% of the stability point at around the 100 min mark. After this, different concentrations of ammonium hydroxide were added into the chamber, as the concentration of ammonia inside the chamber increases, the resonant frequency of the sensing resonator goes down and the resonant frequency of the reference resonator remains unchanged (Fig. 4.7c).

4.5. Conclusion

A depolarizing annular ring tag for volatile sensing applications was presented in this chapter. The cross-polarizing property of the tag was shown to be robust against environmental scattering. This was demonstrated using non resonant objects in near-field zone of the antenna. This improves its practicality compared to traditional radar cross-section-based sensing tags. The ammonia sensing capability of the sensor was demonstrated using a pH electrode biased varactor tuning element added onto one of the resonant slots and keeping another resonant slot as a reference for differential sensing capability. Further study is required towards the improvement of the stability and repeatability of the pH combination electrode pair.

4.6. References

[1] Y. F. Weng, S. W. Cheung, T. I. Yuk, and L. Liu, “Design of chipless UWB RFID system using a CPW multi-resonator,” IEEE Antennas Propag. Mag., vol. 55, no. 1, pp. 13–31, Feb. 2013.

[2] D. Dominic, S. Krafft, N. Safdari and S. Bhadra, "Multiresonator-Based Printable Chipless RFID for Relative Humidity Sensing", Eurosensors Proceedings, vol. 1, no. 4, p. 367, 2017.

[3] E. M. Amin and N. Karmakar, "Development of a chipless RFID temperature sensor using cascaded spiral resonators," Sensors, 2011 IEEE, Limerick, 2011, pp. 554-557.

[4] E. M. Amin and N. C. Karmakar, “Development of a low cost printable humidity sensor for chipless RFID technology,” in 2012 IEEE International Conference on RFID-Technologies and Applications (RFID-TA), 2012, pp. 165–170.

[5] E. M. Amin, N. Karmakar, and B. Winther-Jensen, “Polyvinyl-Alcohol (PVA)-based RF humidity sensor in microwave frequency,” Prog. Electromagn. Res. B, vol. 54, pp. 149–166, 2013.

[6] A. Vena, L. Sydänheimo, M. M. Tentzeris and L. Ukkonen, "A fully inkjet-printed wireless and chipless sensor for CO2 and temperature detection," in IEEE Sensors Journal, vol. 15, no. 1, pp. 89-99, Jan. 2015.

[7] C. Mandel, H. Maune, M. Maasch, M. Sazegar, M. Schüßler and R. Jakoby, "Passive wireless temperature sensing with BST-based chipless transponder," 2011 German Microwave Conference, Darmstadt, 2011, pp. 1-4.

[8] E. M. Amin, N. C. Karmakar, and B. W. Jensen, "Fully printable chipless RFID multi-parameter sensor," Sensors Actuators A Phys., Jul. 2016.

[9] B. Kubina, C. Mandel, M. Schussler, M. Sazegar, and R. Jakoby, "A wireless chipless temperature sensor utilizing an orthogonal polarized backscatter scheme," in 2012 42nd European Microwave Conference, 2012, pp. 61–64.

[10] J. G. D. Hester and M. M. Tentzeris, "Inkjet-printed flexible mm-wave van-atta reflectarrays: a solution for ultralong-range dense multitag and multisensing chipless RFID implementations for iot smart skins," IEEE Trans. Microw. Theory Tech., vol. 64, no. 12, pp. 4763–4773, Dec. 2016.

[11] J. A. Vitaz, A. M. Buerkle, M. Sallin, and K. Sarabandi, "Enhanced detection of on-metal retro-reflective tags in cluttered environments using a polarimetric technique," IEEE Trans. Antennas Propag., vol. 60, no. 8, pp. 3727–3735, Aug. 2012.

[12] R. F. Harrington, "Small resonant scatterers and their use for field measurements," IEEE Trans. Microw. Theory Tech., vol. 10, no. 3, pp. 165–174, May 1962.

[13] R. F. Harrington, "Field measurements using active scatterers (correspondence)," IEEE Trans. Microw. Theory Tech., vol. 11, no. 5, pp. 454–455, Sep. 1963.

[14] J. Kimionis, M. M. Tentzeris, A. Georgiadis, and A. Collado, "Inkjet-printed reflection amplifier for increased-range backscatter radio," 2014 44th European Microwave Conference, Rome, 2014, pp. 5-8.

[15] F. Amato, C. W. Peterson, M. B. Akbar, and G. D. Durgin, "Long range and low powered RFID tags with tunnel diode," 2015 IEEE International Conference on RFID Technology and Applications (RFID-TA), Tokyo, 2015, pp. 182-187.

[16] F. Farzami, S. Khaledian, B. Smida, and D. Erricolo, "Reconfigurable dual-band bidirectional reflection amplifier with applications in Van Atta array," in IEEE Transactions on Microwave Theory and Techniques, vol. 65, no. 11, pp. 4198-4207, Nov. 2017.

[17] P. Chan and V. Fusco, "Bi-static 5.8GHz RFID range enhancement using retrodirective techniques," 2011 41st European Microwave Conference, Manchester, 2011, pp. 976-979.

[18] C. Cho, X. Yi, D. Li, Y. Wang, and M. M. Tentzeris, “Passive wireless frequency doubling antenna sensor for strain and crack sensing,” IEEE Sens. J., vol. 16, no. 14, pp. 5725–5733, 2016.

[19] V. Palazzi et al., “Demonstration of a chipless harmonic tag working as crack sensor for electronic sealing applications,” Wirel. Power Transf., pp. 1–8, Oct. 2015.

[20] H. Huang, P.-Y. Chen, C.-H. Hung, R. Gharpurey, and D. Akinwande, “A zero power harmonic transponder sensor for ubiquitous wireless μL liquid-volume monitoring.,” Sci. Rep., vol. 6, p. 18795, Jan. 2016.

[21] B. Kubina, C. Mandel, M. Schüßler and R. Jakoby, "Compact quasi-chipless harmonic radar sensor with a dielectric resonator antenna," 2015 IEEE MTT-S International Microwave Symposium, Phoenix, AZ, 2015, pp. 1-3.

[22] B. Kubina, J. Romeu, C. Mandel, M. Schüßler and R. Jakoby, "Quasi-chipless wireless temperature sensor based on harmonic radar," in Electronics Letters, vol. 50, no. 2, pp. 86-88, 16 January 2014.

[23] V. Viikari, H. Seppa, T. Mattila and A. Alastalo, "Wireless ferroelectric resonating sensor," in IEEE Transactions on Ultrasonics, Ferroelectrics, and Frequency Control, vol. 57, no. 4, pp. 785-791, April 2010.

[24] A. Lazaro, R. Villarino, and D. Girbau, “A passive harmonic tag for humidity sensing,” International Journal of Antennas and Propagation, vol. 2014, Article ID 670345, 11 pages, 2014.

[25] N. Tahir and G. Brooker, “Toward the development of millimeter wave harmonic sensors for tracking small insects,” vol. 15, no. 10, pp. 5669–5676, 2015.

[26] B. G. Colpitts and G. Boiteau, "Harmonic radar transceiver design: miniature tags for insect tracking," in IEEE Transactions on Antennas and Propagation, vol. 52, no. 11, pp. 2825-2832, Nov. 2004..

[27] A. Vena, E. Perret, and S. Tedjni, “A depolarizing chipless RFID tag for robust detection and its FCC compliant UWB reading system,” IEEE Trans. Microw. Theory Tech., vol. 61, no. 8, pp. 2982–2994, 2013.

[28] O. Rance, R. Siragusa, P. Lemaitre-Auger, and E. Perret, “RCS magnitude coding for chipless RFID based on depolarizing tag,” 2015 IEEE MTT-S Int. Microw. Symp. IMS 2015, pp. 2–5, 2015.

[29] F. Costa, S. Genovesi, and A. Monorchio, “Chipless RFIDs for metallic objects by using cross polarization encoding,” IEEE Trans. Antennas Propag., vol. 62, no. 8, pp. 4402–4407, Aug. 2014.

[30] S. Bhadra, D. Thomson, and G. E. Bridges, "Monitoring acidic and basic volatile concentration using a pH-electrode based wireless passive sensor", Sensors and Actuators B: Chemical, vol. 209, pp. 803-810, 2015.

[31] R. Raju and G. E. Bridges, "Radar cross section based passive wireless sensor for volatile sensing," 2018 18th International Symposium on Antenna Technology and Applied Electromagnetics (ANTEM), Waterloo, ON, 2018, pp. 1-2.

[32] M. a Nolan, S. H. Tan, and S. P. Kounaves, “Fabrication and Characterization of a Solid State Reference Electrode for Electroanalysis of Natural Waters with Ultramicroelectrodes,” *Anal. Chem.*, vol. 69, no. 6, pp. 1244–1247, 1997.

Chapter 5.

A Compact Passive Wireless Harmonic Sensor for Packaged Food Quality Monitoring Applications

In Chapters 3 and 4, radar cross-section-based low-cost sensors were presented for humidity and ammonia sensing respectively. These sensors require a well-calibrated environment for practical applications, thus are limited in application to warehouse like settings where the sensing background can either be easily calibrated or remains constant over the period of measurement. Chapters 5 and 6 present a harmonic sensor that does not require background calibration for their operation, making them more amenable to food monitoring applications further down the food industry supply chain. This chapter is based on the paper "**R. Raju** and G. E. Bridges, "A Compact Passive Wireless Harmonic Sensor for Packaged Food Quality Monitoring," submitted to the *IEEE Trans. Microw. Theory Tech.*, 2021."

5.1. Abstract

There is currently a need to monitor food products while preserving quality and safety during long-term storage. In this paper, a compact low-cost quasi-chipless sensor is presented for monitoring the quality of high-value food items like milk and meat products is presented. The sensor utilizes a dual-band dual-polarized annular ring antenna with an integrated harmonic generator and sensor to receive, modulate, and retransmit the interrogator signal. The resonant frequency of the receiving mode of the antenna is sensitized to the parameter being sensed using a varactor – pH electrode-based transduction scheme. The received signal is doubled using a diode frequency doubler circuit to minimize the clutter from the environment before retransmission. One application of the sensor for monitoring of pH is presented. The sensor was shown to be able to successfully monitor the milk souring process.

5.2. Introduction

Food quality monitoring is crucial for consumers and the food processing industry. Food quality deterioration and extension of shelf life are both of health and economic interest [1], [2].

In recent years smart packaging techniques have gained great popularity. These packages are designed to interact with the food material and its packaged environment in order to provide an extended shelf life of the food products.

Several environmental factors like food temperature, humidity, light, mechanical stress, and pressure affect the quality of food items during long-term storage. Internal factors like initial microbial count, pH and chemical composition affect the rate of degradation of the quality of food products. Additionally, intelligent packaging focuses on the ability to monitor quality indicators inside the packaged food or its environment. Common quality indicators include food freshness indicators, time-temperature indicators, and integrity indicators to detect leaks [1]. Humidity (water activity), temperature and pH are the most essential factors that affect food quality [2], that when monitored and controlled for each specific food commodity, have shown to significantly increase shelf life.

The activity of many pathogens produces chemical bi-products [3], with many of these altering the pH of the food material. For example, microorganisms in meat, like *Enterobacteriaceae*, *Pseudomonas fluorescens* and *Lactobacillus sake* produce various compounds like sulphur-containing molecules, alcohols, acetone, fatty acids, amines and carbon dioxide that alter its pH [4]. Likewise, desserts that are rich in carbohydrates are broken down into simpler molecules like organic acids, ethanol and CO_2 due to microbial action [3]. The detection of spoilage due to microbial action using metabolic biproducts of micro-organisms in different kinds of food can, however, be very distinct from one another. Nevertheless, measurements of these pH and volatile bi-products have successfully been shown to correlate to the microbial count in the food material [5]. The total volatile base nitrogen (TVB-N) and trimethylamine (TMA), for instance are used worldwide as indicators of fish quality and decomposition [6].

With the advancements in printed electronics and material science, package to package non-contact monitoring of volatile gases of high-value food products like milk, fish and meat has been made feasible [1]. One of the most commonly used for detection of acidic/basic biproducts use colorimetric dye-based sensors, that give a qualitative indication of the extent of microbial activity [7][8][9][10]. A viable approach that gives a semi-quantitative insight into microbial activity is through the integration of sensing circuitry into passive RFIDs. The integrated circuit for the

modulation, retransmission and sensing however make them comparatively expensive to techniques that do not require additional sensing circuitry, as shown in [11][12]. These sensors predominantly work via the dielectric loading effect on the RFID antennas. Passive-chipless sensors are another alternative, however, these sensors are limited in practical application due to the high clutter from the sensing environment [13][14]. Several researchers have extended the detection capability of the passive-chipless RFID by using frequency diversity between the incident interrogation signal and the scattered/retransmitted signal, thereby, improving clutter rejection [17][18][19][20]. This is made possible by using a nonlinear element like a diode, either as a passive harmonic frequency generator or a passive mixer, to produce a backscattered signal at

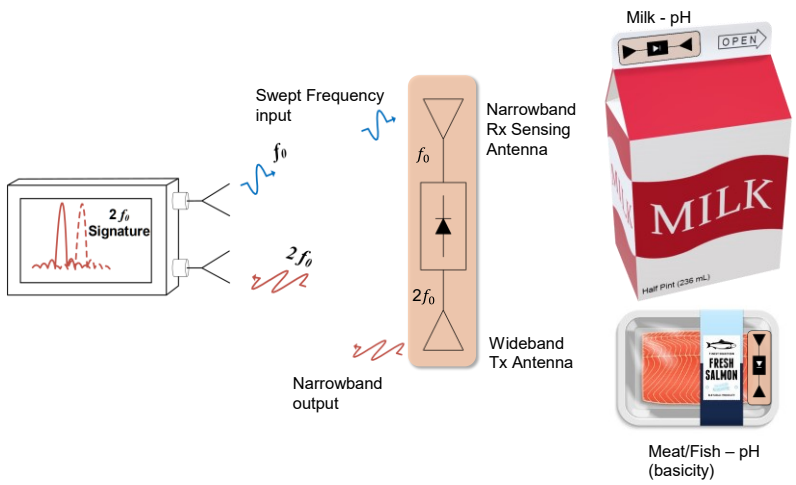

Fig. 5.1 Concept diagram representation of the passive harmonic sensor. The swept frequency interrogation signal at f_0 is orthogonally polarized to the re-transmitted signal at $2f$.

either the harmonic of the incident wave or the product of two incident waves. This technique has previously been demonstrated for sensing physical parameters like temperature [15], [16], [17], humidity [18], dielectric change [19] and pH [20]. Although promising, these sensors are typically large in size and little work has been done for their application directly in food quality monitoring.

In the current chapter, a novel compact quasi-chipless, passive wireless sensor operating based on the principle of harmonic generation is presented. A schematic representation of the sensor concept is shown in Fig. 5.1. The sensor operates in a narrow sensing bandwidth. The application of the sensor in the monitoring of milk souring is demonstrated.

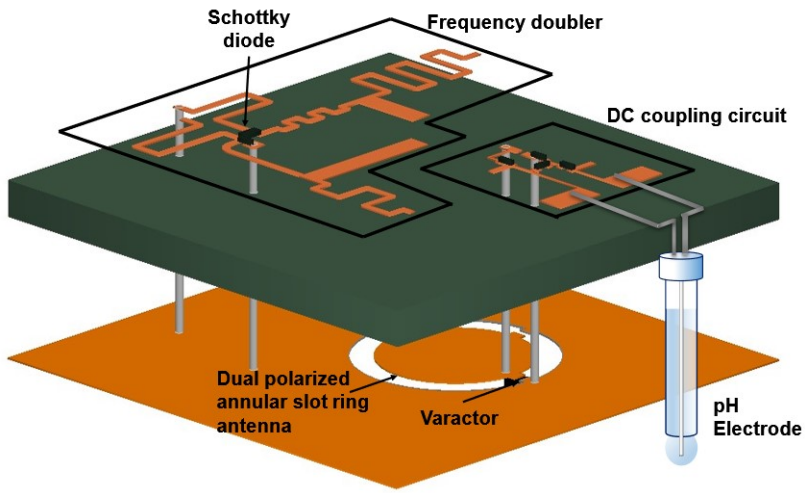

Fig. 5.2 Exploded diagram showing the different functional parts of the harmonic sensor.

5.3. Sensor Design and Operation

The sensor utilizes a dual-band antenna for receiving the interrogating signal at the frequency f_0 and retransmitting the modulated signal at the frequency at $2f_0$ utilizing a frequency doubling circuit. The receiving antenna mode at f_0 performs the required modulation for sensing utilizing a varactor which is biased by the pH electrode. The frequency f_0 was chosen to be 2.5 GHz for implementation using FR4 substrate and integration with commercial off the shelf components. The sensor design can be separated into three parts. The first is the dual-band antenna design, the second is the frequency doubler and the third part is the pH transducer and coupling circuit. Fig. 5.2 shows an exploded conceptual view of all these elements of the sensor. The design and integration of each of these are elaborated in sections 5 3.1.,5.3.2 and 5.3.3, respectively.

5.3.1. Antenna Design and Simulation

An annular slot antenna was chosen owing to its simplicity, ability to combine two polarizations and easy integration with frequency doubling circuitry. A similar antenna design has been previously presented in [27] for a radar cross section-based humidity sensing application. The antenna was designed and simulated using Ansys high-frequency structure simulator (HFSS) simulation software, its geometry is shown in Fig. 5.3. The antenna can operate in two orthogonally polarized modes – the vertically polarized mode at f_0 and the horizontally polarized mode at $2f_0$, using two orthogonal excitations. The aperture field of an unperturbed annular slot antenna of

width much smaller than the operating wavelength and functioning in the fundamental mode can be approximated by an $E_{\rho}^{a} = \cos(\phi)$ distribution [28] (ρ and ϕ are the position vectors in a cylindrical co-ordinate system). The current distributions corresponding to the two orthogonally polarized modes are shown in the Fig. 5.4 insets. Capacitive loading using a variable capacitor like a varactor diode along the direction of the surface current significantly perturbs the resonant frequency. On the other hand, when the direction of the current distribution is orthogonal to the capacitive loading, the resonant frequency remains unperturbed. The equivalent circuit of a slot antenna corresponds to a parallel resonant circuit, and capacitive loading thereby decreases its resonant frequency from the unperturbed case [29]. This also results in the reduction of the operating bandwidth of the antenna. These properties of the antenna can be seen in the return loss plots of Fig. 5.4. The isolation between the antenna ports was -5 dB at both the operating frequencies (due to the small form factor of the antenna). In the current design, the narrow band, vertically polarized, lower frequency tunable mode is used as the receiving antenna and its resonant frequency changes with capacitive loading. The horizontally polarized mode with wider bandwidth remains unperturbed and acts as the transmitting antenna. Both vertically and horizontally polarized modes have a broad radiation pattern as shown in the gain patterns of Fig. 5.5. This makes the sensor less sensitive to misalignment effects between sesing/ antenna the interrogating antennas.

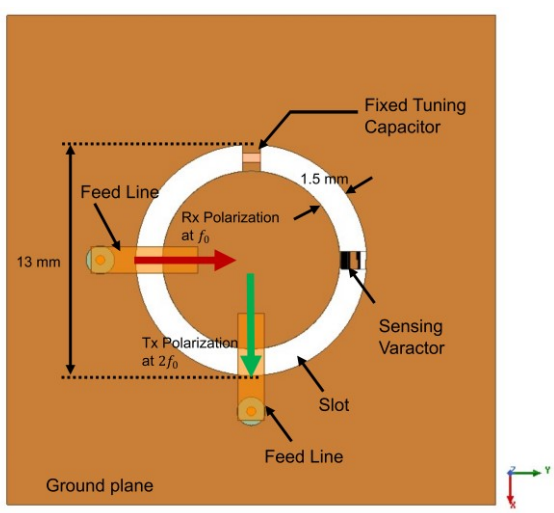

Fig. 5.3 Geometry of the annular slot antenna operating at two distinct frequencies and polarizations, used for HFSS simulations. The antenna is excited using two driven ports to obtain the simulation results without the doubler circuitry.

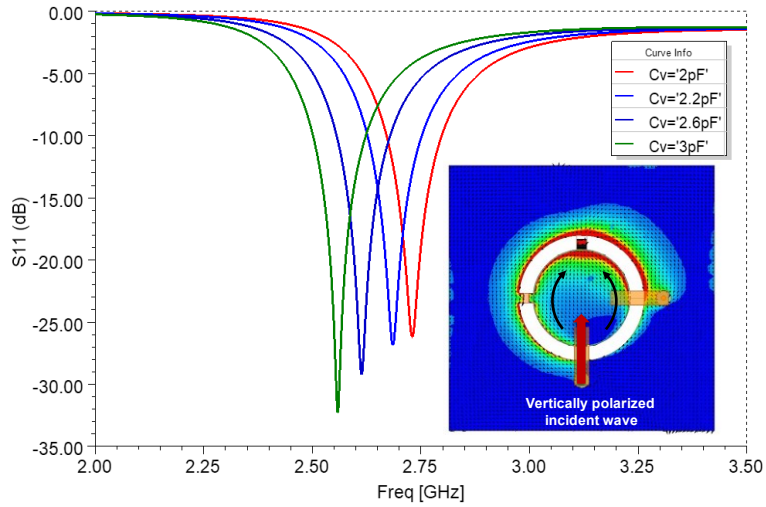

(a)

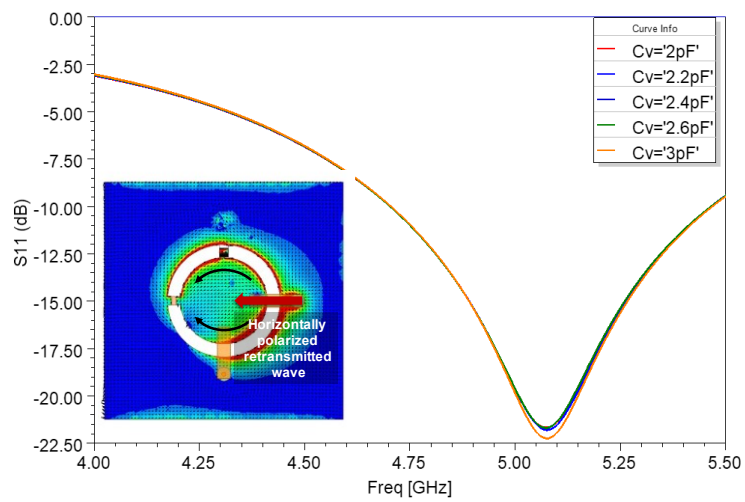

(b)

Fig. 5.4 HFSS simulation showing $|S_{11}|$ plot for the antenna mode corresponding to the (a) receiving mode at f_0 and (b) transmitting mode at $2f_0$, for different capacitance values modeling the varactor diode under different bias conditions. Insets show the surface current distribution for reach of the modes.

The resonant frequency of the receiving mode at f_0 (2.5 GHz) can be sensitized to different sensing parameters by integrating it with a functionalized capacitor like a varactor-pH electrode pair [30] [31] or a gas-sensitive interdigitated capacitor [32] [33]. The maximum sensing range is limited by the bandwidth of the transmitting mode of the antenna. In this paper, a varactor-pH combination electrode pair type of sensing is utilized to demonstrate the proof of concept of operation. In this case, the pH electrode is used to sense the presence of an analyte. The voltage

generated by the electrode in response to a change in concentration and the type of analyte is used to bias the varactor diode and change its capacitance, thereby providing the necessary transduction scheme. The varactor diode used was SMV1405 from Skyworks, and the series resistance of the diode was included in the simulations of the antenna. The capacitance sensitivity of the diode at near-zero bias is 0.23pF/500mV [34]. The effect of antenna miniaturization at the frequency f_0, loss due to the parasitic resistance of the varactor diode and the dielectric loss in the FR4 substrate reduces the radiation efficiency of the antenna. This causes a low gain of -3.9 dBi at this frequency

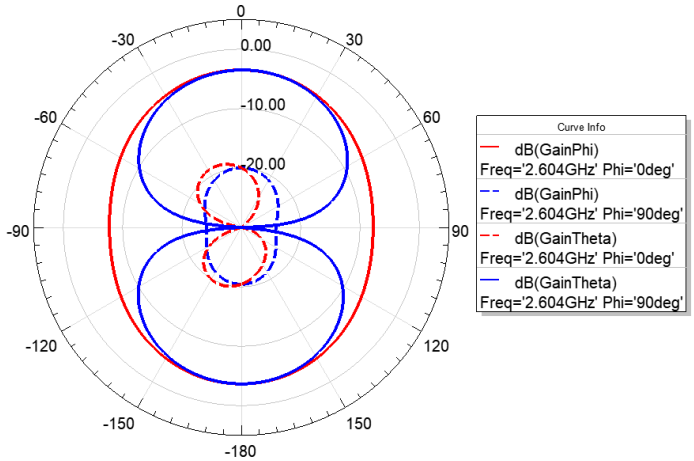

(a)

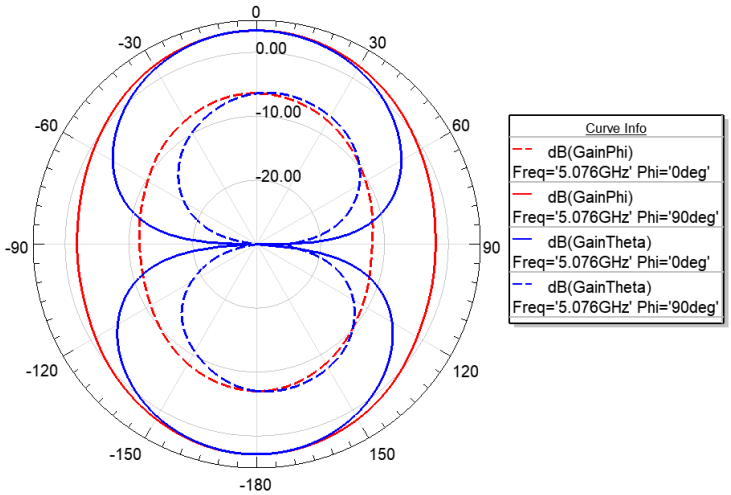

(b)

Fig. 5.5 Gain patterns of the dual polarized annular slot antenna operating at two distinct frequencies (a) at 2.5 GHz and (b) 5 GHz

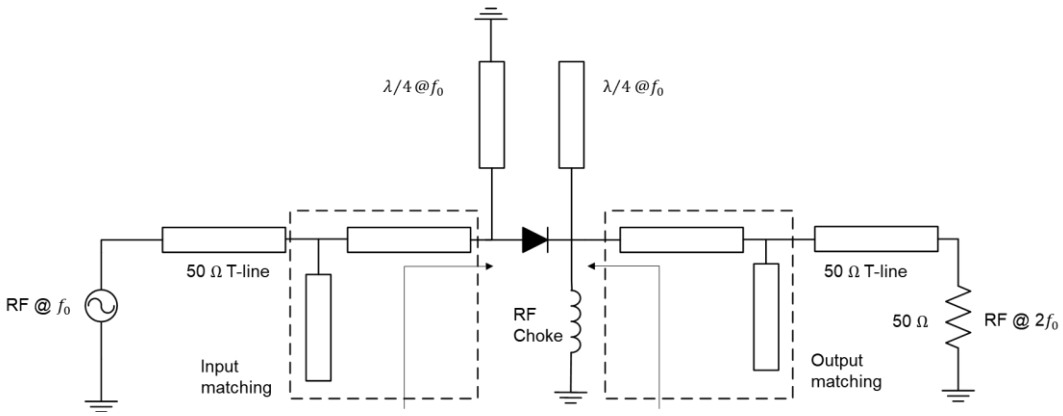

(a)

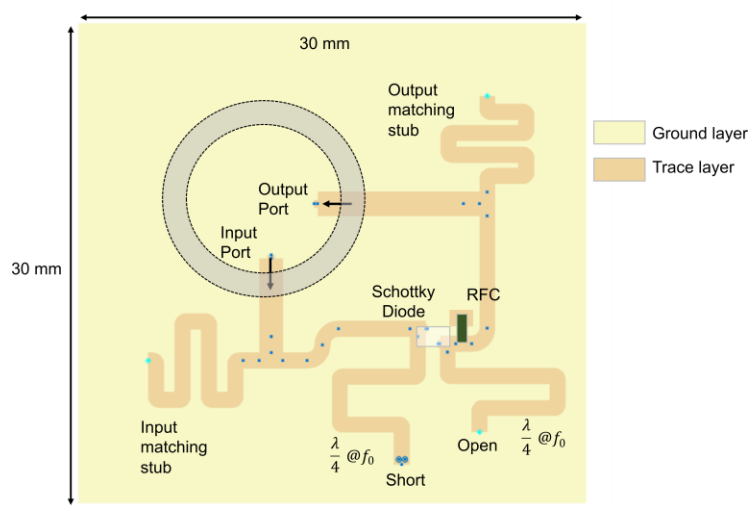

(b)

Fig. 5.6 (a) Circuit schematic showing the harmonic frequency doubler and (b) printed circuit board layout on an FR4 board of thickness 0.7874 mm. The location of the feedlines and the dimensions of meander lines were chosen such that the circuit can be easily integrated with the annular ring antenna of Fig. 2.

5.3.2. Harmonic Generation for Retransmission

The signal modulated by the receiving mode of the antenna is processed using a non-linear resistance-based frequency doubler. The nonlinear resistance is obtained here using a Schottky diode. Fig. 5. 6(a) shows the circuit schematic used to achieve this. It consists of input and output filters centered at f_0 and $2f_0$, respectively. In the current design open and short stubs are used for filtering. When operated in the non-linear region, the harmonic frequency generated by the diode

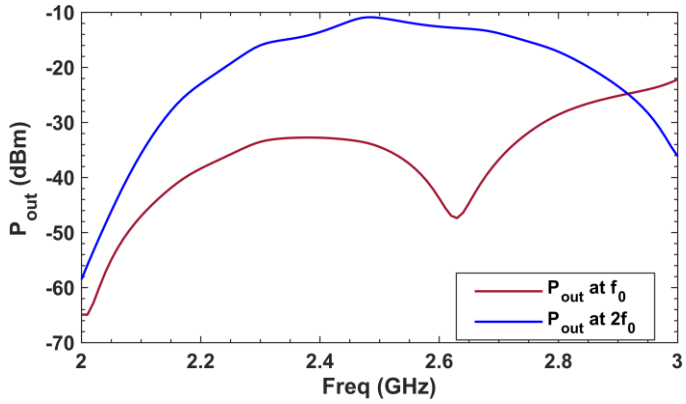

(a)

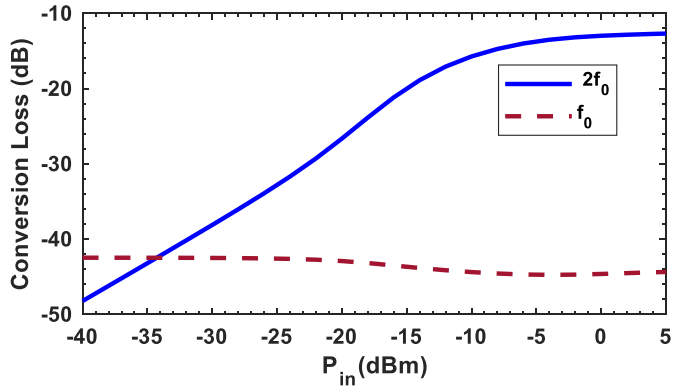

(b)

Fig. 5.7 (a) Wideband harmonic balance EM-circuit co-simulation results of the frequency doubling circuit of the layout shown in Fig. 5.5b obtained using Keysight ADS simulation software. The input power at the fundamental frequency was swept from 2 to 3 GHz while the power was kept constant at 0 dBm. (b) The fundamental and harmonic power at the output port at a fixed frequency of 2.5 GHz.

is directed towards the output and the fundamental frequency at the output of the diode is reflected back to enhance the conversion efficiency. In addition, additional sections of transmission lines and stubs are used for input and output matching of the diode. The input/output impedances of the antenna and the input/output impedances of the doubler were designed to match the 50 Ω ring antenna impedances (see Fig. 5.4). The design and simulation of the doubler circuit were done using the harmonic balance simulator in Keysight's ADS software [35]. Meander lines were used for the transmission line sections to miniaturize the design. The co-simulation tool in the software

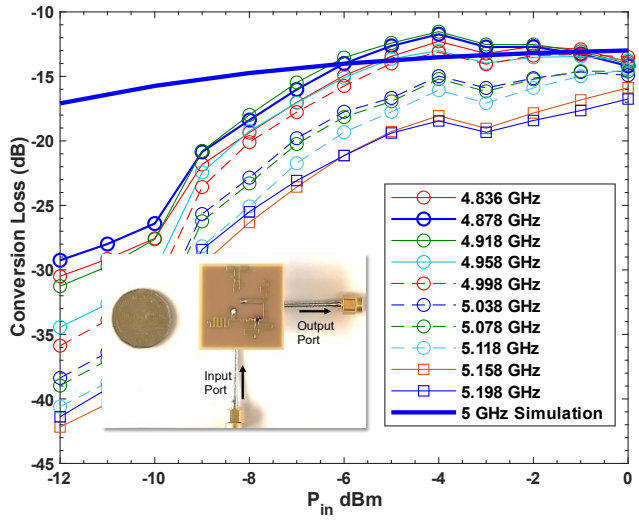

(a)

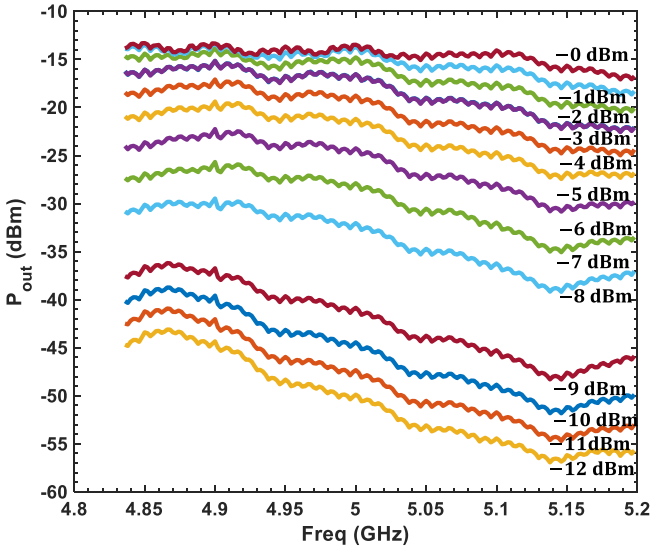

(b)

Fig. 5.8 (a) Measured conversion loss for an output frequency of 5 GHz. (b) Measured frequency response for different input power to the frequency doubling circuit. Inset in (a) shows the fabricated frequency-doubling circuit with connectors added for testing purposes.

was used for accurate simulation of the layout in order to incorporate the finite ground plane and intercoupling effects of the meander line stubs. The optimized layout obtained from the simulation is shown in Fig. 5.6(b). Fig. 5.7 shows the simulated frequency response at the output of the doubler for an input power of 0 dBm. For the input frequency range of around 2.5 GHz, the fundamental frequency is suppressed, and the second harmonic frequency is enhanced at the output. An ideal physical diode model of the Schottky diode (Infineon Tech. BAT15-03W) without

the parasitics was used for the doubler simulation [36]. The difference in the measured and simulated conversion loss at low input power in Fig. 5.8(a) may be attributed to this.

The design was fabricated on FR4 board of thickness 0.7874 mm using microstrip technology. The device is shown in Fig. 5.8(a) inset. The location of the input and output feed lines are chosen such that, the doubler can be easily integrated into the sensing antenna. However, for testing of the doubler input and output have been connected to 50 Ω ports. Fig. 5.8(a) shows the measured conversion loss at $2f_0$ band. For an input power greater than -5 dBm a conversion loss lower than 15 dB is achieved. The circuit provides a relatively flat response for an input power greater than -5 dBm over the intended bandwidth of operation as shown in Fig. 5.8(b).

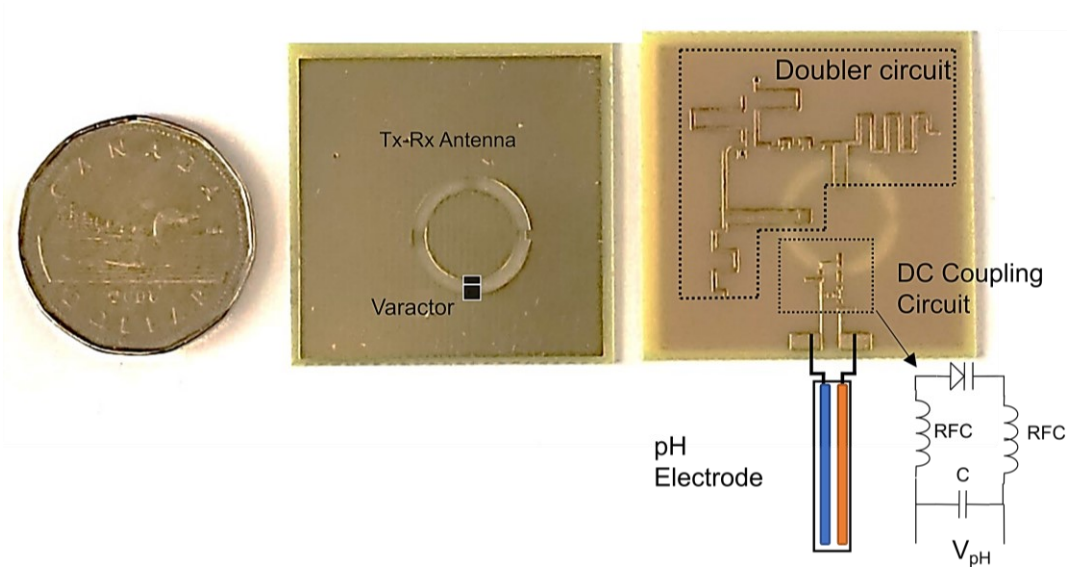

Fig. 5.9 Fabricated harmonic sensor with the annular slot and the doubling circuit integrated with an external pH electrode.

5.3.3. Sensor Integration

Fig. 5.9 shows the fully integrated sensor on a double-sided FR4 substrate of 0.7874 mm thickness. One side consists of the annular ring antenna and the varactor diode and if needed an orthogonal mode fixed tuning capacitor. The other side consists of the doubler circuit and the circuitry for coupling the sensing transducer signal, such as the pH voltage, to the varactor diode (see Fig. 5.2). The coupling circuit consists of two RF chokes and an RF shorting capacitor to

isolate the bias voltage from the RF circuit as shown in Fig. 5.9. A change in the sensing voltage across the varactor modulates its small-signal capacitance, thereby, changing the resonant frequency of the receiving antenna.

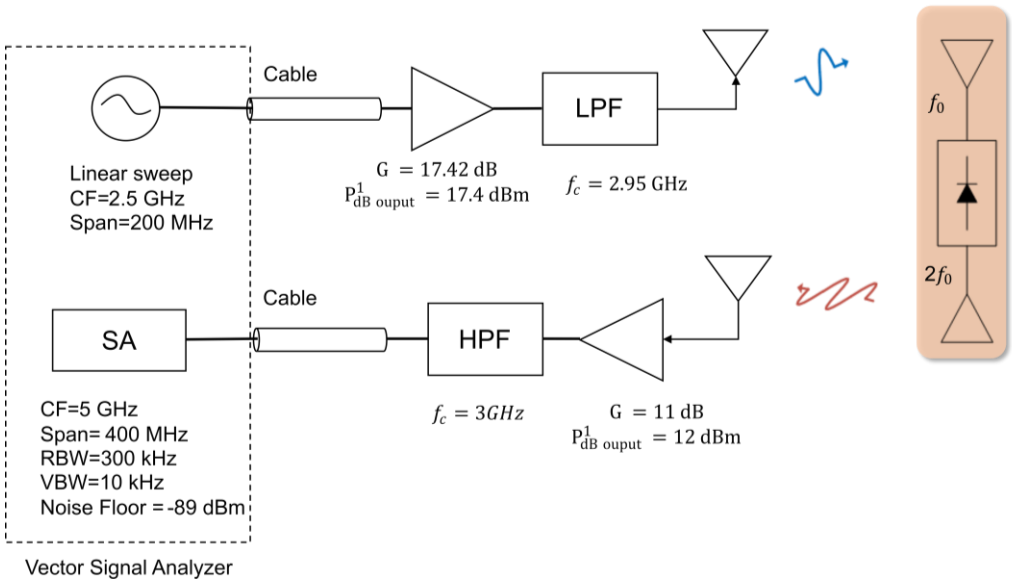

Fig. 5.10 Block diagram of the interrogator for wireless harmonic tag sensing.

5.4. Sensor interrogation and characterization

Fig. 5.10 shows the block diagram of the interrogating system. The transmitter consists of a continuous swept frequency source, an amplifier of gain 17 dB and a low pass filter with a cut-off frequency of 2.95 GHz at the output to minimize the harmonics generated both by the source and the amplifier. The power level of the source is set close to the 1 dB compression point of the amplifier to maximize the interrogation distance. The receiver consists of an amplifier of gain 17 dB, a high pass filter with a cut-off frequency of 3 GHz and a spectrum analyzer. Components from Mini-Circuits and a PXI-based vector signal analyzer from National Instruments were used. The transmitting and receiving antennas (A-INFO JXTXLB-20180) used by the interrogator are orthogonally polarized and both have a gain of 9 dBi. The harmonic tag was placed 30 cm away from the interrogating system. At this distance the tag is in the radiative near-field region of the interrogating antenna. This degrades the gain by a factor of 0.925 [37]. At the sensor, the wideband incoming signal is bandlimited by its narrowband receiving antenna with a maximum at f_0 and is

sent to the doubler circuit after which the signal with a maximum at $2f_0$ is retransmitted back with orthogonal polarization. The horn antennas on the reader system operate with orthogonal polarization. The measured second harmonic when there is no sensor present is below the noise floor of the receiver (-89 dBm).

The link budget of the system can be determined using

$$P_{rec} = G_T^I G_R^{tag} G_T^{tag} G_R^I \, C_L \left(\frac{\lambda/\sqrt{2}}{4\pi R}\right)^4 P_T \mathrm{L}_\mathrm{R}^{tag} \mathrm{L}_\mathrm{T}^{tag}. \qquad (1)$$

Here, P_T and P_R are the transmitted and received powers by the interrogator antennas, G_T^I and G_R^I are the integrator transmit and receive antenna gains, G_T^{tag} and G_R^{tag} are the tag transmit and receive antenna gains, C_L is the conversion loss of the doubling circuit, R is the distance between the integrator and the tag, λ is the operating wavelength at f_0 and $\mathrm{L}_\mathrm{R}^{tag}$ and $\mathrm{L}_\mathrm{T}^{tag}$ are the mismatch losses due to the tag receiving and transmitting antennas. It should be noted that the sensing distance is limited by the transmit power. For a tag distance of 30 cm, the power received by the input of the doubling circuit is -8 dBm. This corresponds to a measured conversion loss of -30 dB (see Fig. 5.8(b)), and a received power of -54 dBm at the receiver output, for an ideal matched condition. Link budget does not take into account the cross-pol loss affect.

The sensitivity of the sensor was first studied using an applied voltage test. This was performed by directly applying different bias voltages to the varactor through the coupling circuit. Fig. 5.11a shows the response of the sensor to applied voltages. Proper cable orientation perpendicular to raditing surface and absorbers were used to minimize the effect of loading of the sensor by the bias wires. The full frequency response of the received signals at the interrogator for example bias voltages are shown in Fig. 5.11b. The resonant frequency is defined here to be the maxima of the received signal and is obtained by fitting the measured data points to a 4th order polynomial and then finding its peak. Secondary peaks beyond the measurement range are discarded. The sensor gives a linear resonant frequency response over the voltage range of interest (3 < pH < 9, suited to most food monitoring applications). The sensor has a larger frequency range of operation in the forward bias mode due to the initial zero-bias position of the resonant frequency being offset from the nominal resonant frequency of the transmitting mode of the sensing antenna. At higher values of the applied voltages the resonant frequency of the sensor moves beyond the

bandwidth of operation of the sensor transmitting antenna, hence diminishing the amplitude level of the received signal as shown in Fig. 5.11 (b).

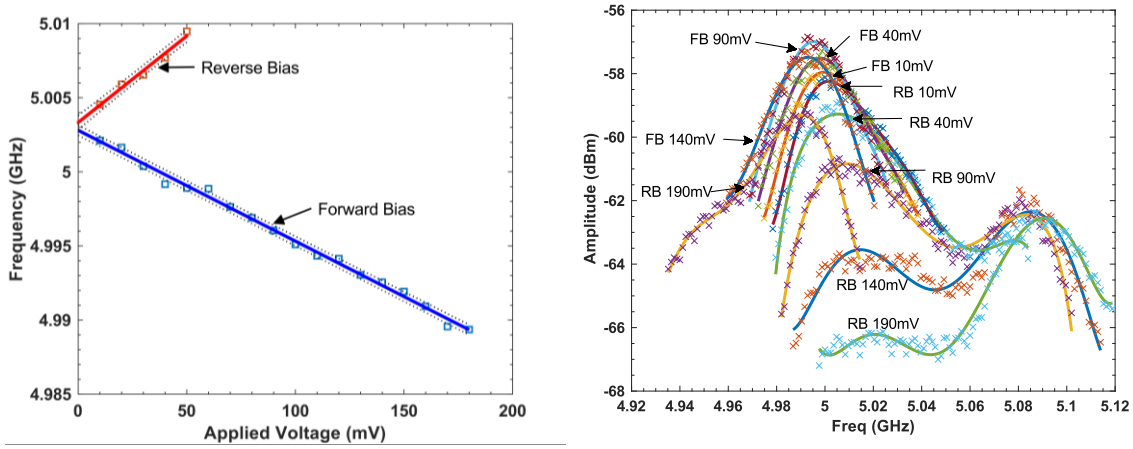

(a) **(b)**

Fig. 5.11 (a) Resonant frequency change and (b) received signal signature of the sensor for different applied voltages across the varactor diode in the forward and reverse bias conditions. Markers indicate the measured data points, and the solid lines are the linear and 4th order polynomial fits in (a) and (b), respectively.

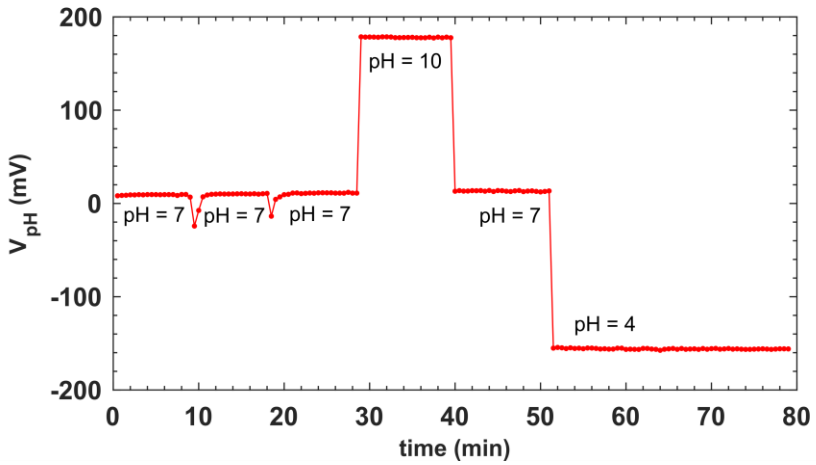

Fig. 5.12 3-point calibration of the commercial pH electrode using buffer solutions measured using Agilent 34401A digital multimeter. The electrode has a sensitivity of ~55mV per unit pH change.

5.5. Sensor Application to pH Sensing

A commercial glass pH electrode was used as the transducer for demonstrating the sensing capability of the sensor. Alternatively, a printed and fully integrated version of the pH electrode can also be implemented as described in [29]. The three-point calibration curve of the pH electrode is shown in Fig. 5.12. The measured DC resistance of the commercial pH electrode was ~180 MΩ

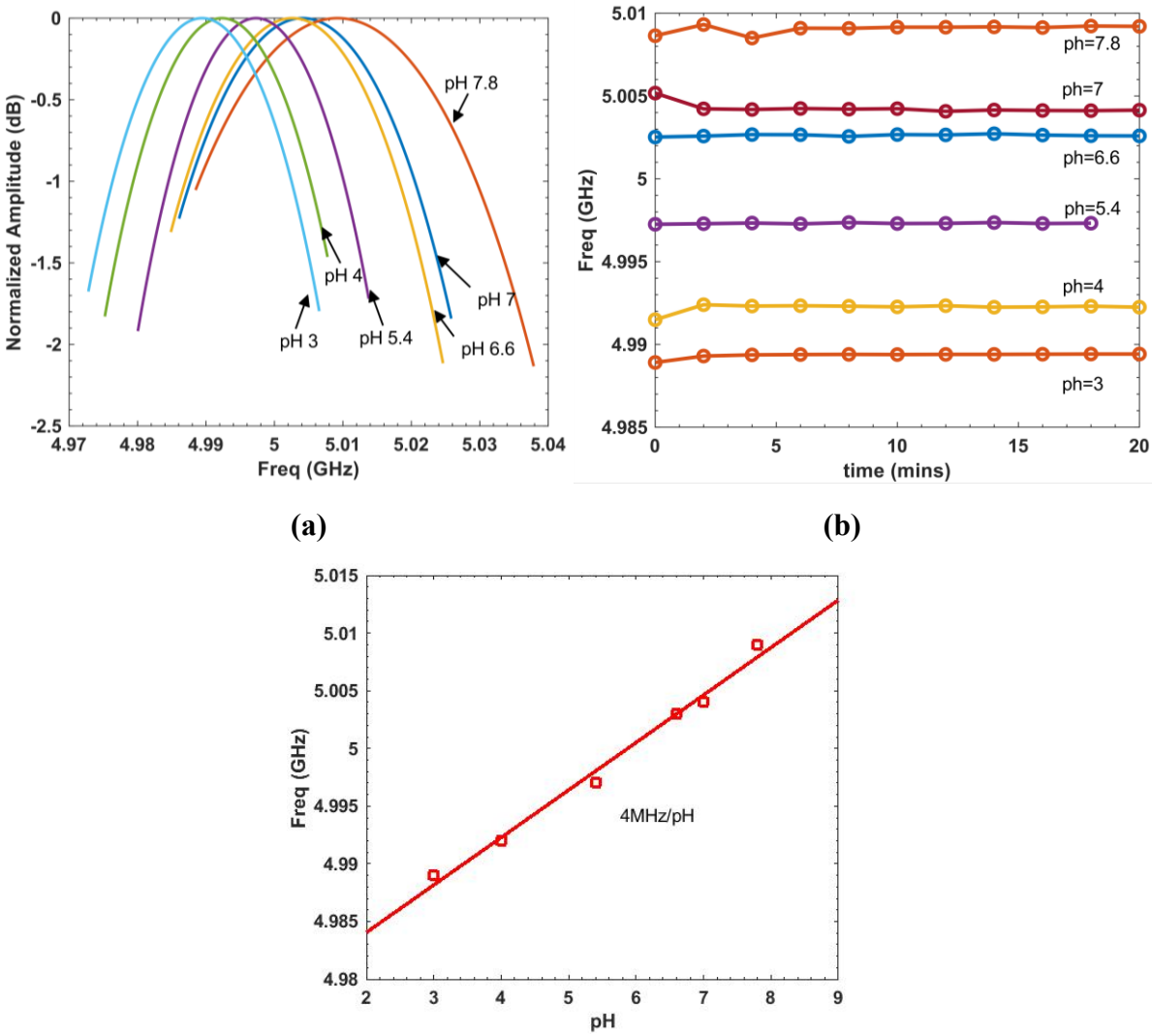

Fig. 5.13 (a) Normalized received signal from the harmonic sensor for different pH buffers, (b) the time response of the sensor's doubled resonant frequency for different pH buffer solutions and (c) the received doubled resonant frequency of the sensor vs the pH of the buffer solution. (data points in (c) are takin from the t=15 min points in (b))

and has a voltage divider effect, which lowers the sensor sensitivity. The pH electrode potential difference, V_{ph}, biases the varactor diode on the slot antenna through the coupling circuitry.

Fig. 5.13 shows the response of the sensor to different pH buffer solutions for the commercial pH electrode attached to the coupling circuit. A sensitivity of 4 MHz per unit change in pH with a dynamic range of 3 < pH < 8 was attained. The polarity of the electrode pair was chosen such that a decrease in pH results in an increase in the forward bias voltage across the varactor diode. This results in the resonant frequency of the sensor decreasing (increased varactor capacitance) and

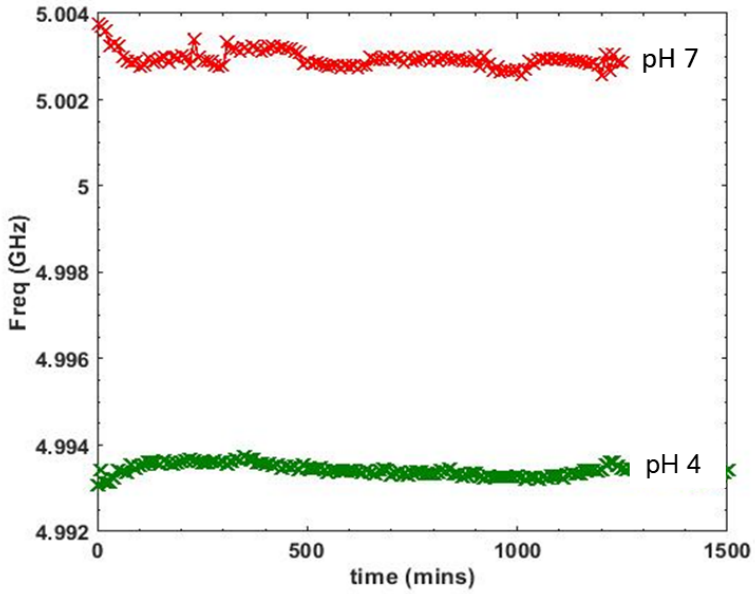

Fig. 5.14. Study of stability of the sensor in two different pH buffer solutions over 25 hour period.

maintains the total change in resonant frequency within the bandwidth of operation of the transmitting mode of the sensor antenna. The stability of the sensor was also investigated for long intervals of time. Fig. 5.14 shows the long-term response of the sensor for a period of 25 hours for two different pH buffer solutions. Note that the measurements were performed in an unshielded lab environment where small temperature fluctuations are expected.

5.5.1. Milk Spoilage Monitoring

Bacterial growth is a major source of milk spoilage. When not stored properly the action of bacteria, increases the pH of milk causing the degradation of milk quality. [39][40][13] show near

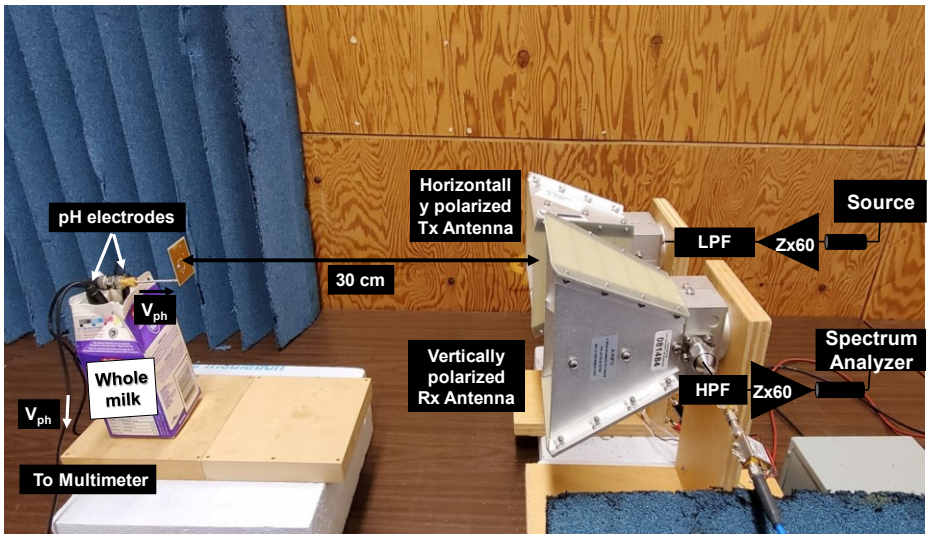

(a)

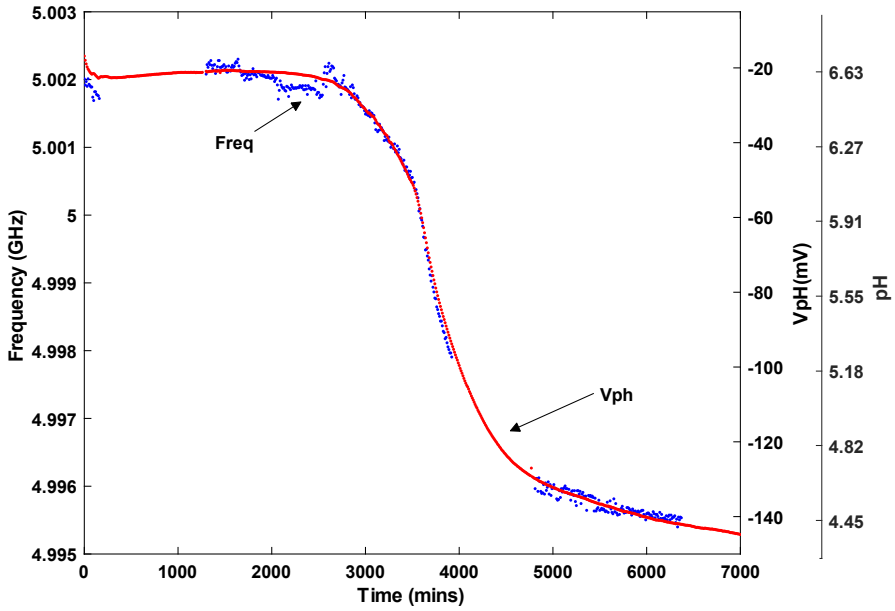

(b)

Fig. 5.15 (a) Experimental setup used for monitoring of milk spoilage and (b) the resonant frequency measured using the harmonic sensor and corresponding pH change measured using a commercial pH electrode with a voltmeter during milk souring process (no temperature compensation).

field sensors used in this application. In this section the proposed harmonic sensor is used to monitor the pH change during the process of milk spoilage. The commercial pH electrode was seen to be stable for the current application. For the milk monitoring experiment whole (3.5%)

milk was used. Two pH electrodes were placed in contact with the milk. One was used to directly monitor the change in the pH voltage using an Agilent 3440 multimeter and the other acted as the transducer for the wireless sensor. The sensor was placed 30 cm from the interrogator and the peak of the received signal was monitored every 10 mins for about 5 days. National instrument's LabView VI was used for automatic data acquisition. The measurement setup is shown in Fig. 15(a). The sample was kept at room temperature over the entire course of the experiment. The measured doubled resonant frequency from the wireless sensor and the direct wired pH measurement results are shown in Fig. 15(b). Both the results overlap and the correlation between the two is evident. This demonstrates the applicability of the sensor in pH-based food monitoring.

5.6. Conclusion

This This paper presented a wireless passive harmonic sensor. We show how the antenna, doubling circuitry and sensing elements can all be integrated into a single small format tag, making it suitable for many packaged food monitoring applications. A dual-band dual polarized annular slot ring antenna was used to receive and retransmit the signal at f_0 and $2f_o$, respectively. In the demonstrated example, the receiving mode of the antenna was sensitized to pH by coupling it to a varactor-pH electrode transduction scheme. A Schottky diode-based frequency doubler was used to generate the harmonic signal. The sensor was shown to have a linear response to pH and with a sensitivity of 4 MHz per unit pH change. A comparison of the sensor to other state harmonic sensors of the art is shown in Table I. The sensor has the advantage of being considerably smaller with comparable range and sensing capability to other previously reported harmonic sensors. The pH electrode may also be completely integrated together with the sensing antenna by using techniques described in [41].

The sensing distance of the sensor is limited by the conversion efficiency of the doubling circuit and the efficiency of the receiving section of the sensor. The interrogator set-up presented operates well below the maximum allowed EIRP level. The sensing distance thus may be increased using a higher output power level, such that the doubler operates in a lower conversion loss regime (see Fig. 5.8). However, EMC issues may have to be considered for the higher transmit power at f_0.

Table 5.1

Comparison of the sensor with state-of-the-art sensors with possible food quality application potential.

	Sensing parameter	Interrogation and sensing technique	RF/Antenna integration	Sensing tag size	Maximum reported distance and output power	Food monitoring demonstration
[25][30][31]	pH, Ammonia, Acetic acid	Near-field coil, resonant frequency change	Yes	$\ll\lambda$	$\ll\lambda$	Yes
[20]	pH	Far-field, harmonic sensor, phase shift change	No	$\sim\lambda$	1.3λ – 15 dBm	No
[19]	Dielectric constant	Far-field, harmonic sensor differential phase shift change	No	$>\lambda$	6λ – 30 dBm	No
[18]	Humidity	Far-field, harmonic sensor, frequency shift with energy harvesting	No	$\sim\lambda$	20λ – 27 dBm	No
[16]	Temperature	Far-field harmonic sensor, frequency shift	No	$\sim\lambda$	7.5λ – 10 dBm	No
This work	pH	Far-filed harmonic sensor, frequency shift	Yes	0.25λ	2.5λ – 17 dBm	Yes

The applicability of the sensor in food quality monitoring was demonstrated with Milk monitoring as an example. The sensor may also be applied in sensing other food commodities like fish [5] and meat [8], [42] by sensing basicity. Bio-compatible materials like gold reference electrodes and IrO_x working electrodes may be a possible alternative for real-world applications, however, further research needs to be carried out for this. Alternatively, a non-contact volatile sensing based transduction scheme may be employed [5]. The tag is targeted towards dielectric packaging with it being located in the head-space region of the packaged food material, with adequate spacing to minimize the effect of dielectric loading from the material being monitored. Additional work is needed to make the sensor compatible with other packaging technologies, such as those that include a metallic foil film.

References

[1] H. Yousefi, H. M. Su, S. M. Imani, K. Alkhaldi, C. D. Filipe, and T. F. Didar, "Intelligent Food Packaging: A Review of Smart Sensing Technologies for Monitoring Food Quality," *ACS Sensors*, vol. 4, no. 4, pp. 808–821, 2019.

[2] R. S. Singhal, P. R. Kulkarni, and D. V. Rege, *Handbook of indices of food quality and authenticity*. Woodhead Pub, 1997.

[3] A. Nopwinyuwong, S. Trevanich, and P. Suppakul, "Development of a novel colorimetric indicator label for monitoring freshness of intermediate-moisture dessert spoilage.," *Talanta*, vol. 81, no. 3, pp. 1126–32, May 2010.

[4] A. E. Ghaly, D. Dave, and A. E. Ghaly, "Meat Spoilage Mechanisms and Preservation Techniques: A Critical Review," *Am. J. Agric. Biol. Sci.*, vol. 6, no. 4, pp. 486–510, 2011.

[5] S. Bhadra, C. Narvaez, D. J. Thomson, and G. E. Bridges, "Non-destructive detection of fish spoilage using a wireless basic volatile sensor," *Talanta*, vol. 134, pp. 718–723, Mar. 2015.

[6] European Commission, "95/149/EC: Commission Decision of 8 March 1995 fixing the total volatile basic nitrogen (TVB-N) limit values for certain categories of fishery products and specifying the analysis methods to be used," 1995. [Online]. Available: https://publications.europa.eu/en/publication-detail/ /publication/91dc1ed4-6450-4a3c-8cab-45009644715c/language-en. [Accessed: 11-Dec-2017].

[7] C. Rukchon, A. Nopwinyuwong, S. Trevanich, T. Jinkarn, and P. Suppakul, "Development of a food spoilage indicator for monitoring freshness of skinless chicken breast," *Talanta*,

vol. 130, pp. 547–554, Dec. 2014.

[8] B. Kuswandi and A. Nurfawaidi, "On-package dual sensors label based on pH indicators for real-time monitoring of beef freshness," *Food Control*, vol. 82, pp. 91–100, Dec. 2017.

[9] A. Nopwinyuwong, S. Trevanich, and P. Suppakul, "Development of a novel colorimetric indicator label for monitoring freshness of intermediate-moisture dessert spoilage," *Talanta*, vol. 81, pp. 1126–1132, 2010.

[10] F. Saliu and R. Della Pergola, "Carbon dioxide colorimetric indicators for food packaging application: Applicability of anthocyanin and poly-lysine mixtures," *Sensors Actuators B Chem.*, vol. 258, pp. 1117–1124, Apr. 2018.

[11] S. Manzari and G. Marrocco, "Modeling and applications of a chemical-loaded UHF RFID sensing antenna with tuning capability," *IEEE Trans. Antennas Propag.*, vol. 62, no. 1, pp. 94–101, 2014.

[12] C. Occhiuzzi, S. Caizzone, and G. Marrocco, "Passive UHF RFID antennas for sensing applications: Principles, methods, and classifcations," *IEEE Antennas Propag. Mag.*, vol. 55, no. 6, pp. 14–34, 2013.

[13] D. Rodriguez, M. A. Saed, and C. Li, "A WPT/NFC-Based Sensing Approach for Beverage Freshness Detection Using Supervised Machine Learning," *IEEE Sens. J.*, vol. 21, no. 1, pp. 733–742, Jan. 2021.

[14] S. Bhadra, D. S. Y. Tan, D. J. Thomson, M. S. Freund, and G. E. Bridges, "A wireless passive sensor for temperature compensated remote pH monitoring," *IEEE Sens. J.*, vol. 13, no. 6, pp. 2428–2436, 2013.

[15] P. Fathi, N. C. Karmakar, M. Bhattacharya, and S. Bhattacharya, "Potential Chipless RFID Sensors for Food Packaging Applications: A Review," *IEEE Sensors Journal*, vol. 20, no. 17. Institute of Electrical and Electronics Engineers Inc., pp. 9618–9636, 01-Sep-2020.

[16] R. Raju, G. E. Bridges, and S. Bhadra, "Wireless passive sensors for food quality monitoring: Improving the safety of food products," *IEEE Antennas Propag. Mag.*, vol. 62, no. 5, pp. 76–89, Oct. 2020.

[17] X. Gu, S. Nikhil, L. Guo, S. Hemour, and K. Wu, "Diplexer-based fully passive harmonic transponder for sub-6-GHz 5G-compatible IoT applications," *IEEE Trans. Microw. Theory Tech.*, vol. 67, no. 5, pp. 1675–1687, May 2019.

[18] V. Palazzi, F. Alimenti, C. Kalialakis, P. Mezzanotte, A. Georgiadis, and L. Roselli, "Highly

Integrable Paper-Based Harmonic Transponder for Low-Power and Long-Range IoT Applications," *IEEE Antennas Wirel. Propag. Lett.*, vol. 16, pp. 3196–3199, Nov. 2017.

[19] V. Palazzi, F. Alimenti, P. Mezzanotte, G. Orecchini, and L. Roselli, "Zero-power, long-range, ultra low-cost harmonic wireless sensors for massively distributed monitoring of cracked walls," *IEEE MTT-S Int. Microw. Symp. Dig.*, pp. 1335–1338, Oct. 2017.

[20] L. Zhu, H. Huang, M. M. C. Cheng, and P. Y. Chen, "Compact, flexible harmonic transponder sensor with multiplexed sensing capabilities for rapid, contactless microfluidic diagnosis," *IEEE Trans. Microw. Theory Tech.*, vol. 68, no. 11, pp. 4846–4854, Nov. 2020.

[21] B. Kubina, C. Mandel, M. Sch, R. Jakoby, M. Schussler, and R. Jakoby, "Compact Quasi-Chipless Harmonic Radar Sensor with a Dielectric Resonator Antenna," *2015 IEEE MTT-S Int. Microw. Symp. IMS 2015*, pp. 2–4, Jul. 2015.

[22] B. Kubina, J. Romeu, C. Mandel, M. Schüßler, and R. Jakoby, "Quasi-chipless wireless temperature sensor based on harmonic radar," *Electron. Lett.*, vol. 50, no. 2, Jan. 2014.

[23] V. Viikari, H. Seppä, T. Mattila, and A. Alastalo, "Wireless Ferroelectric Resonating Sensor," *IEEE Trans. Ultrason. Ferroelectr. Freq. Control*, vol. 57, no. 4, pp. 785–791, Apr. 2010.

[24] A. Lazaro, R. Villarino, and D. Girbau, "A Passive Harmonic Tag for Humidity Sensing," *Int. J. Antennas Propag.*, vol. 2014, pp. 1–11, 2014.

[25] R. Mirzavand and P. Mousavi, "A Zero-Power sensor using multi-port direct-conversion sensing," *IEEE Sens. J.*, vol. 18, no. 22, pp. 9243–9250, Nov. 2018.

[26] S. Mondal, D. Kumar, and P. Chahal, "A Wireless Passive pH Sensor with Clutter Rejection Scheme," *IEEE Sens. J.*, vol. 19, no. 9, pp. 3399–3407, 2019.

[27] R. Raju and G. E. Bridges, "Radar Cross Section Based Chipless Tag with Built-in Reference for Relative Humidity Monitoring of Packaged Food Commodities," *IEEE Sens. J.*, pp. 1–1, Jun. 2021.

[28] R. Garg, Ed., *Microstrip Antenna Design Handbook*. Artech, 2001.

[29] C.-S. Hong, "Small annular slot antenna with capacitor loading," *Electron. Lett.*, vol. 36, no. 2, p. 110, 2000.

[30] S. Bhadra, G. E. Bridges, D. J. Thomson, and M. S. Freund, "Electrode Potential-Based Coupled Coil Sensor for Remote pH Monitoring," *IEEE Sens. J.*, vol. 11, no. 11, pp. 2813–2819, Nov. 2011.

[31] S. Bhadra, D. J. Thomson, and G. E. Bridges, “Monitoring acidic and basic volatile concentration using a pH-electrode based wireless passive sensor,” *Sensors Actuators, B Chem.*, vol. 209, pp. 803–810, Mar. 2015.

[32] B. Wu, X. Zhang, B. Huang, Y. Zhao, C. Cheng, and H. Chen, “High-Performance Wireless Ammonia Gas Sensors Based on Reduced Graphene Oxide and Nano-Silver Ink Hybrid Material Loaded on a Patch Antenna,” *Sensors*, vol. 17, no. 9, p. 2070, Sep. 2017.

[33] G. Bailly, A. Harrabi, J. Rossignol, D. Stuerga, and P. Pribetich, “Microwave gas sensing with a microstrip interDigital capacitor: Detection of NH3 with TiO2 nanoparticles,” *Sensors Actuators, B Chem.*, vol. 236, pp. 554–564, Nov. 2016.

[34] Skyworks “SMV1405 to SMV1430 Series: Plastic-Packaged Abrupt Junction Tuning Varactors,” SMV1405 datasheet, Jan. 2020.

[35] “PathWave Advanced Design System.” Keysight, 2021.

[36] Infinion technologies, “Single silicon RF Schottky diode.”, BAT15-03W datasheet, Jun. 2018.

[37] J. R. Pace, “Asymptotic Formulas for Coupling Between Two Antennas in the Fresnel Region,” *IEEE Trans. Antennas Propag.*, vol. 17, no. 3, pp. 285–291, 1969.

[38] W. D. Huang, S. Deb, Y. S. Seo, S. Rao, M. Chiao, and J. C. Chiao, “A Passive Radio-Frequency pH-Sensing Tag for Wireless Food-Quality Monitoring,” *IEEE Sens. J.*, vol. 12, no. 3, pp. 487–495, 2012.

[39] S. Bhadra, D. J. Thomson and G. E. Bridges, "A wireless passive pH sensor for real-time in vivo milk quality monitoring," *SENSORS, 2012 IEEE*, 2012, pp. 1-4.

[40] R. A. Potyrailo, N. Nagraj, Z. Tang, F. J. Mondello, C. Surman, and W. Morris, “Battery-free radio frequency identification (RFID) sensors for food quality and safety,” *J. Agric. Food Chem.*, vol. 60, no. 35, pp. 8535–8543, Sep. 2012.

[41] S. Kakooei, C. Ismail, and B. Ari-Wahjoedi, “An overview of pH Sensors Based on Iridium Oxide: Fabrication and Application,” *Int. J. Mater. Sci. Innov.*, vol. 1, no. 1, pp. 62–72, 2013.

[42] C. Rukchon, A. Nopwinyuwong, S. Trevanich, T. Jinkarn, and P. Suppakul, “Development of a food spoilage indicator for monitoring freshness of skinless chicken breast.,” *Talanta*, vol. 130, pp. 547–54, Dec. 2014.

Chapter 6.

A Compact Wireless Passive Harmonic Sensor for Ammonia Sensing in Packaged Food

In chapter 5 a passive wireless pH sensor based on harmonic generation was presented. The sensor was easily detectable in cluttered enviroment and was shown to be applicable to practical food monitoring applications like milk spoilage detection. pH sensors however require contact with food material, which make them often undesired. In this chapter, the sensor is modified to sense gasses using a semi-integrated hydrogel-based acidic/basic volatile sensor. The modified sensor is capable of monitoring volatile gasses like ammonia that can be directly correlated to the extent of pathogenic activity like pseudomonas during fish spoilage. This chapter is based on the paper "**R. Raju** and G. E. Bridges, "A compact wireless passive harmonic sensor for ammonia sensing in packaged food," submitted to the *IEEE Sensors Lett.*, 2021."

6.1. Abstract

Sensing of volatile acidic/basic gases play a significant role in early detection of food spoilage. This chapter presents a compact low cost quasi-chipless sensor for monitoring of such gases. The sensor utilizes a dual-band annular ring antenna to receive, modulate, and retransmit an incoming interrogation signal at double the frequency and with an orthogonally polarization. Application of the sensor for monitoring of ammonia is presented. The resonant frequency of the receiving mode of the antenna is sensitized to ammonia using a varactor-based transduction scheme utilizing a hydrogel-coated pH electrode pair. The sensor provides a linear response to the logarithm of the concentration of Ammonia and a sensitivity of 2.3 MHz per unit log concentration and greater than 1 m range for a signal to noise of better than 30 dB.

6.2. Introduction

Monitoring of acidic and basic volatiles is of great importance in environmental monitoring, packaged food monitoring and chemical industries. Quantitative knowledge of the concentration of volatiles can serve as an indicator for food spoilage [1] [2]. Pathogenic activities produce

volatile bi-products [3], many of these acidic or basic in nature. Microorganisms in meat and fish produce various volatile compounds like sulphur-containing molecules, acetone, fatty acids, ammonia and carbon-dioxide [4]. Food items rich in sugars are broken down into organic acids and CO_2 due to microbial action [3]. Total volatile base nitrogen (TVB-N) and trimethylamine (TMA), for example, are used worldwide as indicators of fish quality and decomposition [5].

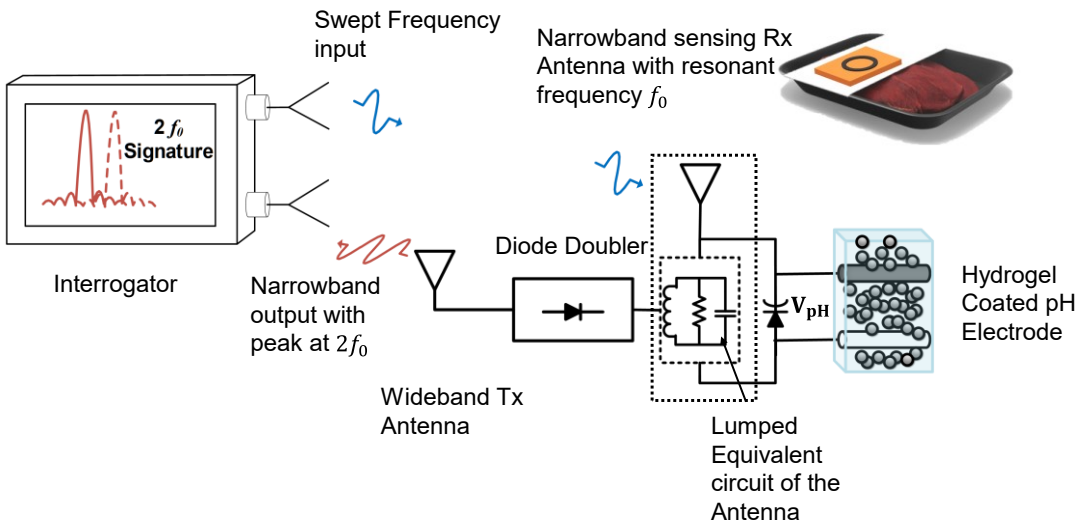

Fig. 6.1 Concept diagram representation of the passive harmonic sensor for volatile gas sensing in packaged food items.

Research in printed electronics and material science has made package-to-package non-contact monitoring of volatile gases of food items like milk, fish and meat feasible [6]. Colorimetric dye-based sensors that give qualitative indication of the extent of microbial activity has been of significant interest in this area [7][8][9][10]. With the advancements in RFIDs, integration of sensing circuitry into passive RFIDs has been presented as one viable approach that gives a semi-quantitative information regarding microbial activity. The integrated circuitry for additional sensing, however, makes them comparatively more expensive than traditional RFIDs. Sensing applications using traditional RFIDs without additional sensing circuitry have also been proposed [11][12]. These sensors predominantly work on the basis of the dielectric loading effect on the RFID antennas. Passive-chipless sensors are another low-cost alternative, however, these sensors are limited in practical application due to the high clutter from the sensing environment [13][14]. Several researchers have presented quasi-chipless passive sensors that utilize frequency

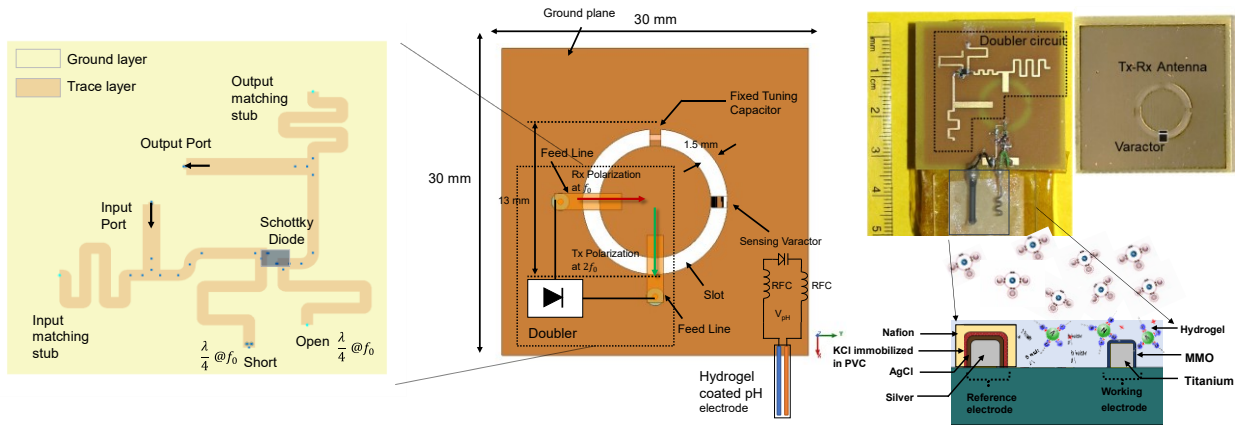

(a) **(b)** **(c)**

Fig. 6.2 (a) Schematic of the frequency doubler circuit on the back side. (b) Dual frequency orthogonal polarized annular ring antenna on the front side and (c) the fabricated sensor and schematic of the amorphous hydrogel coated pH-electrode structure.

diversity between the incident interrogation signal and the scattered/retransmitted signal for clutter rejection. Such sensors utilize a highly nonlinear device such as a diode to generate a harmonic of the incident signal as a backscattered signal. This technique has been demonstrated in the sensing of different parameters [15] [16] [17] [18] [19] [20], however, little research has been dedicated towards their use in low-cost gas sensing applications, such as for packaged food monitoring.

In this chapter a compact quasi-chipless, passive wireless acidic/basic volatile sensor operating based on the principle of harmonic generation is presented. The sensor utilizes a hydrogel coated pH electrode pair previously reported in [4][21][22][23] for near field pH and volatile sensing and fish spoilage monitoring applications.

6.3. Sensor Design and Operation

Fig. 6.1 shows the concept diagram of the sensor. The sensor design is based on the annular ring pH sensing harmonic tag described in detail in [24]. It consists of a dual band annular ring antenna similar to [25], with operating frequencies f_0 and $2f_0$ and orthogonal polarizations. The receiving mode has a resonance at around 2.5 GHz (f_0) with a narrow 10 dB bandwidth of 3%. The receiving mode is functionalized to sense acidic/basic volatile gases using a varactor-pH electrode transduction scheme. A change in concentration of an acidic or basic gas, like ammonia in the environment, causes a change in the pH-electrode voltage, and this intern produces a change

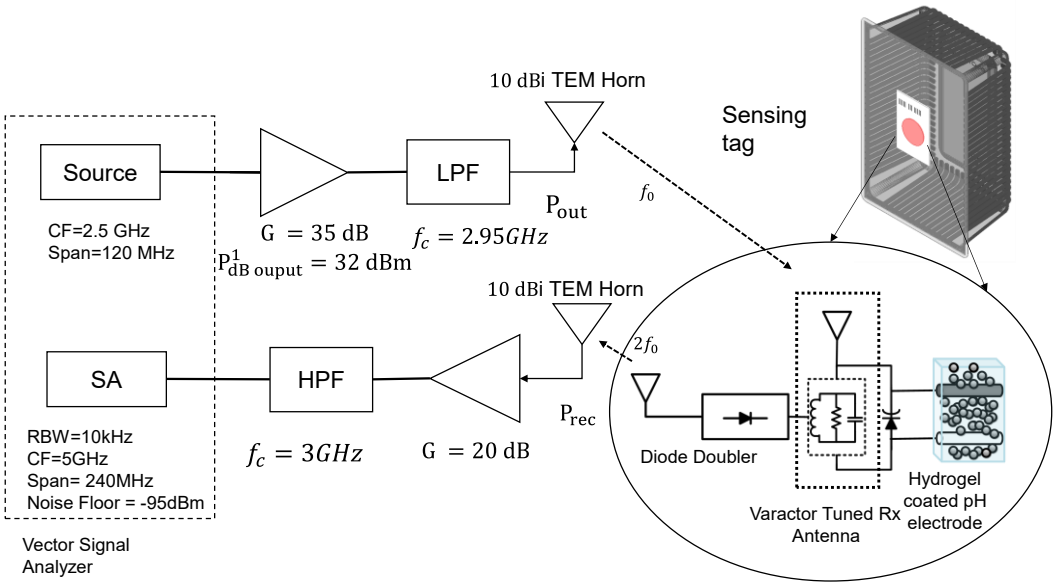

Fig. 6.3 Block diagram of the interrogator used for harmonic wireless sensing.

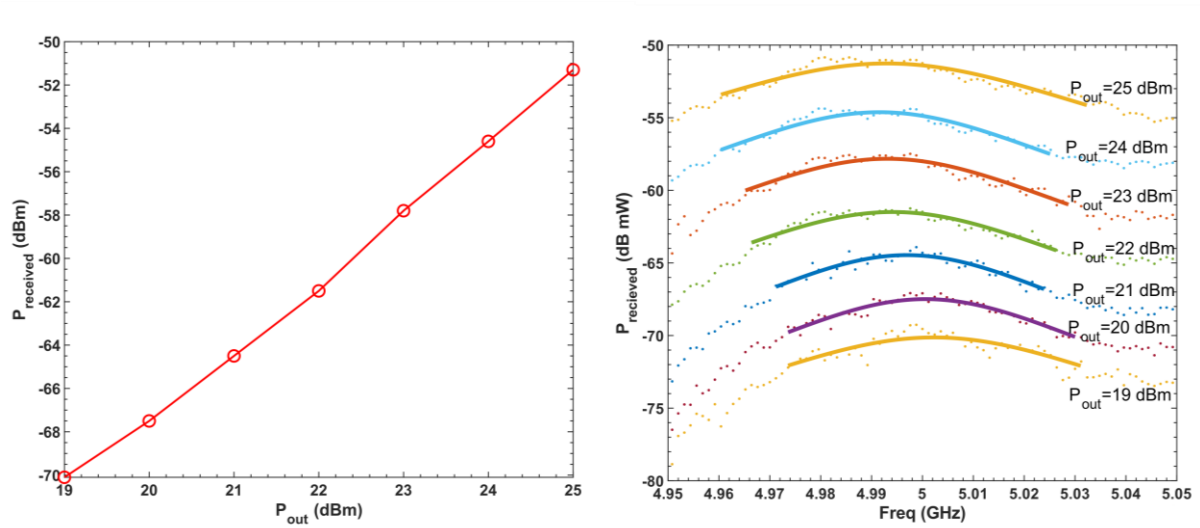

(a) **(b)**

Fig. 6.4 (a) The power received (P_{rec}) by the interrogator for different transmitted power (P_{out}) when the sensing tag is placed at a fixed distance of 80 cm from the reader. (b) The frequency response for the signal received by the interrogator for different P_{out}. Discrete points are actual measured values and solid lines indicates the interpolated data.

in the bias voltage across the varactor diode. The resulting change in the diode junction capacitance causes the resonant frequency, f_0 ,to vary. The fabrication of the pH-electrode is described in subsection 5.3.1. The received and modulated signal passes through a Schottky diode-based

frequency doubling circuit and is subsequently retransmitted back to the interrogator using the orthogonal transmit mode of the ring antenna operating at $2f_0$ that has a wider 10 dB bandwidth of 15%. The location of the varactor diode is chosen such that it gives maximum perturbation of the resonant frequency of the receiving mode at f_0 and minimum to no perturbation of the transmitting mode at $2f_0$. Fig. 6.2 shows the schematic of sensor circuit used to achieve this. The sensor was fabricated on FR4 board, with annular ring antenna on one side and the doubling and sensing voltage coupling circuitry on the other. Fig. 6.3 shows the block diagram of the interrogator which has an EIRP near 32 dBm. The power received by the reader at $2f_0$ at a fixed distance of 80 cm for different transmitted power at f_0 is shown in Fig. 6.4. The sensor gives a linear magnitude response and minimum frequency deviation with a change in the interrogating power. The sensor range may be easily extended to more than 1 m with a signal-to-noise ratio

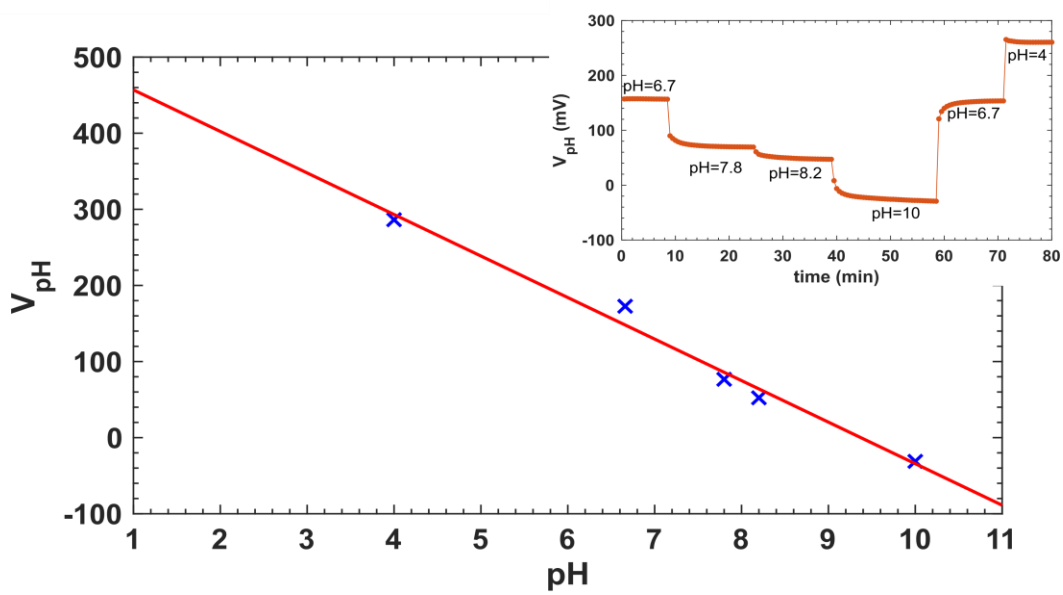

Fig. 6.5 The measured pH response of the MMO-Ag/AgCl electrode pair. The inset shows the time response of the electrodes to different buffer solutions.

higher than 30 dB.

6.3.1. Hydrogel Coated pH Electrode

The pH combination electrode consists of a Silver/Silver Chloride (Ag/AgCl) reference electrode and a commercial mixed metal oxide (MMO) working electrode. The electrodes are coated with hydrogel, which acts as the solid electrolyte completing the electrochemical cell. When

an acidic or a basic gas diffuses and dissolves into the electrolyte, a change in the potential difference is induced between the working electrode and the reference electrode. The potential of the working electrode depends on the pH, while the reference electrode provides a constant potential. For a constant temperature, a pH combination electrode provides a potential difference which is proportional to the pH concentration of the sample. The Ag/AgCl electrode was fabricated using the method as described in [26], that incorporates a nafion coating for long term stability of the electrode. Fig. 6.5 shows the response of the electrode pair for different pH buffer solutions. The electrodes give a sensitivity of ~55mV/pH change. The structure of the electrodes with the hydrogel coating for gas sensing is shown in Fig. 6.2c. The electrodes were placed 0.5 mm from each other, and the hydrogel coating was 5 mm thick. The radii of the commercial MMO and Ag wires were 1.5 mm and 0.5 mm, respectively. The geometry of the electrodes and thickness of the

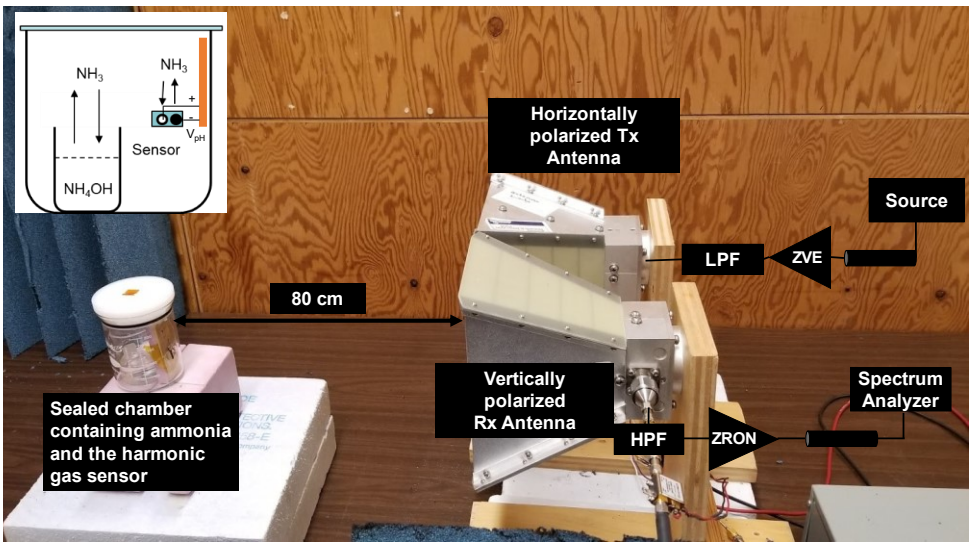

Fig. 6.6 Experimental setup used for ammonia sensing. Inset shows the a schematic of the sensing chamber with the sensor tag inside. Details of the interrogator are in Fig. 3.

hydrogel influence the response time of the sensor and may be optimized as described in [23].

6.4. Ammonia Sensing Application

The harmonic sensing tag is placed inside a sealed chamber with a beaker containing ammonium hydroxide at a distance of 80 cm from the interrogator with a transmit power of 22 dBm. Ammonia gas evaporates and diffuses into the hydrogel electrolyte until an equilibrium concentration is reached. At room temperature, the equilibrium concentration of ammonia gas in

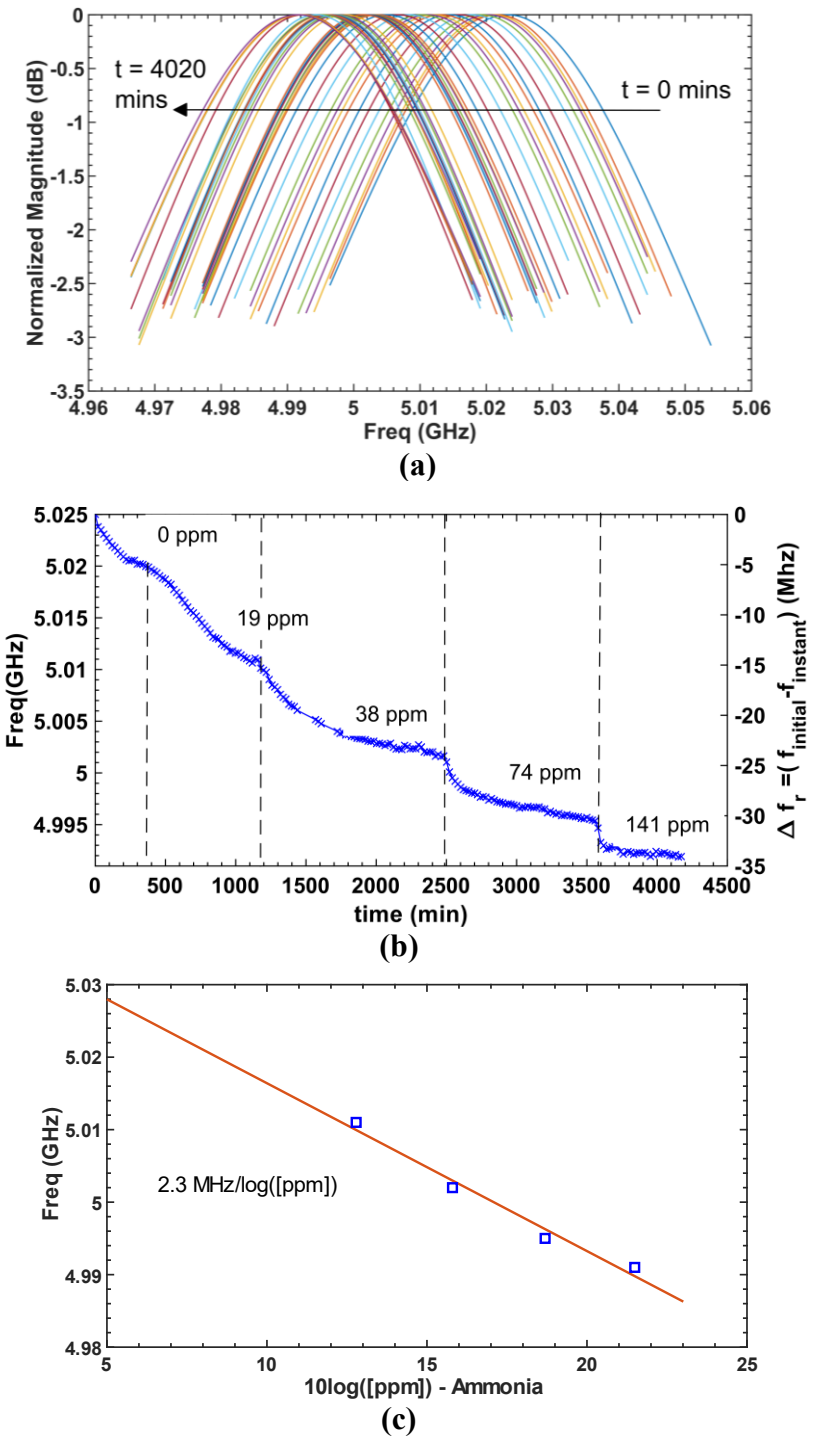

Fig. 6.7 (a) Interpolated normalized magnitude of the received signal at 50 min intervals (b) resonant frequency change with time for different ammonia concentrations introduced into the chamber, and (c) the resonant frequency versus the logarithm of the equilibrium ammonia concentration in ppm (solid line indicates linear interpolation and markers indicate the actual measured points).

the chamber depends on the concentration of ammonium hydroxide and is obtained using Raoult's law. The peak of the received signal was monitored every 2 mins. National instrument's LabView VI was used for automatic data acquisition. This measurement set up is shown in Fig. 6.6. The sample was kept at room temperature over the entire course of the experiment. Fig. 6.7a shows samples of the interpolated normalized magnitude of the received signal at different times during the experiment. The signal received back by the interrogator is 30 dB above the noise floor of the system. The time change in resonant frequency, defined here as the maximum of the magnitude of the received signal, for different concentrations of ammonia is shown in Fig. 6.7b. Both the interpolation and resonant frequency maxima were obtained using a parabolic fit to the magnitude of received signal as described in [27]. The sensor gives a linear resonant frequency shift with the logarithm of the concentration of ammonia as shown in Fig. 6.7c.

6.5. CONCLUSION

This chapter presented a wireless harmonic sensor for applications in packaged food monitoring. A dual-band annular slot ring antenna was used to receive and retransmit the signal at f_0 and $2f_o$, respectively. In this application, the receiving mode of the antenna was also sensitized to acidic or basic volatile by coupling it to a varactor-pH electrode transduction scheme. A schottky diode-based frequency doubler was used to generate the harmonic signal. The sensor was shown to have a linear response to log concentration of ammonia and provided a sensitivity of 2.3 MHz per unit log ppm change in ammonia concentration. Ammonia concentrations of as low as 20 ppm may easily be detected using the presented sensor, making it amenable to applications like fish spoilage detection as described in [4]. Faster response time may be obtained by optimizing the electrode geometries and the hydrogel thickness, and the pH electrode pair may further be integrated into the backside of the antenna [28]. The sensor design may also be scaled to a higher f_0 to further miniaturize it. In this chapter, individual laboratory equipment and connectorized components were used for the implementation of the interrogator and may be simplified using a low-cost software defined radio.

6.6. References

[1] S. Matindoust, M. Baghaei-Nejad, M. H. Shahrokh Abadi, Z. Zou, and L.-R. Zheng, "Food quality and safety monitoring using gas sensor array in intelligent packaging," *Sens. Rev.*, vol. 36, no. 2, pp. 169–183, Mar. 2016.

[2] A. E. Ghaly, D. Dave, and A. E. Ghaly, "Meat Spoilage Mechanisms and Preservation Techniques: A Critical Review," *Am. J. Agric. Biol. Sci.*, vol. 6, no. 4, pp. 486–510, 2011.

[3] A. Nopwinyuwong, S. Trevanich, and P. Suppakul, "Development of a novel colorimetric indicator label for monitoring freshness of intermediate-moisture dessert spoilage.," *Talanta*, vol. 81, no. 3, pp. 1126–32, May 2010.

[4] S. Bhadra, C. Narvaez, D. J. Thomson, and G. E. Bridges, "Non-destructive detection of fish spoilage using a wireless basic volatile sensor," *Talanta*, vol. 134, pp. 718–723, Mar. 2015.

[5] European Commission, "95/149/EC: Commission Decision of 8 March 1995 fixing the total volatile basic nitrogen (TVB-N) limit values for certain categories of fishery products and specifying the analysis methods to be used," 1995. [Online]. Available: https://publications.europa.eu/en/publication-detail/-/publication/91dc1ed4-6450-4a3c-8cab-45009644715c/language-en. [Accessed: 11-Dec-2017].

[6] H. Yousefi, H. M. Su, S. M. Imani, K. Alkhaldi, C. D. Filipe, and T. F. Didar, "Intelligent Food Packaging: A Review of Smart Sensing Technologies for Monitoring Food Quality," *ACS Sensors*, vol. 4, no. 4, pp. 808–821, 2019.

[7] C. Rukchon, A. Nopwinyuwong, S. Trevanich, T. Jinkarn, and P. Suppakul, "Development of a food spoilage indicator for monitoring freshness of skinless chicken breast," *Talanta*, vol. 130, pp. 547–554, Dec. 2014.

[8] B. Kuswandi and A. Nurfawaidi, "On-package dual sensors label based on pH indicators for real-time monitoring of beef freshness," *Food Control*, vol. 82, pp. 91–100, Dec. 2017.

[9] A. Nopwinyuwong, S. Trevanich, and P. Suppakul, "Development of a novel colorimetric indicator label for monitoring freshness of intermediate-moisture dessert spoilage," *Talanta*, vol. 81, pp. 1126–1132, 2010.

[10] F. Saliu and R. Della Pergola, "Carbon dioxide colorimetric indicators for food packaging application: Applicability of anthocyanin and poly-lysine mixtures," vol. 258, pp. 1117–

1124, Apr. .

[11] S. Manzari and G. Marrocco, “Modeling and applications of a chemical-loaded UHF RFID sensing antenna with tuning capability,” *IEEE Trans. Antennas Propag.*, vol. 62, no. 1, pp. 94–101, 2014.

[12] C. Occhiuzzi, S. Caizzone, and G. Marrocco, “Passive UHF RFID antennas for sensing applications: Principles, methods, and classifcations,” *IEEE Antennas Propag. Mag.*, vol. 55, no. 6, pp. 14–34, 2013.

[13] R. Raju, G. E. Bridges, and S. Bhadra, “Wireless passive sensors for food quality monitoring: Improving the safety of food products,” *IEEE Antennas Propag. Mag.*, vol. 62, no. 5, pp. 76–89, Oct. 2020.

[14] P. Fathi, N. C. Karmakar, M. Bhattacharya, and S. Bhattacharya, “Potential Chipless RFID Sensors for Food Packaging Applications: A Review,” *IEEE Sensors Journal*, vol. 20, no. 17. Institute of Electrical and Electronics Engineers Inc., pp. 9618–9636, 01-Sep-2020.

[15] B. Kubina, C. Mandel, M. Sch, R. Jakoby, M. Schussler, and R. Jakoby, “Compact Quasi-Chipless Harmonic Radar Sensor with a Dielectric Resonator Antenna,” *2015 IEEE MTT-S Int. Microw. Symp. IMS 2015*, pp. 2–4, Jul. 2015.

[16] B. Kubina, J. Romeu, C. Mandel, M. Schüßler, and R. Jakoby, “Quasi-chipless wireless temperature sensor based on harmonic radar,” *Electron. Lett.*, vol. 50, no. 2, Jan. 2014.

[17] V. Viikari, H. Seppä, T. Mattila, and A. Alastalo, “Wireless Ferroelectric Resonating Sensor,” *IEEE Trans. Ultrason. Ferroelectr. Freq. Control*, vol. 57, no. 4, pp. 785–791, Apr. 2010.

[18] A. Lazaro, R. Villarino, and D. Girbau, “A Passive Harmonic Tag for Humidity Sensing,” *Int. J. Antennas Propag.*, vol. 2014, pp. 1–11, 2014.

[19] R. Mirzavand and P. Mousavi, “A Zero-Power sensor using multi-port direct-conversion sensing,” *IEEE Sens. J.*, vol. 18, no. 22, pp. 9243–9250, Nov. 2018.

[20] S. Mondal, D. Kumar, and P. Chahal, “A Wireless Passive pH Sensor with Clutter Rejection Scheme,” *IEEE Sens. J.*, vol. 19, no. 9, pp. 3399–3407, 2019.

[21] S. Bhadra, G. E. Bridges, D. J. Thomson, and M. S. Freund, “Electrode Potential-Based Coupled Coil Sensor for Remote pH Monitoring,” *IEEE Sens. J.*, vol. 11, no. 11, pp. 2813–2819, Nov. 2011.

[22] S. Bhadra, D. S. Y. Tan, D. J. Thomson, M. S. Freund, and G. E. Bridges, “A wireless

passive sensor for temperature compensated remote pH monitoring," *IEEE Sens. J.*, vol. 13, no. 6, pp. 2428–2436, 2013.

[23] S. Bhadra, D. J. Thomson, and G. E. Bridges, "Monitoring acidic and basic volatile concentration using a pH-electrode based wireless passive sensor," *Sensors Actuators, B Chem.*, vol. 209, pp. 803–810, Mar. 2015.

[24] R. Raju and G. E. Bridges, "A Compact Passive Wirlress Harmonic Sensor for Packaged Food Quality Monitoring," *IEEE Trans. Microw. Theory Tech.*, 2021.

[25] R. Raju and G. E. Bridges, "Radar Cross Section Based Chipless Tag with Built-in Reference for Relative Humidity Monitoring of Packaged Food Commodities," *IEEE Sens. J.*, pp. 1–1, Jun. 2021.

[26] M. a Nolan, S. H. Tan, and S. P. Kounaves, "Fabrication and Characterization of a Solid State Reference Electrode for Electroanalysis of Natural Waters with Ultramicroelectrodes," *Anal. Chem.*, vol. 69, no. 6, pp. 1244–1247, 1997.

[27] M. P. Robinson and J. Clegg, "Improved determination of Q-factor and resonant frequency by a quadratic curve-fitting method," *IEEE Trans. Electromagn. Compat.*, vol. 47, no. 2, pp. 399–402, May 2005.

[28] T. Y. Kim, S. A. Hong, and S. Yang, "A Solid-State Thin-Film Ag/AgCl Reference Electrode Coated with Graphene Oxide and Its Use in a pH Sensor," *Sensors*, vol. 15, no. 3, pp. 6469–6482, Mar. 2015.

Chapter 7.
Conclusion and Future Work

This research studies the feasibility of high-frequency passive wireless sensors operating in the UHF range for packaged food monitoring applications. Chapter 2 presented a survey of potential passive wireless tags for their application in the package to package food quality monitoring. The most important considerations for the practical implementation of passive wireless sensors for their application in the package to package monitoring were identified to be their cost, size and immunity to environmental loading effects.

Chapter 3 presented a dual-band, dual-polarized annular slot ring antenna for application in relative humidity monitoring in the headspace regions of hermetically packaged food products. The sensor can be effectively used in low clutter environments, such as a factory or warehouse facility, thus being suited to situations when the package integrity is required to be tested after packaging and before shipping. In such a scenario, the packaged commodity is usually on a moving conveyer belt, where in addition to easy background subtraction and time-gated measurements, the doppler shift caused by the moving targets may be used to remove unwanted stationary clutter [1]. The integration of the sensing and reference signal within the same antenna gives the sensor a compact size and differential sensing capability that is usually achieved using an added additional resonator usually used to reduce the de-tuning effects of the immediate environment the sensor is in.

In chapter 4 the annular ring antenna presented in chapter 3 was modified to operate as a depolarizing tag for volatile sensing applications by intelligent placement of capacitive perturbations on the annular slots. The cross-polarizing property of the tag was shown to have better immunity to environmental co-polarized clutter, thereby, improving its practical applications compared to traditional radar cross-section-based sensing tags. The ammonia sensing capability of the sensor was demonstrated using a pH electrode biased varactor tuning element added onto one of the resonant slots and keeping another resonant slot as a reference for differential sensing capability. Further study is, however, required towards the improvement of the stability and repeatability of the pH combination electrode pair. One of the main limitations of the sensors RCS-based sensors is their low-quality factor. This limits the application of signal processing

techniques like a short-time Fourier transform (STFT) and short time matrix pencil method to improve the detection capability of radar cross-section-based [2] [3] [4].

Chapter 5 and chapter 6 presented a harmonic sensor for applications in packaged food monitoring. These chapters show a novel integration of the receive, transmit, doubler circuitry and the sensing circuitry in a compact form factor. A dual-band annular slot ring antenna was used to receive and transmit the signal at f_0 and $2f_o$ respectively. As an example, the receiving mode of the antenna was also sensitized to pH by coupling it to a varactor-pH electrode transduction scheme. A Schottky diode-based frequency doubler was used as the generate the harmonic signal. The sensor was shown to have a linear response to pH and provided a sensitivity of 4 MHz per unit pH change. The sensor was then employed successfully for milk monitoring application. In chapter 6 the harmonic sensor is tailored for the ammonia sensing application and its extended range capability was studied. The sensor utilized semi-integrated wire-electrodes coated with hydrogel for ammonia sensing. The sensor was shown to have a linear response to log concentration of ammonia and provided a sensitivity of 2.3 MHz per unit log ppm change ammonia concentration. The sensor was shown to be capable of detecting ammonia levels as low as 20 ppm, making it suitable for applications like non-contact fish spoilage detection. The addition of the Schottky diode increases the cost of the sensor compared to traditional chipless sensors, this makes them limited to applications for monitoring of high-value food items like poultry and meat.

One of the considerations with practical application and future deployment of the sensors includes low-cost implementation of the interrogator using commercial off-the-shelf parts. Software-defined radio and phase-locked loop-based interrogators may be used for interrogation. The compatibility of the tag with roll-to-roll printing is another consideration to be taken into account. The main component of the passive sensors, the antenna can be easily printed using common inkjet or gravure printers. Both PVA and pH electrodes used for sensing may also be made compatible with printing as shown in [5]. With further advancement in printed electronics, varactor and Schottky diode operating in the giga-hertz range may also be made compatible with printing [6][7] [8]. This brings the cost of the sensors further down and closer to commercialization.

In conclusion, this thesis presents a new paradigm for microwave passive chipless and quasi-chipless wireless sensors in the light of packaged food monitoring. The thesis presented wireless passive sensors operating in microwave frequency range with a sensing range of tens of centimetres to a meter. The sensors were compact in size and were shown to be fitting for sensing in packaged food monitoring applications with improved immunity to the effects of environmental loading.

Some of the recommended future work are listed below-

- The sensor presented in Chapter 3 for sensing relative humidity may be modified to sense volatile gases using the varactor coupled pH combination electrodes. Preliminary work for this has been demonstrated in [9]. Further study may also be carried to integrate the pH electrodes onto the dual-band, dual-polarized annular ring antenna directly.

- The volatile sensors presented in chapters 4 and 6 utilize wire-electrodes for transduction. More work towards more stable electrode, optimized electrode geometries for fast time response and planar electrode integration may be carried out in the future. Experiments to correlate the measured response of the sensor to actual microbial count during the process of spoilage of food items like fish may also be carried out.

- One of the key disadvantages of RCS-based sensors presented in chapters 3 and 4 is that these sensors require a well-calibrated environment for their operation, structures like spiral resonators or planar cavity coupled that are of higher quality factor may be designed. These sensors when coupled to signal processing techniques like short-time Fourier transform and short time matrix pencil method have the potential of superior clutter rejection capability by gating the mid-time response dominated by clutter and using either in the early time response or the late time response of the sensor for detection.

- Chapter 5 demonstrated pH monitoring application using a harmonic sensor, this sensor however utilized a commercial pH electrode for its operation. The integration of the pH electrode directly onto the package of the food commodity may also be studied. The application of the sensor for monitoring bio-reactors and meat/fish spoilage may be explored.

- The harmonic sensors presented in chapters 4 and 5 only demonstrated varactor-based sensing applications. These sensors can also be modified with integrated interdigitated capacitors to obtain dielectric-based capacitive sensing, not only for food monitoring applications but also for other applications where there is a requirement of the sensor being buried inside a high clutter environment like moisture content monitoring in construction industry.

- Lastly, all the sensors presented in the thesis utilize laboratory equipment for the implementation of their interrogators, further work may be carried out to implement these using low-cost commercial hardware like software-defined radio.

7.1. References

[1] M. A. Richards, *Fundamentals of radar signal processing*, 2nd ed. New York, NY: McGraw-Hill, 2014.

[2] A. Fawky, M. Khaliel, A. El-Awamry, M. El-Hadidy, and T. Kaiser, "Novel Pseudo-Noise coded chipless RFID system for clutter removal and tag detection," in *2015 IEEE International Conference on RFID (RFID)*, 2015, pp. 100–104.

[3] F. Costa *et al.*, "Robust Reading Approach for Moving Chipless RFID Tags by Using ISAR Processing," *IEEE Trans. Microw. Theory Tech.*, vol. 66, no. 5, pp. 2442–2451, May 2018.

[4] A. Ramos, E. Perret, O. Rance, S. Tedjini, A. Lazaro, and D. Girbau, "Temporal Separation Detection for Chipless Depolarizing Frequency-Coded RFID," *IEEE Trans. Microw. Theory Tech.*, vol. 64, no. 7, pp. 2326–2337, Jul. 2016.

[5] A. Hayat and J. Marty, "Disposable Screen Printed Electrochemical Sensors: Tools for Environmental Monitoring," *Sensors*, vol. 14, no. 6, pp. 10432–10453, Jun. 2014.

[6] Y. Chu, C. Qian, P. Chahal, and C. Cao, "Printed Diodes: Materials Processing, Fabrication, and Applications," *Adv. Sci.*, vol. 6, no. 6, p. 1801653, Mar. 2019.

[7] K. D. KIM, J. B. KOO, J. K. LEE, Y. S. YANG, I.-K. YOU, and Y.-Y. NOH, "Variations in the Electric Characteristics of an Organic Schottky Diode with the P3HT Thickness," *J.*

Korean Phys. Soc., vol. 57, no. 1, pp. 124–127.

[8] N. Sani *et al.*, "All-printed diode operating at 1.6 GHz.," *Proc. Natl. Acad. Sci. U. S. A.*, vol. 111, no. 33, pp. 11943–8, Aug. 2014.

[9] R. Raju and G. E. Bridges, "Radar Cross Section Based Passive Wireless Sensor for Volatile Sensing," *Proc. - ANTEM 2018 2018 18th Int. Symp. Antenna Technol. Appl. Electromagn.*, vol. 2018-August, Dec. 2018.